

Inaugural-Dissertation
zur
Erlangung der Doktorwürde
der
Gesamtfakultät
Für Mathematik, Ingenieur und Naturwissenschaften
der
Ruprecht – Karls – Universität
Heidelberg

vorgelegt von
Master of Science David Philipp Wohlfart
Aus: Darmstadt, 68283 Deutschland
Tag der mündlichen Prüfung: 05.10.2022

Accumulation of Endogenous Acetaldehyde in Aldehyde
Dehydrogenase 2 Gene Knockout Zebrafish contributes to
Microvascular Complications and Impaired Glucose Metabolism

Gutachter:

Prof. Dr. Rüdiger Hell

Prof. Dr. Jens Kroll

Die vorliegende Arbeit wurde zwischen November 2018 und Juni 2022 in der Abteilung für Vaskuläre Biologie und Tumorangio-genese des „European Center of Angioscience“ der Medizinischen Fakultät Mannheim der Universität Heidelberg angefertigt.

Teile dieser Arbeit sind publiziert und befinden sich unter folgendem Titel in der Zeitschrift *Redox Biology* im Druck:

Accumulation of Acetaldehyde in *aldh2.1*^{-/-} Zebrafish Causes Increased Retinal Angiogenesis and Impaired Glucose Metabolism

David Philipp Wohlfart, Bowen Lou, Chiara Simone Middel, Jakob Morgenstern, Thomas Fleming, Carsten Sticht, Ingrid Hausser, Rüdiger Hell, Hans-Peter Hammes, Julia Szendrödi, Peter Paul Nawroth, Jens Kroll

Hiermit erkläre ich an Eides statt, dass ich die vorliegende Arbeit ohne unzulässige Hilfe Dritter und nur unter Verwendung der angegebenen Quellen und Hilfsmittel verfasst habe. Jegliche Ausführung, die wörtlich oder sinngemäß übernommen wurden, sind als solche kenntlich gemacht. Ich habe weder die Arbeit noch Teile dieser Arbeit an einer Hochschule des In- oder Auslandes als Bestandteil einer Prüfungs- oder Qualifikationsleistung vorgelegt. Ich erkläre hiermit die Richtigkeit der vorstehenden Erklärung und bin mir der Folgen einer unrichtigen oder unvollständigen eidesstattlichen Versicherung bewusst. Ich versichere an Eides statt, dass ich nach bestem Wissen die reine Wahrheit erkläre und nichts verschwiegen habe.

Mannheim, den _____

David Philipp Wohlfart

Danksagung

An erster Stelle danke ich Herrn Prof. Dr. Jens Kroll für die Gelegenheit meine Doktorarbeit in seiner Arbeitsgruppe durchführen zu können inklusive der nachhaltigen Unterstützung in der Projekt-Planung, -Durchführung und -Vollendung.

Herrn Prof. Dr. Rüdiger Hell danke ich dafür, dass er sich die Zeit genommen hat meine Doktorarbeit als Erstgutachter zu unterstützen und hiermit meiner Dissertation an der Gesamtfakultät für Mathematik, Ingenieur und Naturwissenschaften der Ruprecht – Karls – Universität Heidelberg den Weg bereitet hat.

Überdies gilt dem gesamten Team der AG Kroll mein Dank. Namentlich vor allem; Katrin Bennewitz und Björn Hühn und wie sie verlässlich dafür gesorgt haben, dass die Arbeit im Labor und mit den Fischen reibungslos stattfinden konnte; Bowen Lou, Haozhe Qi und Xiaogang Li, welche immer für gute Hilfestellung und wissenschaftliche Diskussion bereit waren; und allen weiteren Mitgliedern des Labors. Ein besonderer Dank geht an Mike Boger und Christopher Tabler, die mir über die Arbeit hinaus moralisch und seelisch beigestanden haben.

Außerdem bedanke ich mich bei meinen Kollaborationspartnern im SFB1118 und GRK 1874/2 DIAMICOM: Dr. Thomas Fleming und Dr. Jakob Morgenstern, Dr. Gernot Poschet und Dr. Elena Heidenreich, Prof. Dr. Hans-Peter Hammes und Chiara Middel, Dr. Carsten Sticht und Dr. Ingrid Hausser-Siller für all die methodische und technische Unterstützung und Expertise, welche mein Projekt vervollständigt haben.

Natürlich möchte ich hier auch meine Freunde erwähnen die immer an meiner Seite standen: Henryk, Seb und Marvin, Jens und Kerstin, sowie Alex, ich danke euch für die wertvolle Zeit die wir gemeinsam haben.

Zuletzt möchte ich noch meiner Partnerin Vera bedanken, welche in jeder Situation alles für mich stehen und liegen lässt und mich in dieser stressigen Zeit aus nächster Nähe unterstützt hat.

Die wichtigsten Menschen für diese Arbeit waren jedoch unumstritten meine Familie: meine Eltern und Brüder, die mir den Weg bis hierhin geebnet haben und immer voller Überzeugung an mich geglaubt haben. Ohne euch könnte ich nicht ich selbst sein.

Vielen Dank.

Table of Contents

Zusammenfassung	V
Summary	VII
1. Introduction.....	1
1.1 Aldehyde dehydrogenase enzyme superfamily.....	1
1.2 Reactive Carbonyl Species and their role in metabolic disorders	2
1.3 Ethanol and Acetaldehyde as risk factors	4
1.4 Microvascular complications and diabetes mellitus.....	5
1.5 <i>Danio rerio</i> as a model organism	9
1.6 Aim of the Thesis	11
2. Results.....	13
2.1 Generation of <i>aldh2.1</i> knockout zebrafish.....	13
2.1.1 Amino acid sequence alignment.....	13
2.1.2 Utilizing CRISPR/Cas9 technology for generation of <i>aldh2.1</i> ^{-/-} knockout mutants.....	14
2.1.3 Distribution of <i>aldh2.1</i> in zebrafish organs.....	15
2.1.4 Validation for loss of Aldh2.1 protein via Western Blot	16
2.2 Phenotypic characterization of <i>aldh2.1</i> ^{-/-} zebrafish.....	17
2.3 Zebrafish vasculature and kidney morphology.....	19
2.3.1 Loss of <i>aldh2.1</i> led to increased angiogenesis in the trunk vasculature and retinal vasculature of zebrafish larvae and adults.....	19
2.3.2 Kidney morphology was not altered in <i>aldh2.1</i> ^{-/-} zebrafish	23
2.4 Metabolome analysis	25
2.4.1 <i>aldh2.1</i> ^{-/-} zebrafish displayed an elevation of endogenous AA and decreased postprandial blood glucose.....	25
2.5 Transcriptomics.....	30
2.5.1 <i>aldh2.1</i> ^{-/-} mutants exhibited aggravated stress-signaling and an impairment of glycolysis.....	30

2.5.2	Angiogenesis factors are unchanged in <i>aldh2.1^{-/-}</i> mutants	32
2.5.3	Inhibition of p38 MAPK and activation of JNK gene expression in <i>aldh2.1^{-/-}</i> mutants.....	32
2.5.4	Inhibition of glucose-6-phosphatase and glucokinase gene expression in <i>aldh2.1^{-/-}</i> mutants.....	33
2.6	Pharmacological interference studies	35
2.6.1	Exogenous AA caused angiogenic alterations in hyaloid vasculature, impairment of glucose metabolism and alteration of MAPK signaling	35
2.6.2	Inhibition of p38 MAPK caused similar, but not identical angiogenic alterations in hyaloid vasculature in <i>aldh2.1^{+/+}</i> zebrafish larvae	38
3.	Discussion	40
3.1	<i>aldh2.1^{-/-}</i> zebrafish display increased angiogenesis and hallmarks of retinopathy without hyperglycemia.....	41
3.2	AA causes an impaired glucose sensitivity and glucose mobilization via inhibition of glycolysis and gluconeogenesis gene expression.....	43
3.3	Loss of Aldh2.1 does not alter glomeruli morphology.....	44
3.4	Reactive metabolites as upstream factors of glucose metabolism and microvascular complications in zebrafish	45
3.5	Conclusion and future perspectives	46
4.	Material and Methods	48
4.1	Material	48
4.1.1	Equipment	48
4.1.2	Chemicals.....	49
4.1.3.	Consumables.....	49
4.1.4	Solutions.....	50
4.1.5	Oligonucleotides	52
4.1.6	Further materials	54
4.1.7	Plasmids.....	55
4.1.9	Antibodies.....	55

4.1.10	55
Zebrafish transgenic lines.....	55
4.2 Methods	55
4.2.1 Study approval.....	56
4.2.2 Zebrafish husbandry	56
4.2.3 Generation of Zebrafish single gene knockout mutants.....	56
4.2.4 Dissection of adult zebrafish and blood glucose measurement	57
4.2.5 Microscopy and analysis of larvae trunks	57
4.2.6 Microscopy and analysis of larvae hyaloids.....	57
4.2.7 Microscopy and analysis of adult retinal vasculature	58
4.2.8 Retinal digest preparation.....	58
4.2.9 Analysis of adult zebrafish kidneys.....	59
4.2.10 Generation of lysates from zebrafish larvae	60
4.2.11 Western Blot analysis	61
4.2.12 Pharmacological treatment of zebrafish embryos / larvae	61
4.2.13 Enzyme Activity assays	61
4.2.14 Measurements of glucose and reactive metabolites	62
4.2.15 Isolation of genomic DNA	63
4.2.16 Isolation of total RNA and reverse transcription.....	63
4.2.17 (Reverse-transcription quantitative) Polymerase Chain Reaction (RT-qPCR)	63
4.2.18 Genotyping	64
4.2.19 RNA-Sequence Analysis	64
4.2.20 Metabolomic Analysis	65
4.2.21 Protein Sequence Alignment	65
4.2.22 Statistical Analysis.....	65
Abbreviations.....	66
References	71

Zusammenfassung

Reaktive Carbonyl Spezies (RCS) werden in jedem Organismus spontan während des Stoffwechsels produziert und sind problematisch, weil sie die Struktur und Funktion von DNA, Proteinen und Lipiden verändern und beeinträchtigen können. Das bekannteste Mitglied dieser Klasse ist Methylglyoxal (MG), welches eine Anhäufung von *advanced glycation endproducts* (AGEs) verursacht und damit zu schweren Organschäden führen kann. MG selbst ist ein Nebenprodukt, das hauptsächlich durch eine nicht-enzymatische Reaktion während der Glykolyse produziert wird, weitere Quellen sind Aminosäuren, Lipide und Aceton. Methylglyoxal wird vorrangig durch das Glyoxalase System detoxifiziert, kann aber auch durch weitere Enzymfamilien wie die Aldehyddehydrogenasen (Aldh) oder die Aldo-Keto Reduktasen (Akr) abgebaut werden. Neueste Studien über den Funktionsverlust des Glyoxalase Systems in Maus, Zebrafisch und *Drosophila* haben offengelegt, dass die Aldehyddehydrogenasen und die Aldo-Keto Reduktasen kompensatorische Aktivität für MG besitzen und so Komplikationen abmildern. In Verbindung zu den Befunden zu Aldh und Akr wird derzeit angenommen, dass die verschiedensten RCS Auslöser für mikrovaskuläre Komplikationen sein können, jedoch sind die inneren Mechanismen zur Anreicherung von RCS wie Acetaldehyd (AA), 4-Hydroxynonenal (4-HNE), Akrolein (ACR) und weitere sowie die nachfolgende Schadensentwicklung nur schlecht verstanden. Daher war das Ziel dieser Studie herauszufinden, welche spezifischen Metabolite von verschiedensten Aldhs primär detoxifiziert werden und welche Auswirkung eine endogene Anhäufung dieser Metabolite auf die Gesundheit verschiedener Organe und den Glukose Metabolismus hat.

Im Zebrafisch führte der Knockout von *glo1*, *aldh3a1* und *akr1a1a* zur Anhäufung von spezifischen primären RCS. Diese RCS enthüllten einen unterliegenden spezifischen Mechanismus zur Regulation des Glukosemetabolismus bis hin zur Hyperglykämie und diabetischen Organschäden. Zusätzlich wurde in den Studien um *glo1* gezeigt, dass diverse Aldh Gene kompensatorisch hochreguliert waren. Zu diesen Genen zählt *aldh2.1*, welches daher als Gen Knockout Mutante im Zebrafisch mittels CRISPR/Cas9 hergestellt und histologisch, metabolisch und transkriptionell analysiert wurde. *aldh2.1*^{-/-} Zebrafische wiesen eine Anhäufung von endogenem AA auf, welche zu einer erhöhten Angiogenese in der retinalen Vaskulatur führte. Diese Aktivierung der Angiogenese wurde getrieben durch ein Ungleichgewicht in der Expression von c-Jun-

N-terminaler Kinase (JNK) und p38 *Mitogen-Activated Protein Kinase* (MAPK). Des Weiteren konnte herausgefunden werden, dass die Anhäufung von AA in *aldh2.1^{-/-}* Zebrafischen keine Hyperglykämie auslöste, sondern über die Inhibierung der Expression von Glucokinase (*gck*) und Glukose-6-phosphatase (*g6pc*) zu einem beschädigten Glukose Metabolismus führte.

Summary

Reactive carbonyl species (RCS) are spontaneously formed during metabolism and modify and impair the function of DNA, proteins, and lipids, leading to several organ complications. The most prominent constituent of this class is methylglyoxal (MG) with its ability to produce and cause the accumulation of advanced glycation endproducts (AGEs). Methylglyoxal is a non-enzymatic byproduct of glycolysis, amino acids, lipids and more, and can be detoxified primarily through the glyoxalase system, aldehyde dehydrogenases (Aldh) and aldo-ketoreductases (Akr). Studies about the glyoxalase system have recently been completed for mice, zebrafish and *Drosophila* and reveal that compensatory mechanisms like Aldh and Akr will significantly reduce complications during loss of function of the glyoxalase system. However, the effect of endogenous elevation of these various RCS like acetaldehyde (AA), 4-hydroxynonenal (4-HNE), and acrolein (ACR) are currently poorly understood. Therefore, this study aimed to identify the specific primary RCS detoxification target of different Aldh family members and to investigate the impact of endogenous elevation on organ complications and glucose metabolism *in vivo*.

In zebrafish, knockout of the RCS detoxifying enzymes glyoxalase 1 (Glo1), aldehyde dehydrogenase 3a1 (Aldh3a1) and aldo-ketoreductase 1a1a (Akr1a1a) showed a signature of elevated RCS which specifically regulated glucose metabolism, hyperglycemia and diabetic organ damage. The isoform *aldh2.1* was compensatory upregulated in *glo1*^{-/-} animals as well and therefore implemented as a single gene knockout mutant in zebrafish. The knockout mutant was analyzed on a histological, metabolic and transcriptional level, because *aldh2.1*^{-/-} zebrafish displayed increased endogenous acetaldehyde (AA) inducing an increased angiogenesis in retinal vasculature. Furthermore, expression and pharmacological interventional studies identified an imbalance of c-Jun N-terminal kinase (JNK) and p38 MAPK induced by AA, which mediated an activation of angiogenesis. However, the increased AA in *aldh2.1*^{-/-} zebrafish did not induce hyperglycemia, instead AA inhibited the expression of glucokinase (*gck*) and glucose-6-phosphatase (*g6pc*), which led to an impaired glucose metabolism akin to hypoglycemia.

In conclusion, the data have identified AA as the preferred substrate for Aldh2.1's detoxification ability, which subsequently caused microvascular organ damage and impaired glucose metabolism independently of ethanol exposure.

1. Introduction

1.1 Aldehyde dehydrogenase enzyme superfamily

The aldehyde dehydrogenase (Aldh) enzyme superfamily exists in most known life forms from bacteria and eukaryotes to mammals and fish and they are expressed within all organs of their organism^{1,2}. Up to date 555 *aldh* genes are known, including 20 functional *aldh* genes in the human genome and 21 *aldh* genes in the zebrafish genome¹. Enzymes of this superfamily classify as oxidoreductases as their primary function is NAD(P)⁺ / NAD(P)H-dependent detoxification of endogenous and exogenous aldehydes to their respective carboxylic acid as seen in Figure 1³. However, Aldh enzymes can have additional enzymatic functions such as esterase activity for various carboxylic acid esters and non-enzymatic functions like absorbing ultraviolet light and binding endobiotic or xenobiotic molecules⁴⁻⁹.



Figure 1 General reaction equation of Aldh enzymes.

Due to their involvement with aldehydes and carboxylic acids and their protective function from reactive metabolites, the Aldh family is also often involved in many other physiological processes such as regulation of oxidative stress and cell proliferation¹⁰⁻¹². Consequently, mutations that lead to altered or impaired enzyme activity in *aldh* genes have been found to cause a variety of pathologic organ developments. These afflictions comprise of cardiovascular complications¹³, cancer^{3,14}, epileptic seizures and many more¹². Furthermore, Aldh have an impact on metabolic health in major organs, as it has been shown recently, that a defective aldehyde metabolism can lead to several issues in glucose, amino acid and fatty acid metabolism¹⁴⁻¹⁷.

Aldehyde dehydrogenase family member 2 is an enzyme known for its mitochondrial activity, and its highest gene expression is accordingly found in liver and other tissues with high mitochondrion count^{14,18}. The most investigated function of Aldh2 is the clearance of endogenous acetaldehyde (AA), which can accumulate during alcohol consumption and other risk factors¹⁹. Biochemically and structurally, Aldh2 may be

counted as a member of the Aldh1 family. However, the specific association with ethanol metabolism results in a strong differentiation to the Aldh1³. It has been observed, that dysfunction of Aldh2 can increase the risk of several complications, especially during alcohol abuse. For instance, a role of Aldh2 has been described in multiple cancer types^{20–23}, Alzheimer's disease^{24,25}, alcoholic and non-alcoholic fatty liver disease^{26–33} as well as heart diseases^{34–37}. Among East Asians a common occurring gene polymorphism *aldh2*2* is causing a lowered tolerance for alcohol due to accumulation of acetaldehyde framed as “Asian Flushing Syndrome”. Polymorphisms in the *aldh2* gene also evidently increase the risk of the carcinogenic effect of alcohol, especially for head and neck cancer^{38–41}. Additionally, it has been observed that *aldh2* polymorphism impairs the glycemic control⁴², is related to fasting blood glucose levels^{43,44} and can be a risk factor for type 2 diabetes mellitus⁴⁵.

Based on AA detoxification alone, Aldh2 proves to be a promising therapeutic target for numerous diseases. However, Aldh2 also has additional explored and non-explored functions. Aldh2 is involved in the clearance of further endogenous aldehydes as well, especially aldehydes produced during oxidative stress and lipid peroxidation like 4-hydroxynonenal (4-HNE) and malondialdehyde (MDA). Similarly, Aldh2 is involved in clearance of metabolites of neurotransmitter like 3,4-dihydroxyphenylacetaldehyde and –glycoaldehyde (DOPAL, DOPGAL)⁹. Although Aldh2 data has established the enzyme as an essential factor for risk reduction in several diseases. Its underlying mechanisms and potential are not yet fully explored. Further investigations for a better comprehension are needed.

In conclusion, the Aldh enzyme superfamily shows enormous potential for research and therapeutic targeting. It is now essential to thoroughly understand the mechanism with which each family member plays a role in proliferation disorders like cancer and metabolic diseases like diabetes mellitus.

1.2 Reactive Carbonyl Species and their role in metabolic disorders

In the past two decades, reactive carbonyl species (RCS) have drawn significant attention in disease research areas due to their roles in several biological processes and complications. RCS are commonly derived from the oxidation of carbohydrates, lipids and amino acids^{46–48}. The cellular environment constantly changes through

stress factors and metabolomic changes, therefore the endogenous concentration of RCS may be fluctuating. Dysfunctional RCS detoxification may be a key factor for carbonyl stress in aging, diabetes, late-diabetic microvascular complications and further metabolic disorders ^{17,49–53}.

Their generation *in vivo* can generally be split into five subgroups. Firstly, the non-enzymatic glycation includes metabolites like methylglyoxal (MG) and glyoxal which have been linked to formation of advanced glycation end products (AGEs) and diabetes, cancer and atherosclerosis respectively. Secondly, production of 3-deoxyglucosone and 3-deoxyfructose through the enzymatic polyol pathway is likewise related to formation of AGEs and the subsequent complications ^{54,55}. Thirdly, the peroxidation of lipids is the main underlying cause for accumulation of malondialdehyde (MDA) and 4-hydroxynonenal (4-HNE), acrolein (ACR), hexanal and more. This group of RCS has recently been associated with an imbalance of pancreas development and the insulin signaling pathway and subsequent diabetic organ damage ^{15–17,56–58}. Additionally, another group of RCS is produced through enzymatic glycation during metabolism and detoxification of various commonly occurring metabolites such as acetaldehyde (AA) from ethanol and glyceraldehyde-3-phosphate (G3P) from fructose-1,6-bisphosphate or dihydroxyacetone phosphate. Lastly, oxidation of amino acids results in a mixture of RCS from the pathways as mentioned above. Since amino acids are highly diverse, their catabolism results in various saturated and unsaturated RCS like MG, glyoxal and acrolein but also glycolaldehyde and 2-hydroxypropanal ⁵⁹. The most commonly occurring RCS associated with complications *in vivo* are shown in Figure 2 ⁴⁷. These RCS do not have to occur endogenously but also include exogenous sources such metabolites of drug products, cigarette smoke, food additives, and fried, smoked or otherwise processed food.

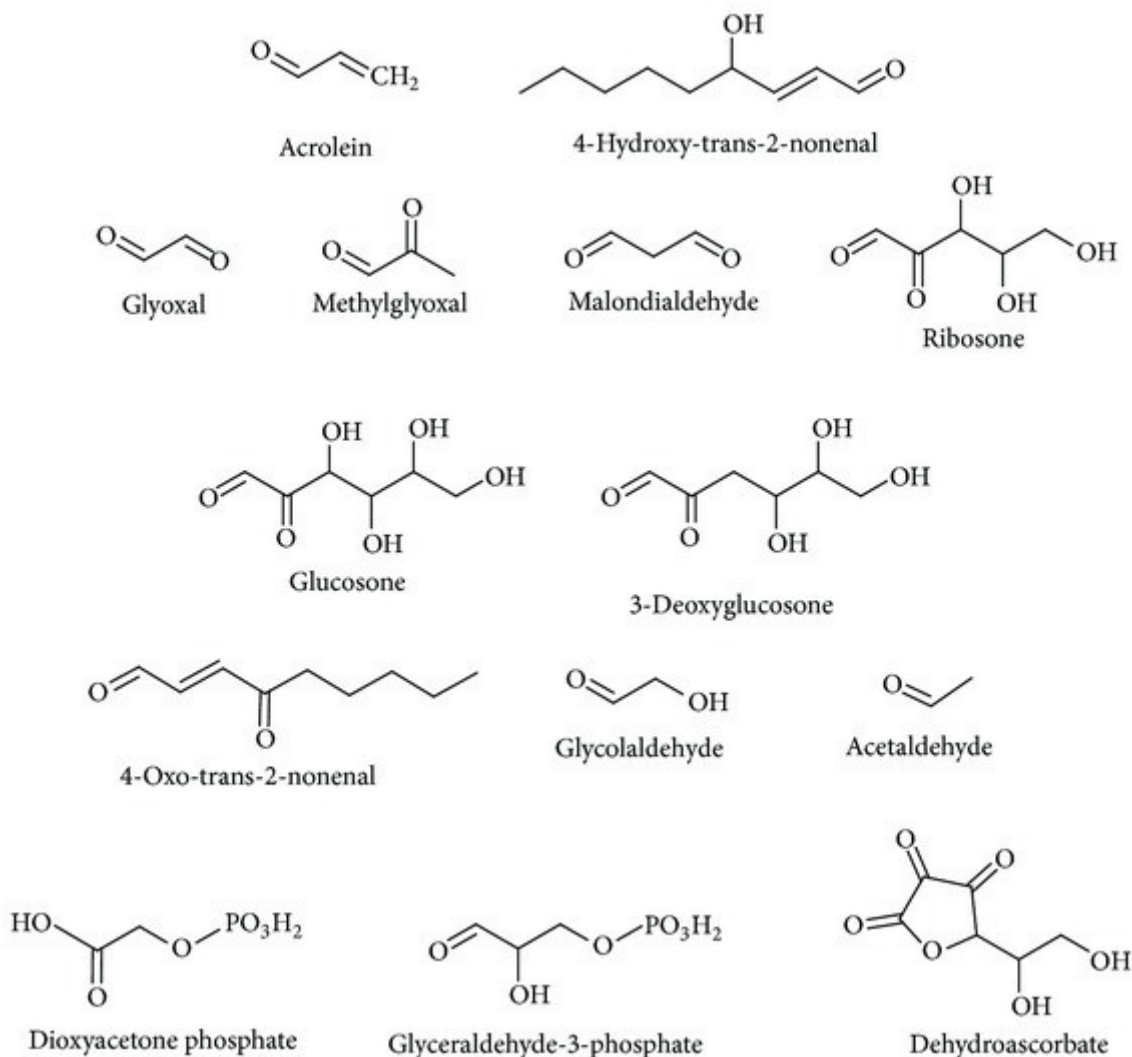


Figure 2 The Chemical Structures of most common Mono- and Di-Carbonyl Species. Picture taken from Semchyshyn *et al*⁴⁷.

1.3 Ethanol and Acetaldehyde as risk factors

One of the most notorious risk factors due to its cultural incorporation in many countries are ethanol and its metabolites. Ethanol is associated with many complications such as alcoholic fatty liver disease, cardiovascular disease, cardiomyopathy and cancer^{34,60–70}. Although there have been many attempts to understand alcohol-related complications, decisive evidences for the mechanisms and responsible toxins are still vague. Molecular candidates suggested to be the driving force are ethanol itself, but also its main downstream metabolic product acetaldehyde and fatty acid ethyl-esters^{63,71–73}. Ethanol is mainly metabolized in the liver by alcohol dehydrogenase (*adh*) to AA. AA is then further oxidized into acetate, enzymatically coupled to Coenzyme A

(CoA) and introduced into TCA cycle or fatty acid metabolism as acetyl-CoA. Additional sources for AA are further xenobiotics such as tobacco additives or diethyl ether. In mammals AA is also enzymatically produced from threonine to complement acetyl-CoA metabolism ^{74,75}.

The high reactivity of AA causes decreased antioxidant defenses (i.e. GSH levels) and is linked to production of free radicals through aldehyde / xanthine oxidase-associated oxidation. For this reason, its corresponding detoxification enzyme Aldh2 has been found to be essential for protection from mitochondrial dysfunction induced by oxidative stress in many of the major organ systems such as its primary location the liver, but also the heart, pancreas, gastrointestinal tract and the brain ^{22,76,77}. If AA metabolism is impaired, the oxidative stress in affected cells will rise and lead to a cycle of accumulating ROS and RCS, causing further oxidative stress and modification of the structure and function of macromolecules like DNA, lipids and proteins through reaction with amino, hydroxyl and sulfhydryl groups. Hence, evidence suggests that AA plays the key role in some of the pathogenesis mentioned above of alcohol-induced cardiomyopathy, liver disease and cancer either directly via oxidative stress or indirectly through inflammatory cytokines like tumor necrosis factor α (TNF- α) ⁷⁸⁻⁸¹.

In conclusion, even though AA has a verifiable impact on many major organs and takes part in various complications, the role of this RCS and its detoxification enzyme Aldh2 in metabolic diseases has been neglected in past studies ⁸². Especially, *in vivo* studies are missing, which investigate the role of *aldh2.1* independently of chronic toxification by exogenously added ethanol.

1.4 Microvascular complications and diabetes mellitus

Diabetic complications include not only micro- and macrovascular complications, but also partially cover dysfunction of immune system. Under the term microvascular complications three different subtypes are categorized: diabetic retinopathy (DR), diabetic nephropathy (DN) and diabetic neuropathy, which are causative for blindness, kidney failure, lower limb amputation, stroke and heart attacks. Furthermore, they are commonly described in context with diabetes mellitus. Diabetes mellitus (DM) is a metabolic disorder that is characterized by its chronic hyperglycemia in affected patients. Traditionally, DM is categorized at least into two different types. Type 1 DM

is an autoimmune disorder in which destruction of beta cells in the pancreas leads to insufficient insulin production and secretion^{83–85}. Type 2 DM, on the other hand, originates from an insulin resistance and hyperinsulinemia. It successively progresses into decreased β -cell function and insulin secretion. Patients with T2DM attributes are the majority of all DM cases (>90%) and may split up into further disease subtypes, as its heterogenous underlying mechanisms are not well understood⁸⁶.

Microvascular complications are commonly linked to diabetes mellitus due to high frequency of risk factors like hyperglycemia, inflammation and oxidative stress. However, the unique cause of these late diabetic complications is far from being understood. Recently, comprehensive studies revealed a limitation in the reduction of the relative risk for microvascular complications through glucose lowering treatment^{87–90}. These results show that glucose and hyperglycemia may have only an auxiliary impact to different underlying metabolic and genetic changes^{91,92}.

In 2001, Michael Brownlee proposed a hypothesis that four different molecular pathways are sufficient to explain all microvascular complications (Figure 3)⁹³. These four pathways, the polyol pathway, hexosamine pathway, protein kinase C (PKC) pathway and the AGE pathway, all cause metabolic disorder and microvascular damage by increasing oxygen and carbonyl stress. Since then, this concept has been adapted and extended by additional research groups^{46,94,95}. One weakness of this molecular pathway-oriented view is, that it does not address the full heterogeneity of diabetic complications, especially in T2DM patients. In order to better understand this heterogeneity Ahlqvist *et al* proposed in 2018 a novel stratification into five T2DM subgroups supported by cluster analysis based on six clinical parameters in 2018. The six parameters are, age, body-mass index, glutamate decarboxylase (GADA) antibodies, HbA_{1c}, HOMA 2B (beta cell function) and HOMA2 IR (insulin sensitivity). The severe autoimmune diabetes (SAID) incorporates 6-15 % of all diabetic patients. Patients with this form of T2DM have an early onset of the disease, with high HbA_{1c} values, impaired insulin production and GADA antibodies. The severe insulin-deficient diabetes (SIDD) makes up 9 – 20 % of diabetic patients and has the highest risk for diabetic retinopathy. It is accompanied by high HbA_{1c} values, impaired insulin secretion and moderate insulin resistance. The severe insulin-resistant diabetes (SIRD) is characterized by adiposity with high insulin resistance. These patients make up 11 – 17 % of all diabetic patients and have the highest risk for diabetic nephropathy and

coronary complications. The first of two mild variants, mild obesity-related diabetes (MOD) has its onset in young patients, is mostly related to overweight and makes up 18-23% all diabetic patients. While the second, mild age-related obesity diabetes (MARD), is developed in old age and makes up the biggest part of diabetic patients with 39-47 %. This stratification eases the process of prediction for late diabetic complications and improves their therapeutic treatment ⁹⁶.

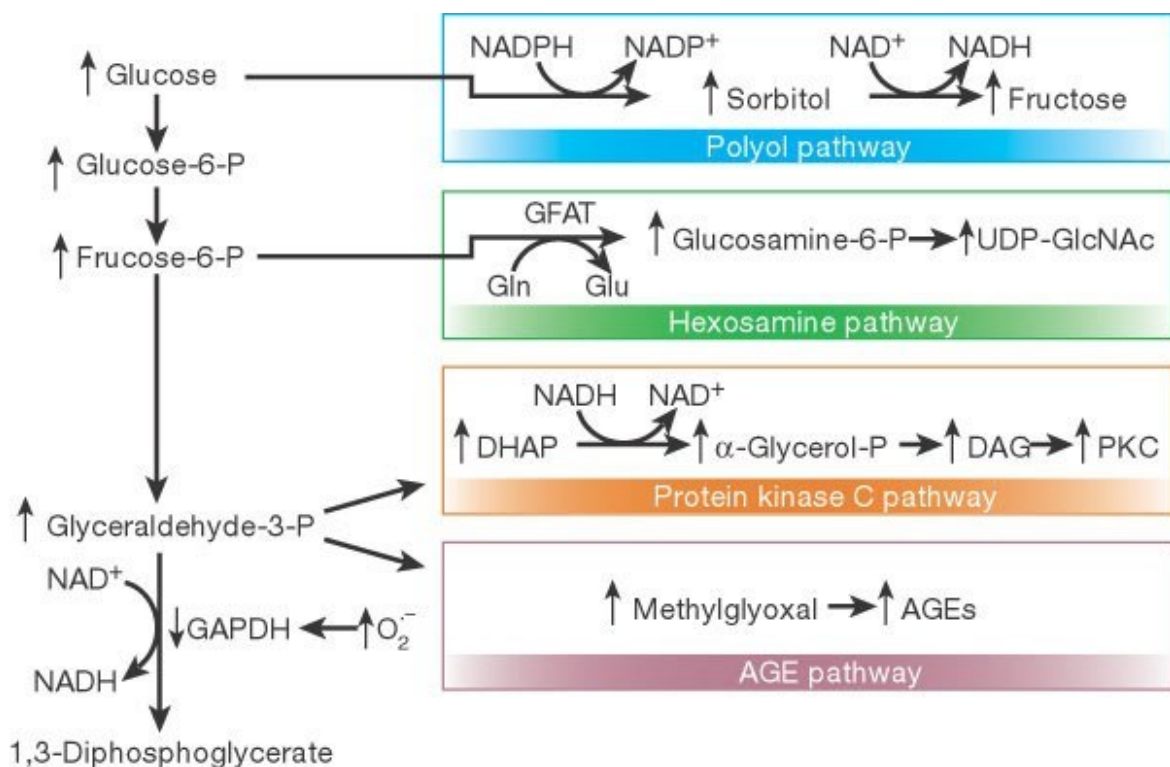


Figure 3 Potential mechanism by which hyperglycemia-induced mitochondrial superoxide overproduction activates four pathways of hyperglycemic damage. Picture Taken from Brownlee *et al* ⁹³.

Diabetic retinopathy as a complication has a varying prevalence of up to a third in patients suffering from diabetes. These high numbers establish diabetic retinopathy as one of the leading causes of vision loss in developed countries. Clinically, diabetic retinopathy is grouped into five phenotypic classifications based on anatomical features. Mild, moderate and severe non-proliferative diabetic retinopathy (NPDR) is accompanied by microaneurysms, microvascular lesions, and intraretinal hemorrhages, depending on the severity. In contrast, patients with proliferative diabetic retinopathy (PDR) show signs of vitreous hemorrhages but more importantly mild to

severe neovascularization in the optic disc or elsewhere. Macular edema are characterized by retinal thickening and hard exudates in the vicinity of the macula. The pathophysiological mechanisms underlying the development of any of these anatomic changes are not fully understood and matter of ongoing research. Currently it is believed, that chronic exposure of the retina to hyperglycemia and other risk factors will induce numerous detrimental biochemical pathways within retinal compartments, which on mid- and long-term damage the retinal neurovascular units and induce retinal dysfunction. This hypothesis is consistent with identified risk factors for DR, which include hyperglycemia, hypertension, dyslipidemia, and the duration of the diabetes. The biochemical cascades suggested to be involved are oxidative stress, AGEs, inflammation, protein kinase C activation and ultimately the vascular endothelial growth factor (VEGF) pathways. None of the current therapies for DR address all of these pathways. Therefore, several targets and respective therapeutic agents are awaiting clinical proof of concept studies to add new approaches to treat diabetic retinopathy 97–100 .

Unlike DR, other diabetic complications, especially DN is associated with worse morbidity and mortality. With its high prevalence and incidence in all civilizations, DN established itself in the past years as the leading cause for end-stage renal disease (ESRD) worldwide. Pathological characteristic of DN include glomerular basement membrane (GBM) thickening, mesangial proliferation and podocyte loss leading to glomerular dysfunction. In addition, endothelial cell dysfunction and impairment of the glomerular filtration barrier are observed. Similar to DR, the few established current therapeutic treatments of DN result in short-term amelioration only and are more symptomatic than really providing a cure. A clear reason for this insufficient therapy is, that they do not address the complexity of complications due to a lack of understanding of underlying pathogenic mechanisms. Because both DN and DR are part of microvascular complications, the involved biochemical processes that are suggested to be important for development and progression may overlap. While inhibiting an activated renal renin-angiotensin aldosterone system (RAAS) is an important treatment for renal disease, additionally covering oxidative stress through reactive oxygen and carbonyl species, as well as inflammatory processes may offer new promising opportunities 101–106 .

Finally, and analogous to DN and DR, diabetic neuropathy is also the leading form of neuropathy in developed countries. Strikingly, patients suffering from DM with diabetic neuropathy complications account for more hospitalizations than DN and DR combined as well as accounting for up to 75% of amputations not caused by trauma. Diabetic neuropathy is generally divided into two main forms, diabetic sensorimotor polyneuropathy (DSPN) which affects extremities and autonomic neuropathy which affects the digestive tract, the genitourinary system and the cardiovascular system. Especially the latter is associated not only with high morbidity but also with the two other microvascular complications DN and DR^{107–111}.

1.5 *Danio rerio* as a model organism

The zebrafish (*Danio rerio*) is a recently established new model organism for investigating diabetic complications. Its popularity is rising due to many advantages compared to other animal models like mice¹¹². However, there are also a few disadvantages which have to be considered when working with zebrafish. On one side, Zebrafish only shares about 70% of their genome with humans, therefore not every biochemical pathway is identical to molecular pathways in higher species¹¹³. In several cases, metabolic pathways are less complex in zebrafish, compared to higher vertebrata like humans. Some metabolic pathways are even not existing or totally divers, because zebrafish live in water and not on land¹¹⁴. Another challenge working with zebrafish is the lack of specific protocols and methods developed for them, not only in technical equipment and utensils, but also in existence of suitable research tools like antibodies and analytical assays, which are rarely implemented. However, when these challenges can be addressed, using zebrafish provides a lot of advantages over other vertebrata models. Husbandry of zebrafish is cheaper and more cost effective compared to commonly used animal models. It is also faster due to the high throughput and reproduction rate. While both mice and zebrafish take about three months to reach adulthood and become fertile, zebrafish can reproduce once a week and yield 200 – 300 eggs¹¹⁵. Furthermore, these fast-growing zebrafish eggs are easy to manipulate. High throughput screening, genetic modification – transient and permanent - and exposure to exogenous factors are now well-established experiments with zebrafish larvae. Additionally, the zebrafish reference genome is fully sequenced and published and many different methods for manipulation of gene expression have

been established especially for zebrafish. Transient knockdown is achieved in zebrafish eggs during the first stages of embryogenesis through splice or translation blocking by using morpholinos, methodologies which are incomparably more complex in mammals ¹¹⁶. Respectively, permanent knockout is realized by genome editing technologies clustered regularly interspaced short palindromic repeats (CRISPR) / CRISPR-associated systems (CAS) ¹¹⁷.

Most importantly, the role of zebrafish as a model for diabetes mellitus has been advanced significantly in the past decade, leading to new and insightful knowledge for diabetic complications. Since zebrafish are vertebrates, they have a closed circulatory system with arteries, veins and capillaries and all major organs affected by this metabolic disorder are present. Moreover, the glucose metabolism in zebrafish is highly preserved, the respective pathways and enzymes are similar in form and function to mammals, consequently zebrafish operate glycolysis and gluconeogenesis normally ¹¹⁴. They respond to insulin by decreasing blood glucose, store and catabolize glycogen and produce glucose during fasting periods ^{118–120}. Accordingly, many zebrafish models and methods have been implemented to research diabetes complications including gene knockout of *pdx1*, *glo1*, *aldh3a1* and *akr1a1a* ^{15,16,121–123}. While the *pdx1* knockout is a powerful tool to research hyperglycemia and its effects earlier on, the latter three, *glo1*, *aldh3a1* and *akr1a1a*, reveal the importance of various RCS like MG, 4-HNE and acrolein to glucose homeostasis and hyperglycemia. Specifically, research of these gene knockout zebrafish resulted in a confirmation of the novel hypothesis, that RCS are upstream factors to hyperglycemia. *glo1* knockout resulted in increased insulin resistance, *aldh3a1* knockout and 4-HNE caused hyperglycemia due to a disruption of the pancreas and *akr1a1a* knockout zebrafish developed impaired insulin receptor signaling.

Simultaneously, methods to research organ complications and vasculature has become more sophisticated. In general, development of organ systems like vasculature, pronephros or pancreas including their physiological processes can be imaged and followed over several days due to the fact, that zebrafish embryos develop externally and are transparent. In combination with transgenic fluorescent reporter gene lines this allows the unique approach for *in vivo* imaging using (confocal) fluorescent microscopy ^{112,114,124}. In addition, methods to observe late diabetic complications in adult zebrafish organs have also been improved. Diabetic retinopathy

research has been advanced via new methods for fluorescence microscopy and trypsin digestion with hemalum staining ^{122,125–127}. While methods for diabetic nephropathy have been advanced similarly using fluorescence microscopy and histology methods like electron microscopy. These improvements of procedures also made it possible to connect the aforementioned gene knockout of *glo1*, *aldh3a1* and *akr1a1a* and their respective RCS to late diabetic complications in eyes and kidneys of larvae and adult zebrafish, highlighting the importance of intact RCS detoxification and metabolism for Diabetes mellitus as potential gatekeepers.

In conclusion, the zebrafish model became more and more attractive in research areas, where common mammalian models have limitations in costs and efforts in time and resources needed. One example for such a research area would be diabetes and related microvascular complications ^{122,127}. Consequently, hyperglycemic fish and glucose-induced alteration of retina, kidney and neuronal tissues could already be observed ^{15,16,123,128,129}. This makes the research on diabetes and related complications in zebrafish highly interesting especially as an extension to typically used animal models.

1.6 Aim of the Thesis

Microvascular organ damages are usually associated with diabetes-related complications like hyperglycemia and accumulation of advanced glycation end products (AGEs) ^{54,130}. However, in recent investigations reactive metabolite detoxification enzymes like the glyoxalase system emerge as powerful regulator and upstream factors of metabolic and transcriptomic processes. In zebrafish, glyoxalase 1 (Glo1) implemented its importance in glucose homeostasis by regulating insulin resistance in permanent knockout animals ^{123,131}. Additionally, analysis of gene expression in *glo1* and *pdx1* knockout zebrafish introduced two further detoxification enzyme families in context of diabetes and diabetic complications: the aldehyde dehydrogenases (Aldh) and the aldo-keto reductases (Akr) ¹³². Subsequently, family members of these detoxification systems *aldh3a1* and *akr1a1a* revealed a signature of specifically elevated reactive carbonyl species which caused altered glucose metabolism, hyperglycemia and diabetic organ damage ^{15,16}.

Similarly to *aldh3a1* and *akr1a1a*, *aldh2.1* gene expression was increased in *glo1*^{-/-} knockout and *pdx1* knockdown zebrafish. Additionally, the human isoform Aldh2 is known to detoxify a variety of short-chained and aliphatic aldehydes including AA, 4-HNE, MDA and MG. Because these RCS have been identified as regulators for glucose metabolism and are causative to organ damages like microvascular complications up to onset of diabetic retinopathy, the aim of this study was to evaluate the detoxification ability of *aldh2.1 in vivo* as well as to identify a potential regulatory function of Aldh2.1 on glucose metabolism, organ physiology and diseases such as diabetes mellitus. Therefore, after generation and validation of the *aldh2.1*^{-/-} knockout zebrafish line, the first step was to identify the primary detoxification target of Aldh2.1 in zebrafish followed by a characterization of morphological changes in trunk vasculature, retinal vasculature and kidney as well as metabolome and transcriptome changes in *aldh2.1*^{-/-} zebrafish. Lastly, the mechanism and underlying cause for alterations was to be investigated. Thus, the working hypothesis was that loss of *aldh2.1* leads to dysfunction of RCS detoxification. The dysfunction then leads to accumulation of specific RCS, which in turn results in organ damages like microvascular complications and metabolic changes i.e. hyperglycemia in zebrafish.

2. Results

Parts of this chapter have been published in Wohlfart *et al* (2022) and have been originally written by myself:

“Accumulation of Acetaldehyde in *aldh2.1*^{-/-} Zebrafish Causes Increased Retinal Angiogenesis and Impaired Glucose Metabolism”

David Philipp Wohlfart, Bowen Lou, Chiara Simone Middel, Jakob Morgenstern, Thomas Fleming, Carsten Sticht, Ingrid Hausser, Rüdiger Hell, Hans-Peter Hammes, Julia Szendrödi, Peter Paul Nawroth, Jens Kroll

2.1 Generation of *aldh2.1* knockout zebrafish

This study aimed to find and evaluate the detoxification ability of Aldh2.1 for different RCS in zebrafish *in vivo* specifically in context with methylglyoxal detoxification and its detrimental long-term effects ^{46,49,50,130}. An additional objective was to identify a potential regulatory function of Aldh2.1 on glucose metabolism, organ physiology and diseases such as diabetes mellitus. Thus, *aldh2.1*^{-/-} gene knockout zebrafish lines were generated.

2.1.1 Amino acid sequence alignment

The first step in the investigation of Aldh2.1 enzyme and RCS detoxification was to identify similarities between human, mouse and zebrafish regarding their amino acid sequence and their respective active sites. An alignment of the Aldh2.1 amino acid sequence between zebrafish and human, and zebrafish and mouse revealed a 78.2 % similarity between zebrafish and human and likewise 77.4 % for zebrafish and mouse and an overall similarity of 83.1%. Amino acids important for the enzymatic activity are boxed in green (cysteine active site) red (glutamic active site). These amino acids in Aldh2 homologues are completely preserved across all three species (Figure 4).

Aldh2.1_ZF	MLRTVFSR--TFPQ--VFRISSCQHSTIPAPNVQPDVHYNKIFINNEWHDAVSKKTFPTI	56
Aldh2_Human	MLRA-- --AARFGPRLGRRLLSAAATQAVPAPNQOPEVFCNQIFINNEWHDAVSRKTFPTV	57
Aldh2_Mouse	MLRAALTTVRRGPRLS-RLLSAAATSAVPAPNHQPEVFCNQIFINNEWHDAVSRKTFPTV	59
	: *: :*. . .:* *.*. *:*****:*****:	
Aldh2.1_ZF	NPATAEVICHVAEGDKADVDAKAVKAARDAFKLGSPWRRMDASQRGLLLSRLADCIERDAA	116
Aldh2_Human	NPSTGEVICQVAEGDKEDVDKAVKAARAAAFQLGSPWRRMDASHRGRLLNRLADLIERDRT	117
Aldh2_Mouse	NPSTGEVICQVAEGNKEDVDKAVKAARAAAFQLGSPWRRMDASDRGRLLYRLADLIERDRT	119
	:*.*.*:****:* ***** **:******.* ** ** ** **	
Aldh2.1_ZF	YLAELETLDNGKPYTLSFCVDLPMVVKCLRYYAGWADKWEGKTIPIDGNFYCYTRHEPIG	176
Aldh2_Human	YLAAELETLDNGKPYVISYLVLDLMDVLKCLRYYAGWADKYHGKTIPIDGDFSYTRHEPVG	177
Aldh2_Mouse	YLAAELETLDNGKPYVISYLVLDLMDVLKCLRYYAGWADKYHGKTIPIDGDFSYTRHEPVG	179
	*** *****.:*: ** **:******:*****:.*.*****:.*.*****:*	
Aldh2.1_ZF	VCGQIIPWNFPLLMQALKLGPALATGNTVVMKVAEQTPLTALYIASLIKEVGFAPGVNI	236
Aldh2_Human	VCGQIIPWNFPLLMQAWKLGALATGNVVMKVAEQTPLTALYVANLIKEAGFPPGVNI	237
Aldh2_Mouse	VCGQIIPWNFPLLMQAWKLGALATGNVVMKVAEQTPLTALYVANLIKEAGFPPGVNI	239
	***** *****.* *****:.*.***.* ** **	
Aldh2.1_ZF	IPGFGPTAGAAIASHMDVDKVAFTGSTDVGHLIQQASSASNLKNSVLELGGKSPNIILSD	296
Aldh2_Human	VPGFGPTAGAAIASHEDVDKVAFTGSTEIGRVIQVAAGSSNLKRVTLLELGGKSPNIIMSD	297
Aldh2_Mouse	VPGFGPTAGAAIASHEGVDKVAFTGSTEVEGHLIQVAAGSSNLKRVTLLELGGKSPNIIMSD	299
	:*****.* *****:.*:.* ** *.:****.*:*****:***	
Aldh2.1_ZF	ANMEEAVEQAHSALFFNQGQCCAGSTRFVQESIYDEFVRSVERAKNRIVGDPFDLNT	356
Aldh2_Human	ADMDWAVEQAHFALFFNQGQCCAGSTRFVQEDIYDEFVRSVARAKSRVGNPFDKTE	357
Aldh2_Mouse	ADMDWAVEQAHFALFFNQGQCCAGSTRFVQENVYDEFVRSVARAKSRVGNPFDSTRTE	359
	*.: ***** *****:*****.* ***** **.*:.*:*** **	
Aldh2.1_ZF	QGPQVDEDEQFKKVLGYISSGKREGAKLMCGGAPAAERGYFIQPTVFGDVKDDMTIAREEI	416
Aldh2_Human	QGPQVDEDEQFKKILGYINTGKQEGAKLLCGGGIAADRGYFIQPTVFGDVQDGMTIAKEEI	417
Aldh2_Mouse	QGPQVDEDEQFKKILGYIKSQQEGAKLLCGGGAAADRGYFIQPTVFGDVKDGMTIAKEEI	419
	***** ***:***.:*:.*:*****:***.* **:******:.*.***:***	
Aldh2.1_ZF	FGPVMQILKFKSLEEVIERANDSKYGLAGAVFTQDIDKANYISHGLRAGTVWINCYNVFG	476
Aldh2_Human	FGPVMQILKFKTIEEVVGRANNSTYGLAAAVFTKDLKANYLSQALQAGTVWNCYDVFG	477
Aldh2_Mouse	FGPVMQILKFKTIEEVVGRANDSKYGLAAAVFTKDLKANYLSQALQAGTVWINCYDVFG	479
	*****:.*:***.* **:*.*.***.* *****:.*:****.*:***:***	
Aldh2.1_ZF	VQAPFGGYKASGIGRELGEYGLDIYTEVKTVTIKVPQKNS	516
Aldh2_Human	AQSPFGGYKMSGSGRELGEYGLQAYTEVKTVTIKVPQKNS	517
Aldh2_Mouse	AQSPFGGYKMSGSGRELGEYGLQAYTEVKTVTIKVPQKNS	519
	.*:***** ** *****: *****:*****	

Figure 4 Amino acid alignment of Aldh2 across zebrafish, human and mouse. The amino acid sequence displays a ~80% similarity between zebrafish (first line), human (second line) and mouse (third line); glutamic acid active site (red) and cysteine active site (green) are indicated and are completely preserved in each species.

2.1.2 Utilizing CRISPR/Cas9 technology for generation of *aldh2.1*^{-/-} knockout mutants

Before this study, rarely any *aldh* knockout zebrafish lines had been generated. However, there were a variety of studies indicating their involvement with either MG

and RCS or more complex disease backgrounds like diabetes mellitus^{2,3,14,46,123,133–136}. Thus, a gene knockout for *aldh2.1* by using CRISPR/Cas9 technology was established in zebrafish in collaboration with Dr. Bowen Lou. First, Dr. Bowen Lou synthesized CRISPR-guideRNA (gRNA) targeting exon 3 of *aldh2.1* and injected together with Cas9 mRNA into one-cell stage *Tg(fli1:EGPF)* zebrafish embryos. The resulting adults – termed F0 generation – were analyzed on germline transmission using Sanger sequencing. Afterwards I crossed the positive F0 mosaic mutants with the *Tg(fli1:EGPF)* wild type zebrafish line and identified and selected different heterozygous mutations of the respective genes again via Sanger-sequencing. For *aldh2.1*, a reading frameshift mutation due to a deletion of five nucleotides, resulting in an early stop-codon, was selected (Figure 5).

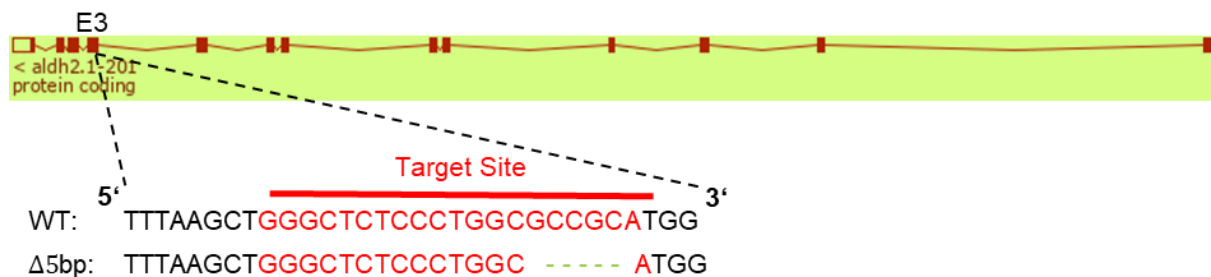


Figure 5 Generation of *aldh2.1* knockout zebrafish using CRISPR-Cas9 technology. *aldh2.1*-CRISPR-target site (red line) was designed in exon 3 and CRISPR/Cas9-induced deletion of 5 nucleotides (green) was selected for mutant generation. The genotypes were analyzed using sanger sequencing chromatograms of PCR-amplified *aldh2.1* region containing the target sites.

2.1.3 Distribution of *aldh2.1* in zebrafish organs

In zebrafish, the gene expression pattern for most *aldh* variants has not been determined before. Therefore RT-qPCR analysis was utilized to investigate the mRNA levels of *aldh2.1* in various zebrafish organs (Figure 6). Highest *aldh2.1* gene expression was found in liver (15 %), followed by brain (6.8 %) and eyes (5 %) when compared to the expression of the house keeping gene b2m. Overall, these results confirmed that the expression of *aldh2.1* in zebrafish is comparable to other vertebrates like human and mouse.

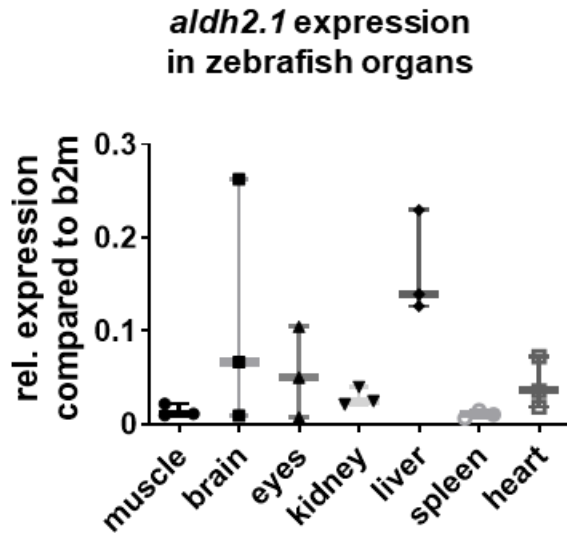


Figure 6 Distribution of *aldh* genes in different zebrafish organs. *aldh2.1* mRNA expression in wild type zebrafish was highest in liver (15%) followed by brain (6.8%) and eyes (5%). Expression of genes was determined using RT-qPCR and normalized to b2m, n = 3, one organ per sample.

2.1.4 Validation for loss of Aldh2.1 protein via Western Blot

In order to demonstrate that the genetic knockout also resulted in a loss of function or loss of protein. Western Blot using specific anti-antibodies were performed. For this purpose, antibodies against the zebrafish isoform was generated with the support of GPCF Unit Antibodies, DKFZ Heidelberg, Germany. Peptide sequences of Aldh2.1, was generated and subsequently injected into guinea pigs for immunization. The produced antibodies for Aldh2.1 were functional and visualized the protein in denatured liver, muscle and brain lysates in a western blot (Figure 7), proving that *aldh2.1*^{-/-} zebrafish mutants have no Aldh2.1 protein.

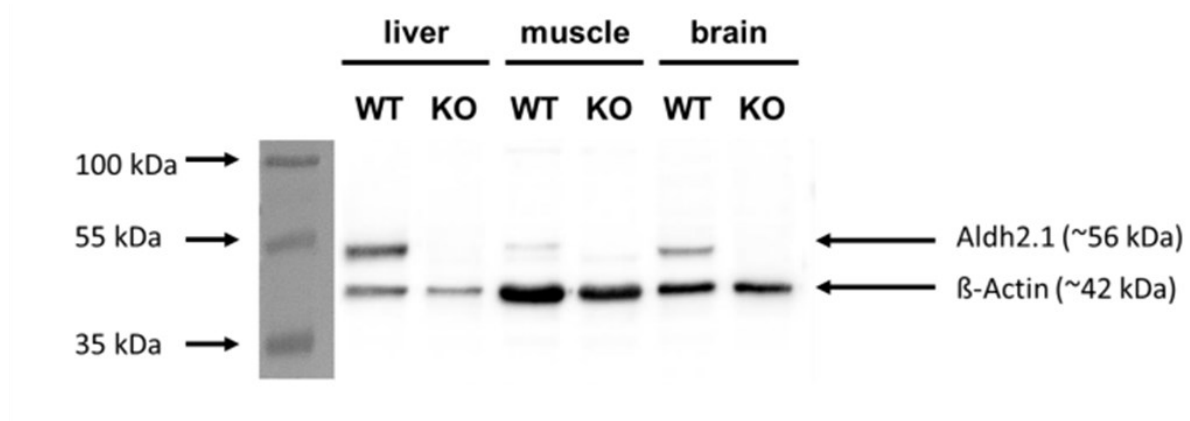


Figure 7 Validation for loss of Aldh2.1 protein via Westernblot was successful. Representative Western blot for Aldh2.1 and Actin proteins in adult liver confirmed the loss of Aldh2.1 in *aldh2.1*^{-/-} mutants.

2.2 Phenotypic characterization of *aldh2.1*^{-/-} zebrafish

The investigation of *aldh2.1*^{-/-} zebrafish started with a phenotypic characterization of larvae and adult animals. The gross morphology of *aldh2.1*^{-/-} larvae at 5 day-post-fertilization (dpf) was not altered compared to *aldh2.1*^{+/+} littermates; however, in a few *aldh2.1*^{-/-} embryos / larvae the livers appeared enlarged (Figure 8A). Intriguingly, the survival rate of adult *aldh2.1*^{-/-} animals deviated from the estimated Mendelian distribution and were significantly lower than expected. Out of 282 adult zebrafish from *aldh2.1*^{+/+} matings, 99 (35.1 %) were *aldh2.1*^{+/+}, 122 (43.2 %) were *aldh2.1*^{+/+} and only 61 (21.7 %) had the Δ 5 bp deletion *aldh2.1*^{-/-} (Figure 8B), these results suggested that permanent loss of Aldh2.1 negatively affects the survival of zebrafish.

Aldh enzyme activity measurements were performed to confirm that the *aldh2.1* knockout resulted in reduction of total Aldh enzyme activity. With the following RCS as substrates a significant reduction of total Aldh enzyme activity in lysates from *aldh2.1*^{-/-} larvae could be observed compared to the respective *aldh2.1*^{+/+} lysates. The Aldh enzyme activity was reduced by 67% for acetaldehyde (Figure 8D), by 31% for methylglyoxal (Figure 8C), by 23% for 4-hydroxynonenal (Figure 8E) and by 16% for malondialdehyde (Figure 8F) as substrates. Total Aldh enzyme activity with acrolein (Figure 8G) as substrate was also reduced by 28 %, but was not statistically significant within the replicate numbers included. On the other hand, total enzyme activity of Glo1 (Figure 8H) and Akr (Figure 8I) with MG as a substrate did not change in *aldh2.1*^{-/-} zebrafish. These results not only further confirmed the successful generation and loss of function of *aldh2.1*^{-/-} mutants, but also identified a capacity of the Aldh2.1 enzyme in

the detoxification of several RCS in zebrafish besides its known function in ethanol and acetaldehyde detoxification, indicating the involvement in various metabolic disorders through the respective RCS: MG, 4-HNE and ACR and their complications.

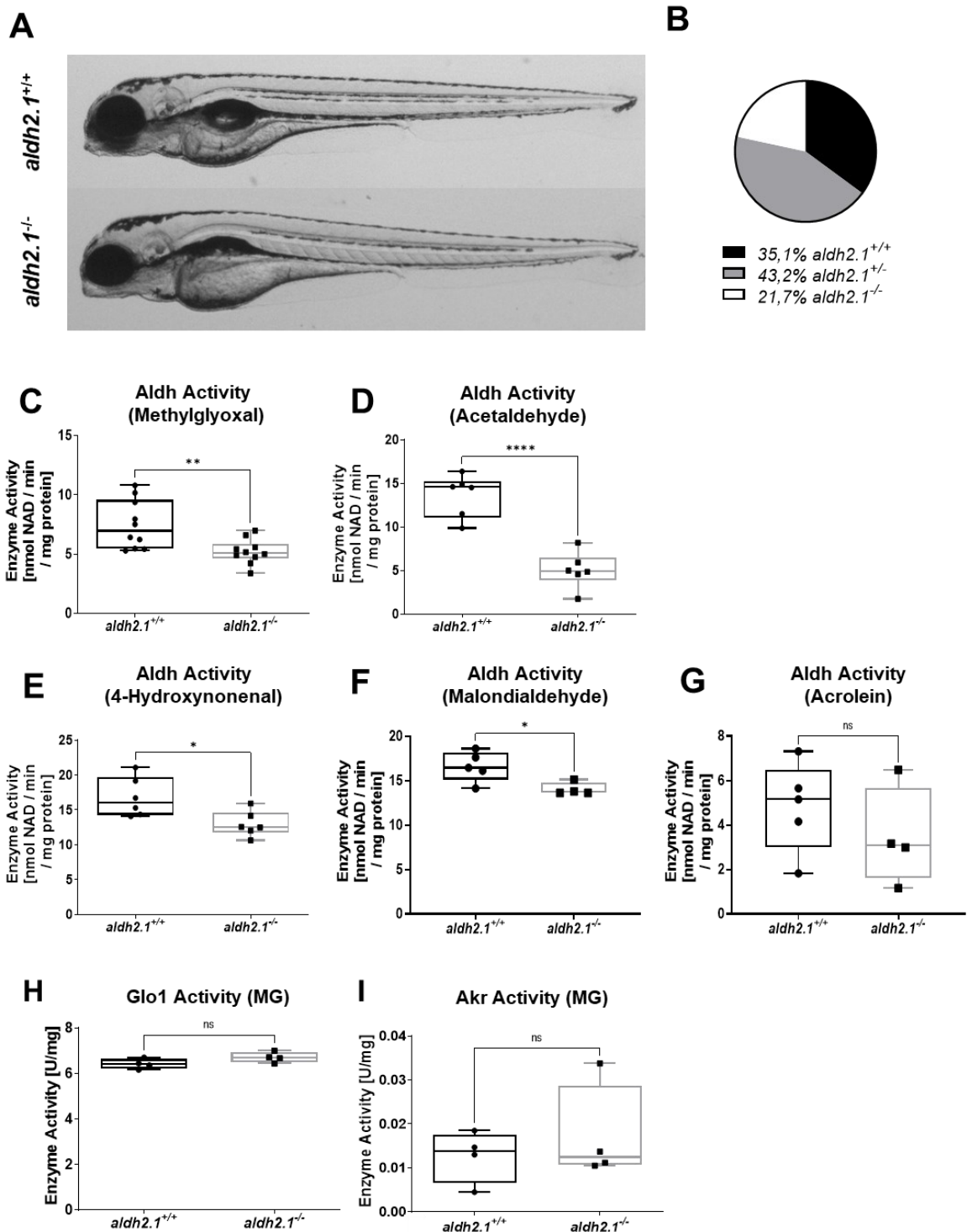


Figure 8 *aldh2.1*^{-/-} zebrafish larvae exhibit significantly lowered RCS detoxification and survivability. **A** Images of *aldh2.1*^{+/+} and *aldh2.1*^{-/-} larvae showed no difference at 5 dpf. Black scale bar: 500 μ m. **B** Adult *aldh2.1*^{+/+} and *aldh2.1*^{-/-} animals are underrepresented in *aldh2.1*^{+/+} matings according to the Mendelian distribution. *aldh2.1*^{+/+} = 99 (35.1%), *aldh2.1*^{+/-} = 122 (43.2%) and *aldh2.1*^{-/-} = 61 (21.7%). Statistical analysis was done via chi-square test. **C-G** *aldh2.1*^{-/-} mutants displayed decreased Aldh enzyme activity with MG (**C**) as substrate, n = 10; AA (**D**) as substrate, n = 6; 4-HNE

(E) as substrate, n = 6 and MDA (F) as substrate, n = 4-5, but unaltered Aldh enzyme activity with ACR (G) as substrate, n = 4-5. Enzyme activity was quantified via spectrophotometry of NAD metabolic rate (nmol NAD \ min \ mg protein) in zebrafish lysates. H Quantification of total Glo1 enzyme activity showed no difference between *aldh2.1^{+/+}* and *aldh2.1^{-/-}* zebrafish lysates, n = 4. Glo1 enzyme activity was determined spectro-photometrically monitoring the change in absorbance at 235 nm caused by the formation of S D lactoylglutathione. I Quantification of total Akr enzyme activity showed no difference between *aldh2.1^{+/+}* and *aldh2.1^{-/-}* zebrafish lysates, n = 4. Total Akr enzyme activity was measured spectro-photometrically via the rate of reduction of NADPH at 340 nm Zebrafish lysates were produced from clutches of 50 larvae. Statistical analysis was done via Student's t-test, ns = not significant, *p < 0.05, **p < 0.01, ***p < 0.001, ****p < 0.0001. Enzyme activity data was produced jointly with Dr. Jakob Morgenstern from the Department of Internal Medicine I and Clinical Chemistry, Heidelberg University Hospital, Heidelberg 69120, Germany.

2.3 Zebrafish vasculature and kidney morphology

2.3.1 Loss of *aldh2.1* led to increased angiogenesis in the trunk vasculature and retinal vasculature of zebrafish larvae and adults

In previous studies, it could be shown that elevated exogenous and endogenous reactive metabolites damaged the microvasculature via an impaired glucose metabolism in zebrafish^{15,16,123}. Because the results of the enzyme activity assays for total Aldh showed that a broader range of RCS are detoxified by Aldh2.1, a set of microvasculature experiments utilizing fluorescence and confocal microscopy was performed to investigate whether the loss of Aldh2.1 potentially affected vascular development and subsequently organ health.

The trunk vasculature of *aldh2.1^{-/-}* zebrafish larvae at 120 hpf (Figure 9) revealed a slight, but statistically significant increase of hyperbranches between intersomitic vessels (ISM) compared to *aldh2.1^{+/+}* zebrafish. Furthermore, this increase in angiogenesis in *aldh2.1^{-/-}* zebrafish was also exhibited during an investigation of preretinal hyaloid vessels in 120 hpf larvae. Here an increase in branch points in the hyaloid vasculature of *aldh2.1^{-/-}* zebrafish larvae compared to *aldh2.1^{+/+}* larvae was identified (Figure 10A, C).

To assess whether these changes in the vasculature of trunk and hyaloid vessels were a transient phenomenon only found in larvae but not in adult zebrafish, a visualization and quantification of retinae of 12 mpf zebrafish was performed additionally. The quantification of vasculature in adult retinae confirmed the preceding results of an increased angiogenesis and instated the effect as a permanent phenotype. The *aldh2.1^{-/-}* adults had an increase of branch points in the high-density areas of the retinae vasculature compared to *aldh2.1^{+/+}* adults (Figure 10B, D).

To finalize the investigation of retinal vasculature a digest preparation of adult retinae using trypsin and subsequent Mayers's hematoxylin staining was performed (Figure

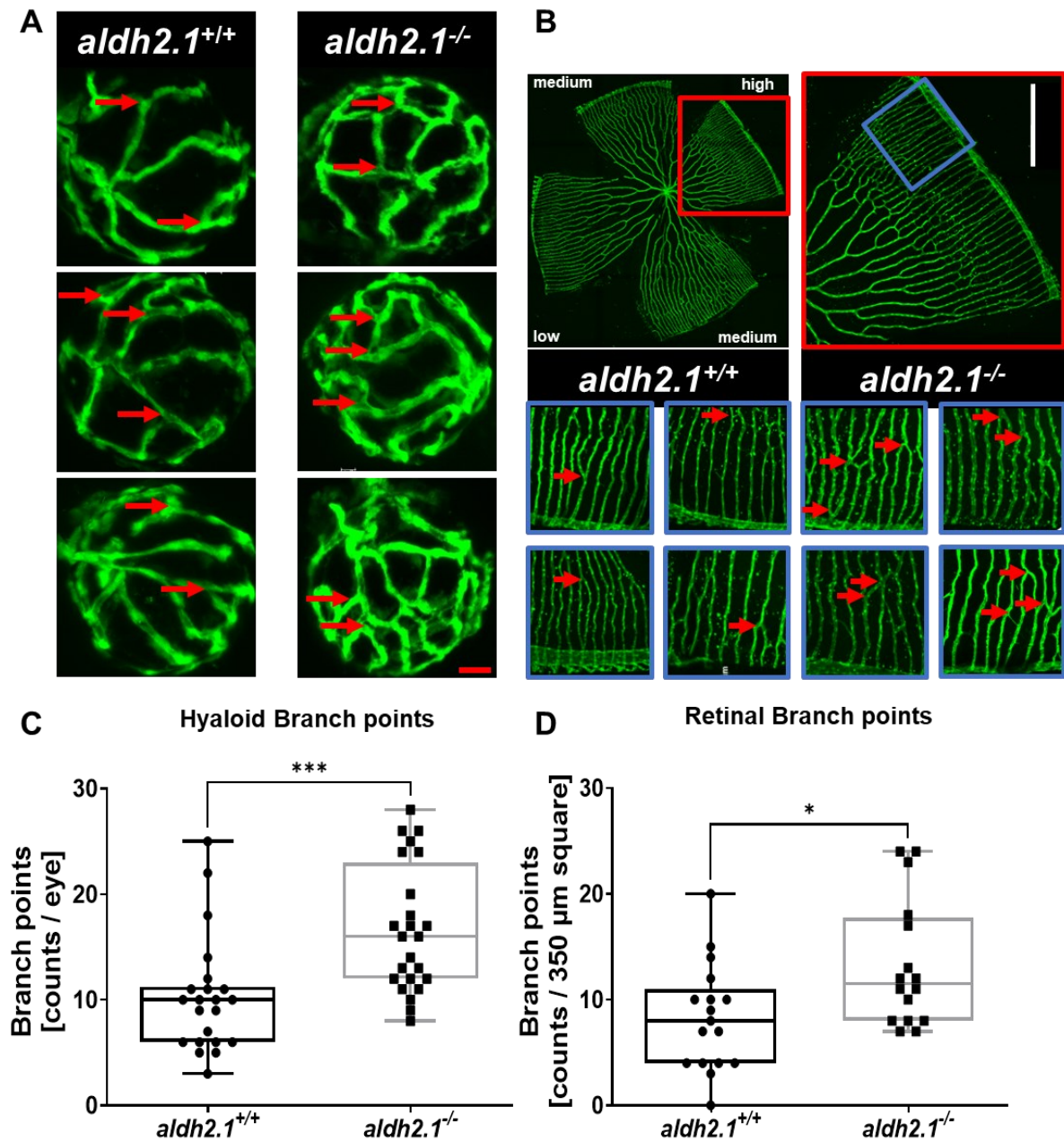


Figure 10 Loss of *aldh2.1* led to increased angiogenesis in the retinal vasculature of zebrafish larvae and adults. **A** Representative confocal images of hyaloid vasculature in zebrafish larvae at 120 hpf displayed increased branching. Red scale bar: 20 μ m, red arrows: branch points as counted for quantification. **B** Representative confocal images of adult zebrafish retinae showed increased angiogenesis. White Scale Bar: 350 μ m, red rectangle: high-density subdivision, blue rectangle 350 μ m square, red arrows: branch points as counted for quantification. **C** Quantification of larval hyaloid vasculature showed increased numbers of branch points in *aldh2.1*^{-/-} mutants, n = 22-24 eyes per group. **D** Quantification of retinal vasculature showed increased numbers of branch points in *aldh2.1*^{-/-} adults, n = 16-17 350 μ m squares per group, statistical analysis was done via Student's - test, *p < 0.05, ***p < 0.001.

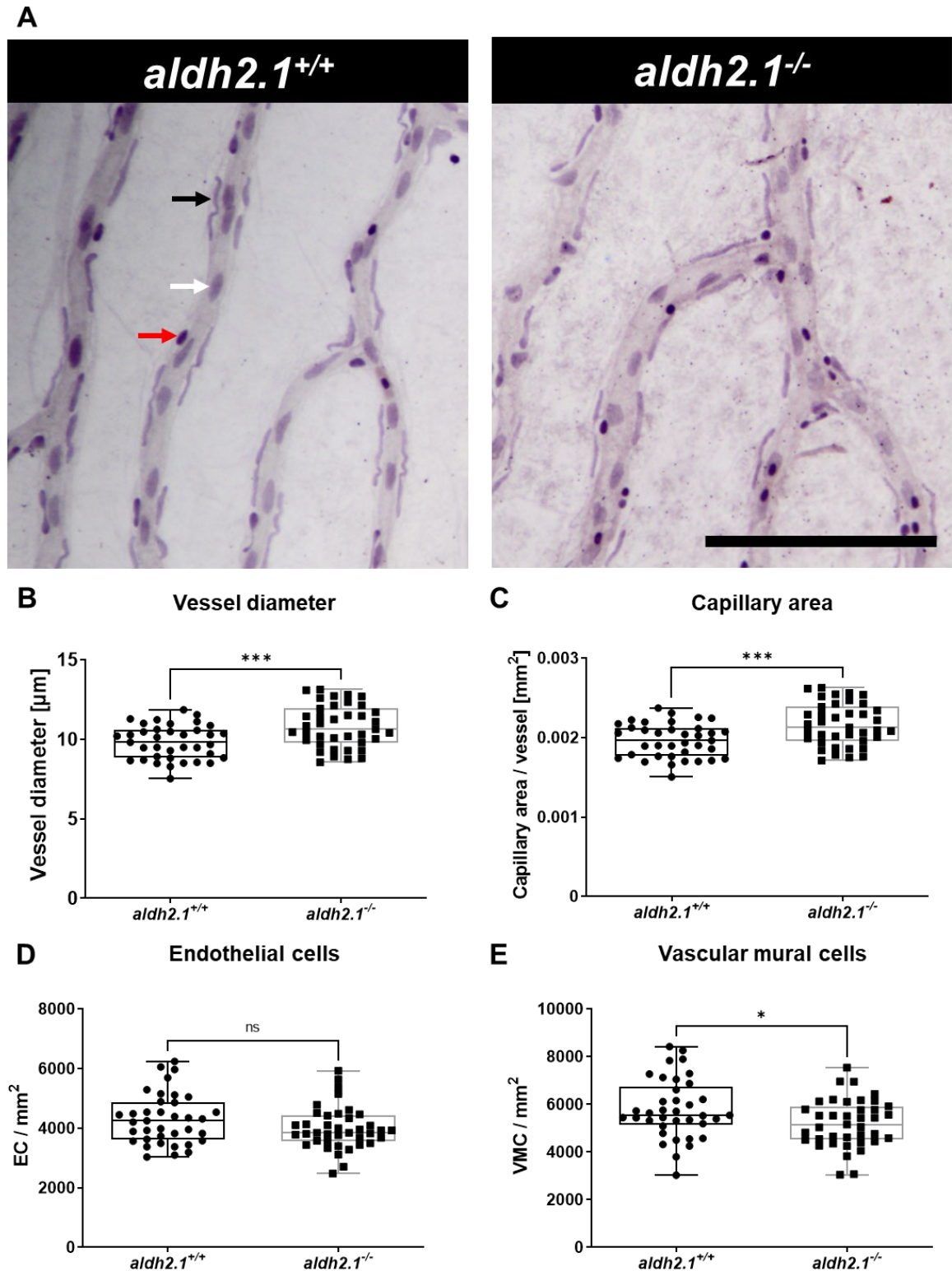


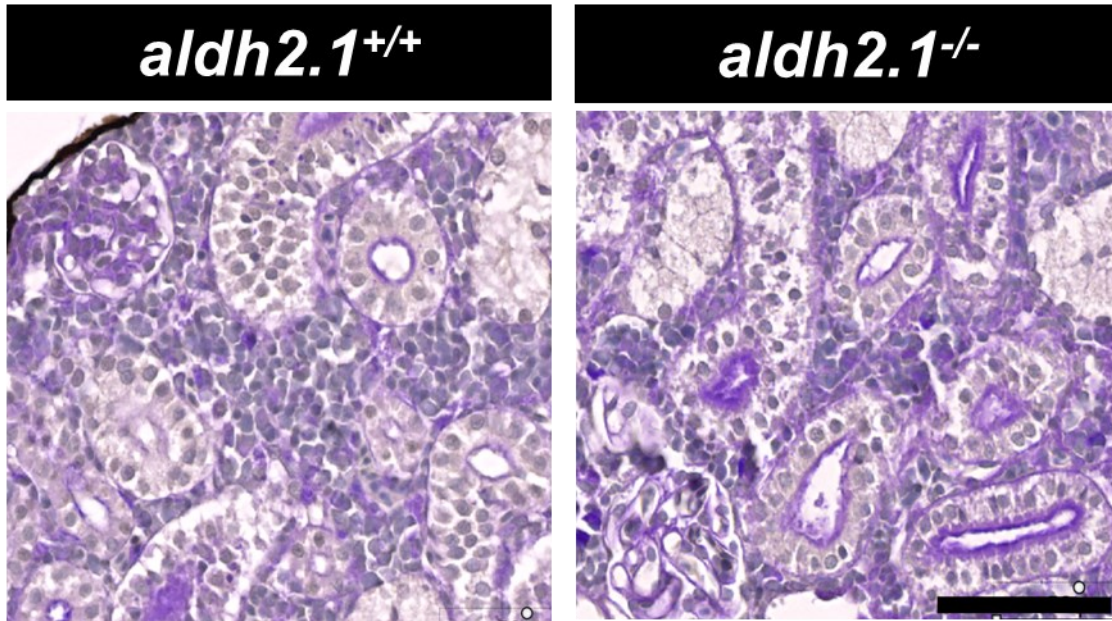
Figure 11 Thickening of blood vessels and reduction of vascular mural cell coverage in *aldh2.1^{-/-}* retinæ. A Representative light microscopy images of zebrafish retinæ prepared with trypsin digestion and hematoxylin staining. Red Arrow: erythrocyte, black arrow: pericyte, white arrow: endothelial cell, black scale bar: 100 μm . **B-E** Quantification of vascular parameters. **B** Increased vessel diameter, **C** Increased capillary area, **D** Unaltered endothelial cell count and **E** Reduced vascular mural cell count. $n = 37-39$. Statistical analysis was done via Student's t-test, ns = not significant, $*p < 0.05$, $***p < 0.001$. Data was produced jointly with Chiara Simone Middel from the Department of Vascular Biology and Tumor Angiogenesis, European Center for Angioscience (ECAS), Medical Faculty Mannheim, Heidelberg University, Mannheim 68167, Germany

2.3.2 Kidney morphology was not altered in *aldh2.1*^{-/-} zebrafish

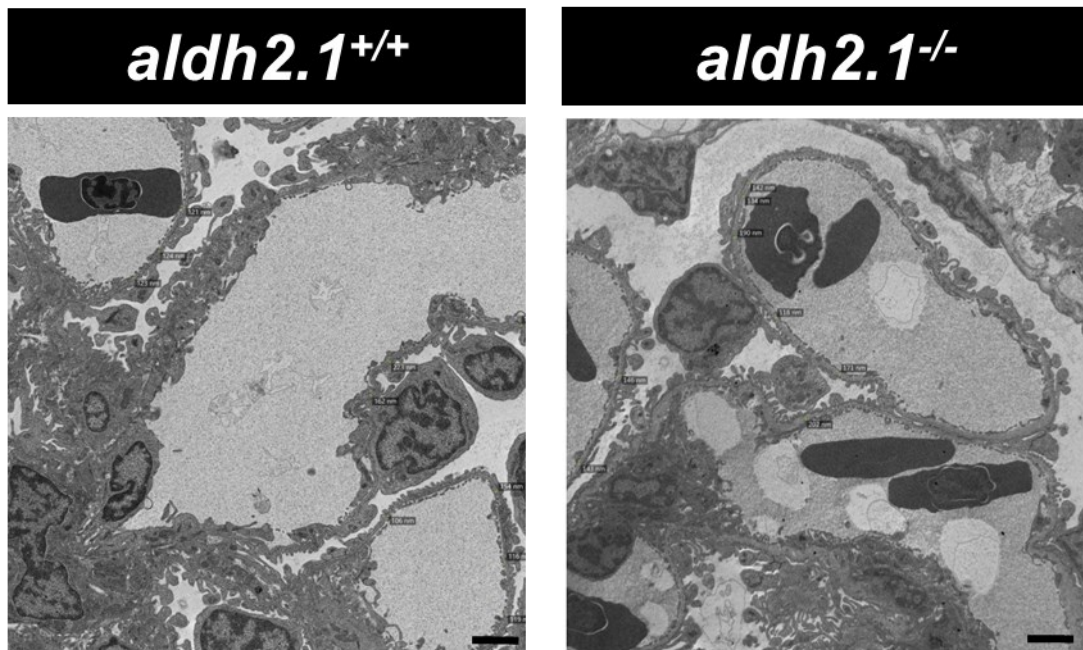
In addition to the vasculature of retinae, zebrafish kidneys were also analyzed via Periodic Acid-Schiff (PAS) staining (Figure 12A) and electron microscopy (EM) (Figure 12B). However, there was no change of the kidney morphology between *aldh2.1*^{+/+} and *aldh2.1*^{-/-} in either visualization. Neither the Mesangium nor the Bowman-space was expanded as seen in the PAS stainings resulting in normal sized glomeruli of *aldh2.1*^{-/-} compared to *aldh2.1*^{+/+} (Figure 12C). The close-up visualization of glomeruli also did not reveal any pathogenic changes. The mesangium of *aldh2.1*^{-/-} was normally proliferated, the semipermeable layer of the capillary was not damaged and lastly, the podocytes were not deformed as seen in diabetic nephropathy (Figure 13D).

In conclusion *aldh2.1* knockout did not cause pathological phenotypes in zebrafish kidneys.

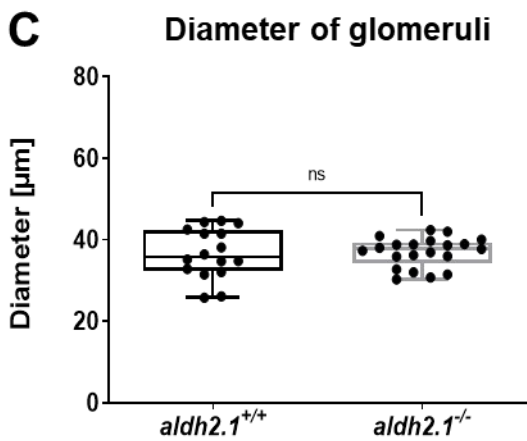
A



B



C



D

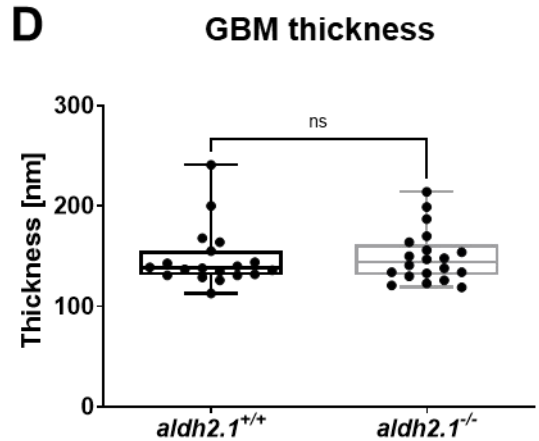


Figure 12 Kidney morphology is unaltered in adult *aldh2.1*^{-/-} zebrafish. **A** Representative Periodic acid-Schiff (PAS) staining showed no alterations in gross morphology of *aldh2.1*^{-/-} kidneys. Black scale bar: 50 μ m. **B** Representative electron microscopy images showed no alterations in *aldh2.1*^{-/-} glomeruli. Black scale bar: 2 μ m. **C** Quantification of glomerular diameter in zebrafish kidneys showed no changes between *aldh2.1*^{+/+} and *aldh2.1*^{-/-} zebrafish. **D** Quantification of GBM thickness in *aldh2.1*^{-/-} zebrafish glomeruli showed no changes. Statistical analysis was done via Student's t-test, ns = not significant. EM data was produced jointly with the Institute of Pathology IPH, EM Lab, Heidelberg University Hospital, Heidelberg 69120, Germany.

2.4 Metabolome analysis

2.4.1 *aldh2.1*^{-/-} zebrafish displayed an elevation of endogenous AA and decreased postprandial blood glucose

Previous studies on diabetic organ complications with the Aldh3a1 enzyme revealed an impaired RCS detoxification as the cause for the increases in angiogenesis of retinal blood vessels¹⁵. Whether the impaired detoxification activity (Figure 8C-E) in *aldh2.1*^{-/-} mutants translated into a similar elevation of endogenous reactive metabolites or impairment of glucose metabolism remained unknown. Thus, a series of measurements for glucose and reactive metabolites was conducted in 96 hpf old larvae and adult zebrafish organs. In larvae, no changes in whole-body glucose (Figure 13A), MG (Figure 13B), 4-HNE (Figure 13D) and ACR (Figure 13E) were found. However, an elevation of the reactive metabolite AA could be identified (Figure 13C), which was 4.2-fold higher in *aldh2.1*^{-/-} larvae than in *aldh2.1*^{+/+}. Additionally, a metabolome screening for thiols and adenosines (Figure 14), amino acids (Figure 15), fatty acids (Figure 16), the tricarboxylic acid cycle (Figure 17) and primary metabolites (Figure 19) was performed in 96 hpf *aldh2.1*^{+/+} and *aldh2.1*^{-/-} zebrafish larvae. No consistent, significant changes between wildtype and genetic knockout could be detected in these metabolite categories. In adult zebrafish, AA concentration was increased 4.3-fold in liver of fasted *aldh2.1*^{-/-} zebrafish (Figure 13H). Yet, fasting and postprandial MG (Figure 13G, J) were unchanged. Interestingly, while fasting blood glucose levels were unchanged in *aldh2.1*^{-/-} adults (Figure 13F), postprandial measurements revealed reduced levels of blood glucose (Figure 13I).

In summary, the data implies acetaldehyde as the primary RCS of Aldh2.1's detoxification activity in zebrafish. Even though *aldh2.1* knockout has an impact on total Aldh enzyme activity for a wide spectrum of RCS (Figure 1G-K), only AA accumulated in vivo, while leaving the remaining the metabolome mostly unaltered.

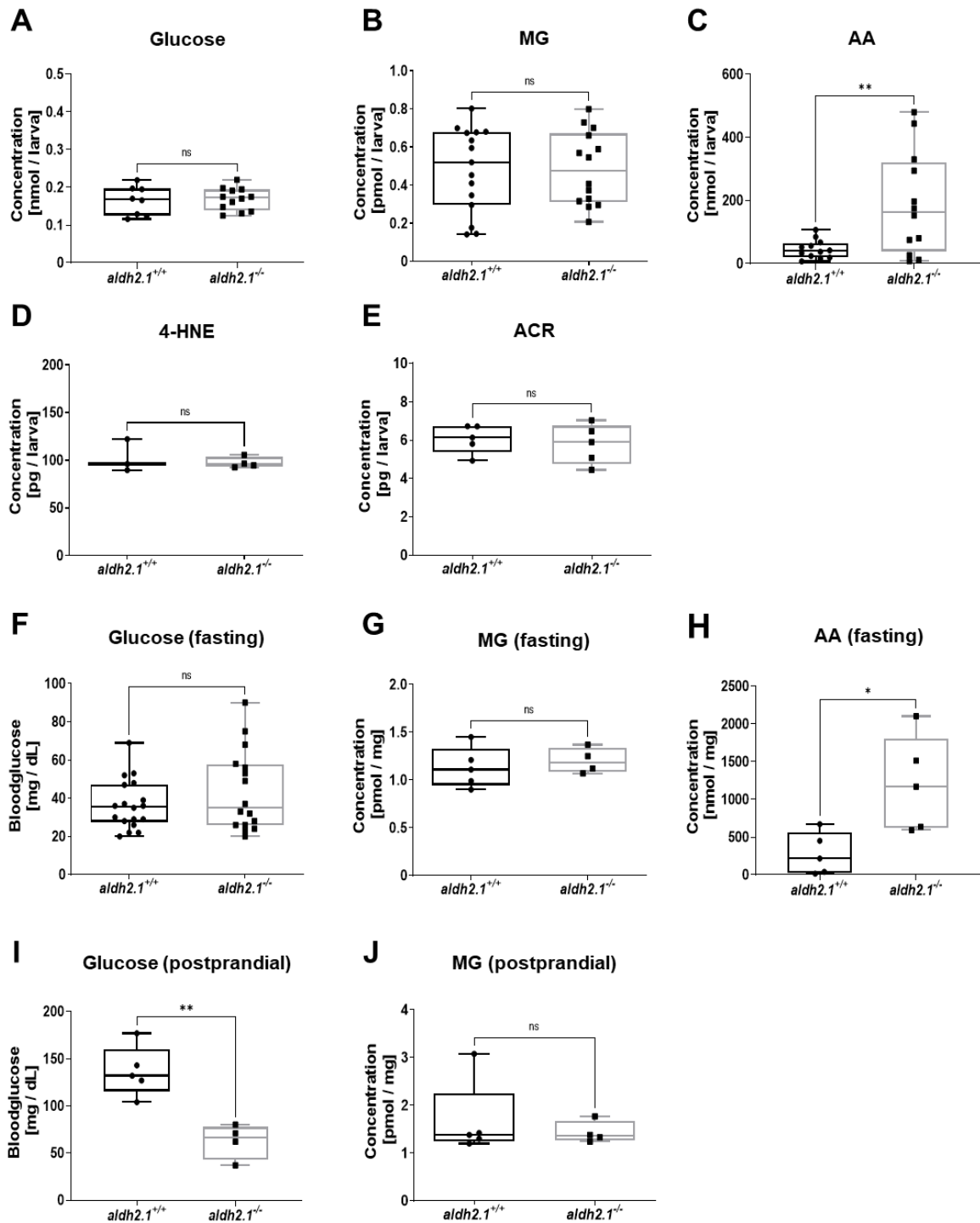


Figure 13 *aldh2.1^{-/-}* mutants displayed an elevation of endogenous AA and lowered postprandial blood glucose. **A-E** Determination of glucose and endogenous reactive metabolites in 96 hpf old zebrafish larvae displayed significantly increased AA (**C**) in *aldh2.1^{-/-}* mutants, but no changes for glucose (**A**), MG (**B**), 4-HNE (**D**) or ACR (**E**), $n = 3-15$ clutches, 50 larvae per clutch. Measurements were done via ELISA (**A,D,E**) or GC-MS / LC-MSMS (**B,C**). **F-J** Glucose and endogenous reactive metabolites in adult zebrafish displayed significantly increased AA (**H**) in *aldh2.1^{-/-}* liver and decreased postprandial blood glucose (**I**). MG (**G,J**) in fasted and postprandial zebrafish eyes as well as fasting blood glucose (**F**) stayed unaltered in *aldh2.1^{-/-}* zebrafish, $n = 4-18$. Measurement of blood glucose was performed with a glucometer. MG and AA were measured via GC-MS and LC-MSMS respectively. Statistical analysis was done via Student's t-test, ns = not significant, * $p < 0.05$, ** $p < 0.01$. MG and AA measurements were produced jointly with Dr. Thomas Fleming and Dr. Jakob Morgenstern from the Department of Internal Medicine I and Clinical Chemistry, Heidelberg University Hospital, Heidelberg 69120, Germany.

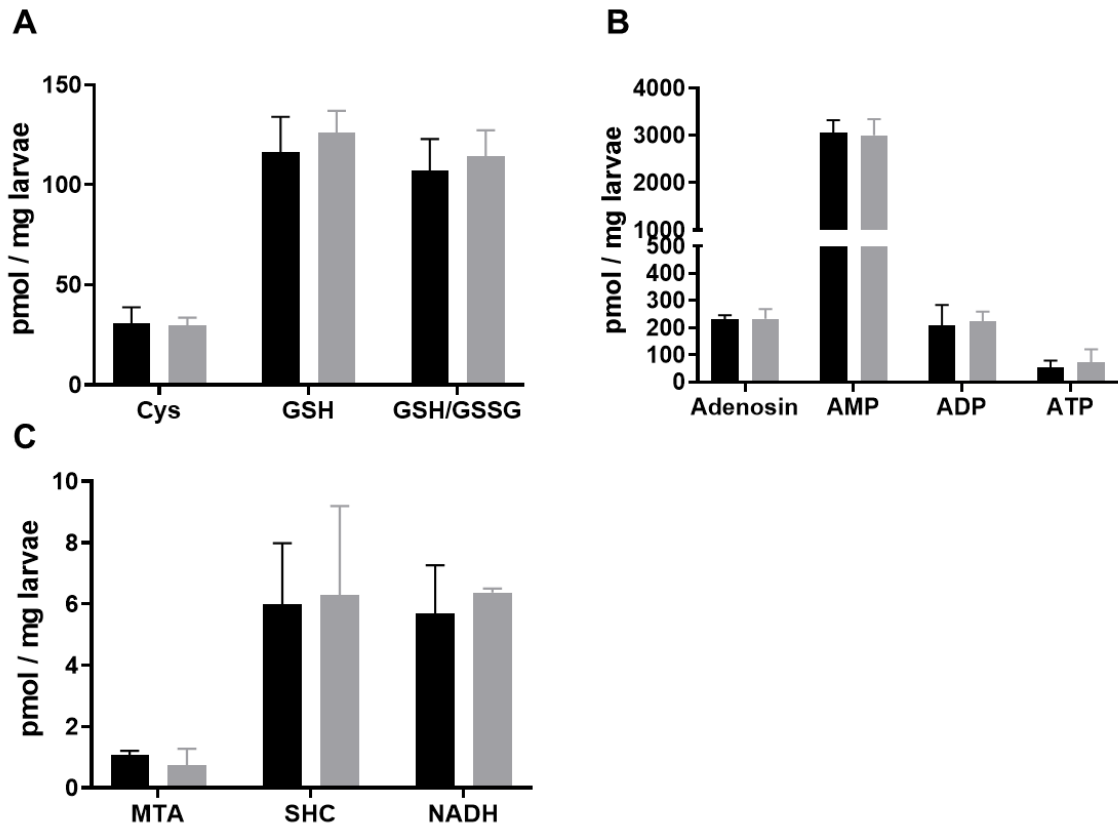


Figure 14 Thiols and adenosines are unaltered in *aldh2.1*^{-/-} zebrafish larvae. **A** Determination of Cysteine, GSH and GSH/GSSG concentration showed no difference between *aldh2.1*^{+/+} and *aldh2.1*^{-/-} zebrafish larvae. **B** Adenosine, AMP, ADP and ATP are unaltered between *aldh2.1*^{+/+} and *aldh2.1*^{-/-} zebrafish larvae. **C** MTA, SHC and NADH are not changed between *aldh2.1*^{+/+} and *aldh2.1*^{-/-} zebrafish larvae. Adenosine compounds and thiols were measured in 96 hpf old zebrafish larvae lysates with n = 3 utilizing ultra-performance liquid chromatography with fluorescence detection (UPLC-FLR). Statistical analysis was done via Student's t-test, ns = not significant. Cys: cysteine, GSH: glutathione, GSSG: glutathione disulfide, MTA: methylthioadenosine, SHC: S-adenosylhomocystein, NAD: Nicotinamide adenine dinucleotide, NADH: Nicotinamide adenine dinucleotide hydride, AMP: Adenosine monophosphate, ADP: Adenosine diphosphate, ATP: Adenosine triphosphate. Data was produced jointly with the Metabolomics Core Technology Platform, Centre for Organismal Studies, Heidelberg University.

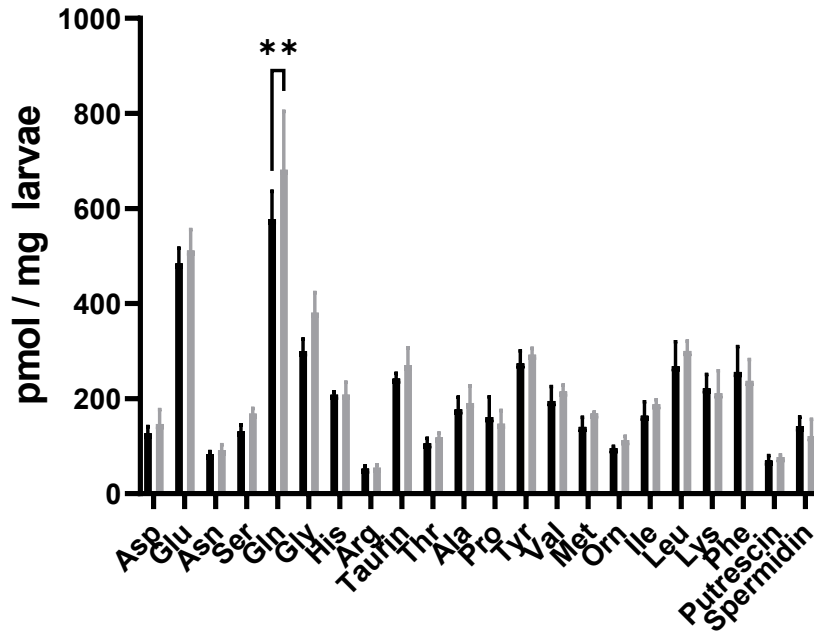


Figure 15 Amino acids concentration are mostly unaltered in *aldh2.1*^{-/-} zebrafish larvae. Amino acids showed no alteration between genotypes except for glutamine in zebrafish larvae. Amino acids were measured in 96 hpf old zebrafish larvae lysates with n = 3 utilizing ultra-performance liquid chromatography with fluorescence detection (UPLC-FLR). Statistical analysis was done via Student's t-test, ns = not significant, *p < 0.05, **p < 0.01. Data was produced jointly with the Metabolomics Core Technology Platform, Centre for Organismal Studies, Heidelberg University.

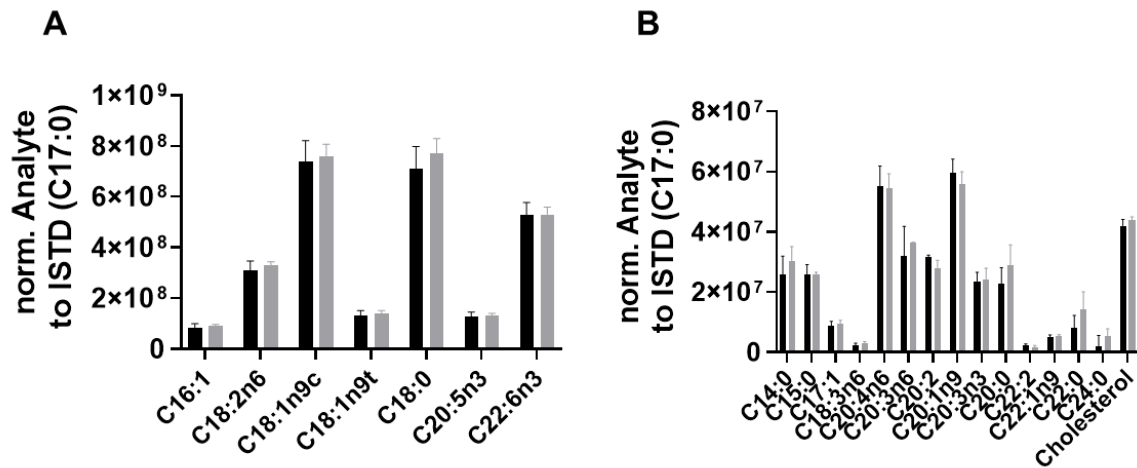


Figure 16 Fatty acids are unaltered *aldh2.1*^{-/-} zebrafish larvae. Fatty acids were measured in 96 hpf old zebrafish larvae lysates with n = 3 utilizing ultra-performance liquid chromatography with fluorescence detection (UPLC-FLR). Statistical analysis was done via Student's t-test, ns = not significant, *p < 0.05, **p < 0.01. Data was produced jointly with the Metabolomics Core Technology Platform, Centre for Organismal Studies, Heidelberg University.

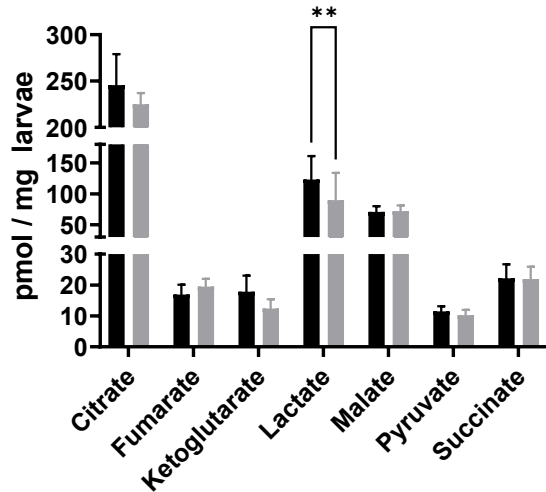


Figure 17 TCA cycle intermediates are mostly unaltered in *aldh2.1*^{-/-} zebrafish larvae. TCA cycle metabolites showed no alteration between genotypes except for a slight significant decrease of lactate in *aldh2.1*^{-/-} zebrafish larvae. Metabolites were determined using GC / MS analysis in zebrafish larvae lysates at 96 hpf, n = 8-9. Statistical analysis was done via Student's t-test, ns = not significant, *p < 0.05, **p < 0.01. Data was produced jointly with the Metabolomics Core Technology Platform, Centre for Organismal Studies, Heidelberg University.

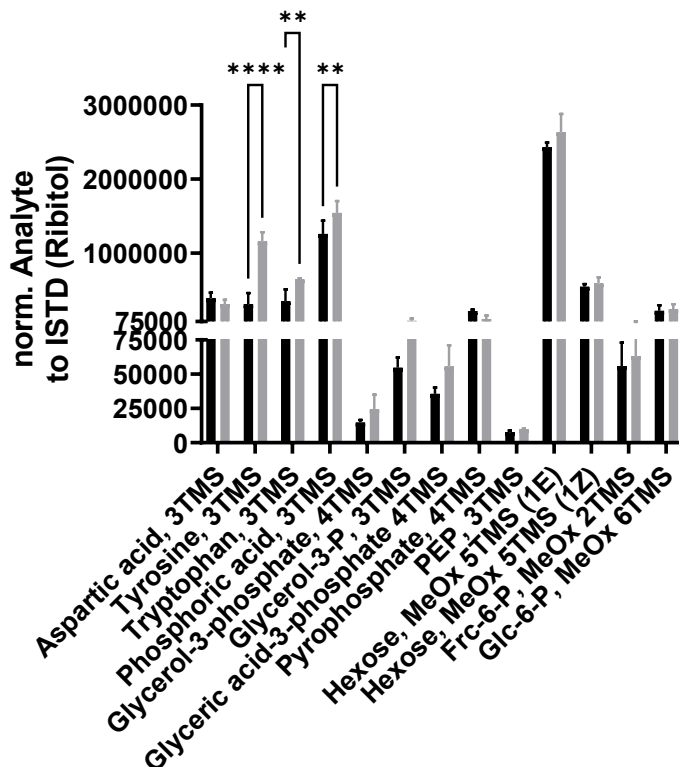


Figure 18 Primary Metabolites are mostly unaltered in *aldh2.1*^{-/-} zebrafish larvae. Semi-targeted GC-MS revealed a mostly unaltered primary metabolite screening with the exception of Tyrosine, Tryptophan and Phosphoric acid. Primary metabolites were measured in 96 hpf old zebrafish larvae lysates with n = 3 utilizing semi-targeted GC-MS. Statistical analysis was done via Student's t-test, ns = not significant, *p < 0.05, **p < 0.01, ****p < 0.0001. Data was produced jointly with the Metabolomics Core Technology Platform, Centre for Organismal Studies, Heidelberg University.

2.5 Transcriptomics

2.5.1 *aldh2.1*^{-/-} mutants exhibited aggravated stress-signaling and an impairment of glycolysis

In order to investigate the underlying mechanism causing the vascular alterations in *aldh2.1*^{-/-} mutants and to address why *aldh2.1*^{-/-} mutants developed a decrease in postprandial blood glucose, RNA-sequencing and expression analysis in zebrafish larvae with an emphasis on pathways analysis was performed. The Kyoto-encyclopedia of gene and genomes (KEGG) pathway analysis revealed several pathways significantly regulated by the *aldh2.1* knockout, including upregulated stress signaling and a downregulated energy metabolism (Figure 19A). Apoptosis, ferroptosis and cell senescence were among those pathways with a normalized enrichment score (NES) between 1.5 – 1.7. More importantly, overexpression of VEGF pathway components with a NES of 1.46 (Figure 19B) and Mitogen-Activated-Protein-Kinases (MAPK) with a NES of 1.58 (Figure 19C) were identified, providing a first hint on the mechanism in *aldh2.1*^{-/-} blood vessels (Figure 9, Figure 10 and Figure 11). On the other side, the downregulated energy metabolism pathways included fatty acid degradation and amino acid metabolism, but also pyruvate metabolism and glycolysis / gluconeogenesis were identified (Figure 19D). Gene set enrichment analysis (GSEA) for glycolysis / gluconeogenesis revealed a NES of -1.82 and -2.02 for pyruvate metabolism (Figure 19E) respectively, suggesting that *aldh2.1* is indeed involved in glucose metabolism, even though the metabolomics screening could not identify the location.

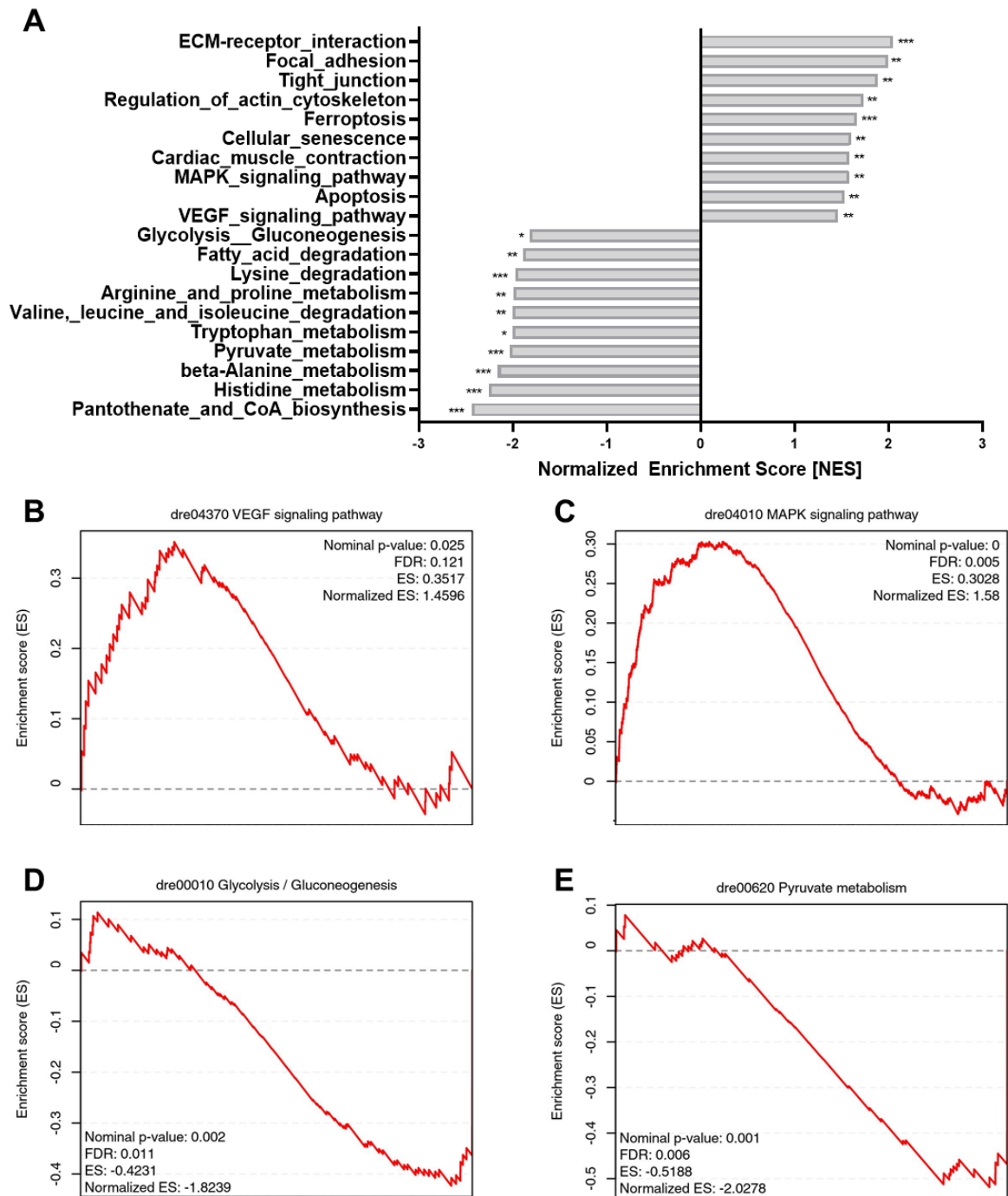


Figure 19 *aldh2.1*^{-/-} mutants exhibited aggravated stress-signaling and an impairment of glycolysis and gluconeogenesis. **A** Bar diagram for highest, significantly increased or decreased pathways in a Kyoto-encyclopedia of gene and genomes (KEGG) pathways analysis in *aldh2.1*^{-/-} larvae. **B-E** Gene set enrichment analysis (GSEA) plots for VEGF (**B**), MAPK (**C**), glycolysis / gluconeogenesis (**D**), pyruvate metabolism (**E**) pathways. RNA-seq was done with mRNA in 120 hpf zebrafish larvae, quantification via normalized enrichment score (NES), n = 5 clutches, 50 larvae per clutch, ns = not significant, *p < 0.05, **p < 0.01, ***p < 0.001. Data was produced jointly with Beijing Genomic Institution, www.bgi.com, BGI and Carsten Sticht from the NGS Core Facility, Medical Faculty Mannheim, Heidelberg University, Mannheim 68167, Germany.

2.5.2 Angiogenesis factors are unchanged in *aldh2.1*^{-/-} mutants

Based on the RNA-seq data (Figure 19), we explored expression of selected genes within the identified pathways which may explain the underlying mechanism of increased retinal angiogenesis and impaired glucose homeostasis in *aldh2.1*^{-/-} zebrafish¹³⁷. Interestingly, the gene expression of common angiogenesis marker, such as *fgfr2*, *vegfr2* and *notch1a* was not changed between *aldh2.1*^{-/-} and *aldh2.1*^{+/+} larvae (Figure 20), indicating that different pathways are involved in the underlying mechanism. Statistical analysis was done via Student's t-test, ns = not significant, *p < 0.05, **p < 0.01.

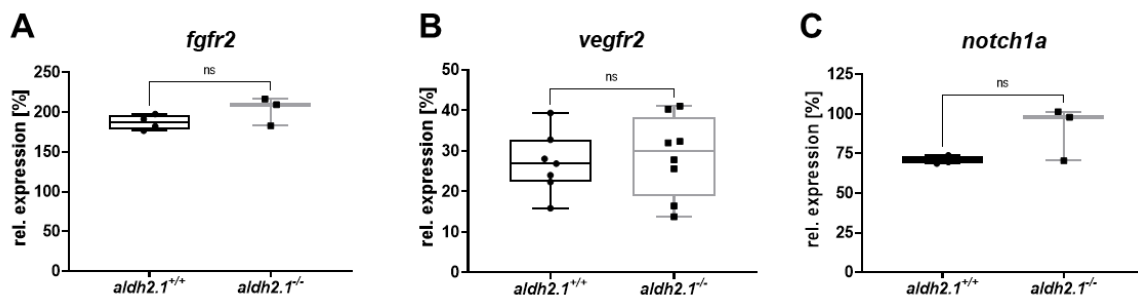


Figure 20 *aldh2.1*^{-/-} larvae displayed unaltered angiogenesis related factors. Quantification of gene expression of angiogenesis related factors: *fgfr2* (E), *vegfr2* (F) and *notch1a* (G) showed no change in *aldh2.1*^{-/-} larvae compared to *aldh2.1*^{+/+} larvae. Expression was quantified via RT-qPCR with 96 hpf zebrafish larvae and normalized to *arnt2*, n = 5-8 clutches, 50 larvae per clutch.

2.5.3 Inhibition of p38 MAPK and activation of JNK gene expression in *aldh2.1*^{-/-} mutants

Subsequently members of the MAPK family were investigated more in detail, since ERK1, JNK and p38 MAPK are all known for their abilities to alter endothelial cell activation and angiogenesis^{138–144}. Quantitative PCR results revealed a two-fold increase in expression for *mapk8b*, also known as JNK1 (Figure 21C). *mapk11-14*, known as p38 MAPKs, were downregulated up to two-fold (Figure 21D, E, F). Expression of other ERK / MAPK genes such as *mapk3* (ERK1, Figure 21A) and *mapk7* (ERK5, Figure 21B) was not changed. Therefore, the confirmation of gene expression by quantitative PCR is in accordance with RNA-seq data and raised the further hypothesis, that increased angiogenesis in retinal vessels of *aldh2.1*^{-/-} mutants is due to altered JNK and p38 MAPK signaling in zebrafish larvae. In order to provide further evidences for this mechanism, zebrafish were treated with specific pharmacological inhibitors of MAPK signaling.

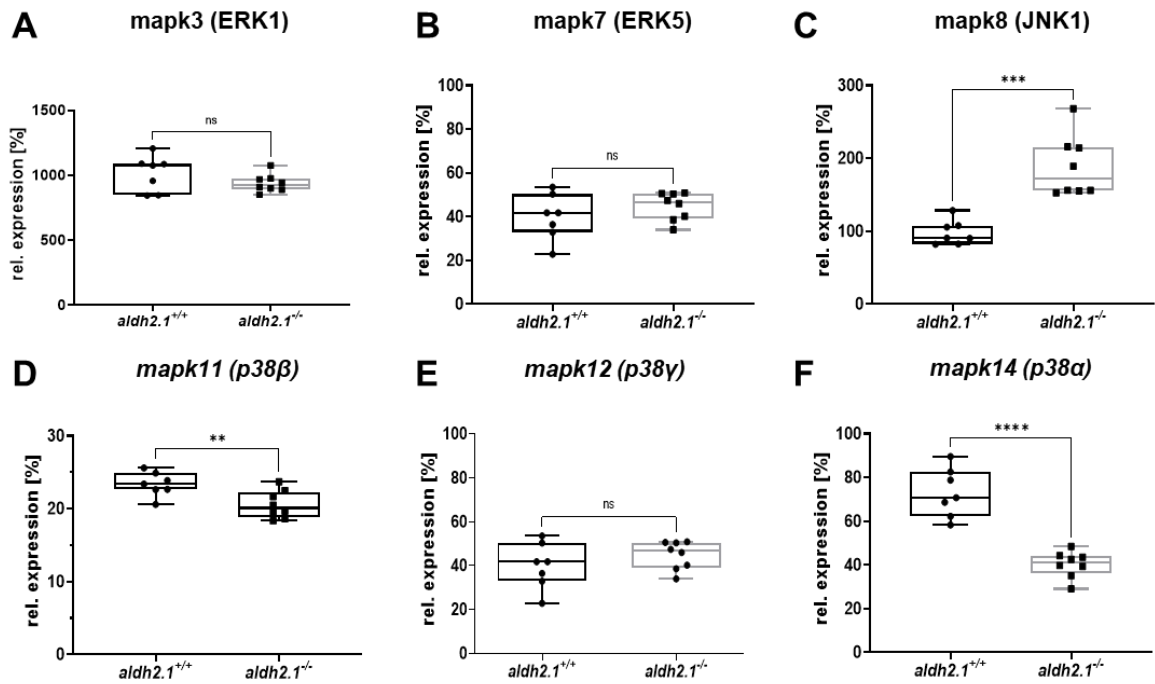


Figure 21 *aldh2.1*^{-/-} zebrafish larvae revealed an imbalance of MAPK gene expression. **A-F** Expression of MAPK family members. ERK1 (**A**), ERK5 (**B**) and p38 γ (**E**) were unaltered in *aldh2.1*^{-/-} larvae. JNK1 (**C**) is significantly upregulated; p38 α (**F**) and p38 β (**D**) were significantly downregulated in *aldh2.1*^{-/-} animals. Gene expression was quantified via RT-qPCR with 96 hpf zebrafish larvae and normalized to *arnt2*, n = 5-8 clutches, 50 larvae per clutch. Statistical analysis was done via Student's t-test, ns = not significant, *p < 0.05, **p < 0.01, ***p < 0.001, ****p < 0.0001.

2.5.4 Inhibition of glucose-6-phosphatase and glucokinase gene expression in *aldh2.1*^{-/-} mutants

Simultaneously to stress signaling in zebrafish larvae, we explored the cause for lowered postprandial blood glucose concentrations in adult *aldh2.1*^{-/-} mutants by measuring the expression of selected genes important in glycolysis, gluconeogenesis and glucose internalization. Quantitative PCR identified a four-fold decrease of glucose-6-phosphatase (*g6pc*) expression (Figure 22A) in zebrafish larvae, which is a key regulating point in gluconeogenesis converting glucose-6-phosphate into glucose^{145–147}. Intriguingly, several years ago a single report has indeed hypothesized that AA suppresses glucose-6-phosphatase expression¹⁴⁸ and our data now shows this regulation for the first time in vivo since AA is highly increased in the *aldh2.1*^{-/-} mutant (Figure 13C,H). Correspondingly, phosphoenolpyruvate decarboxylase expression (*pepck*) (Figure 22C), another key regulator of gluconeogenesis¹⁴⁹, was downregulated 1.7-fold. Moreover a three-fold decrease of glucokinase (*gck*) (Figure 22F), which mediates the first step in glycolysis by phosphorylation of glucose to glucose-6-phosphate, was observed in *aldh2.1*^{-/-} mutants¹⁵⁰ and glucose-6-phosphate

dehydrogenase (*g6pd*) (Figure 22B), which is stimulated by its substrate – glucose-6-phosphate, was also downregulated 1.3-fold. Finally, insulin (*ins*) expression as well as *pdx1* expression in *aldh2.1*^{-/-} mutant larvae was similarly significantly downregulated (Figure 22G, H). Together, this data suggests a new mechanism of impaired glucose metabolism in which an increase of endogenous AA, which inhibits glucokinase and glucose-6-phosphatase expression, causes a delayed reaction to glucose intake up to hypoglycemia-like metabolomics behavior.

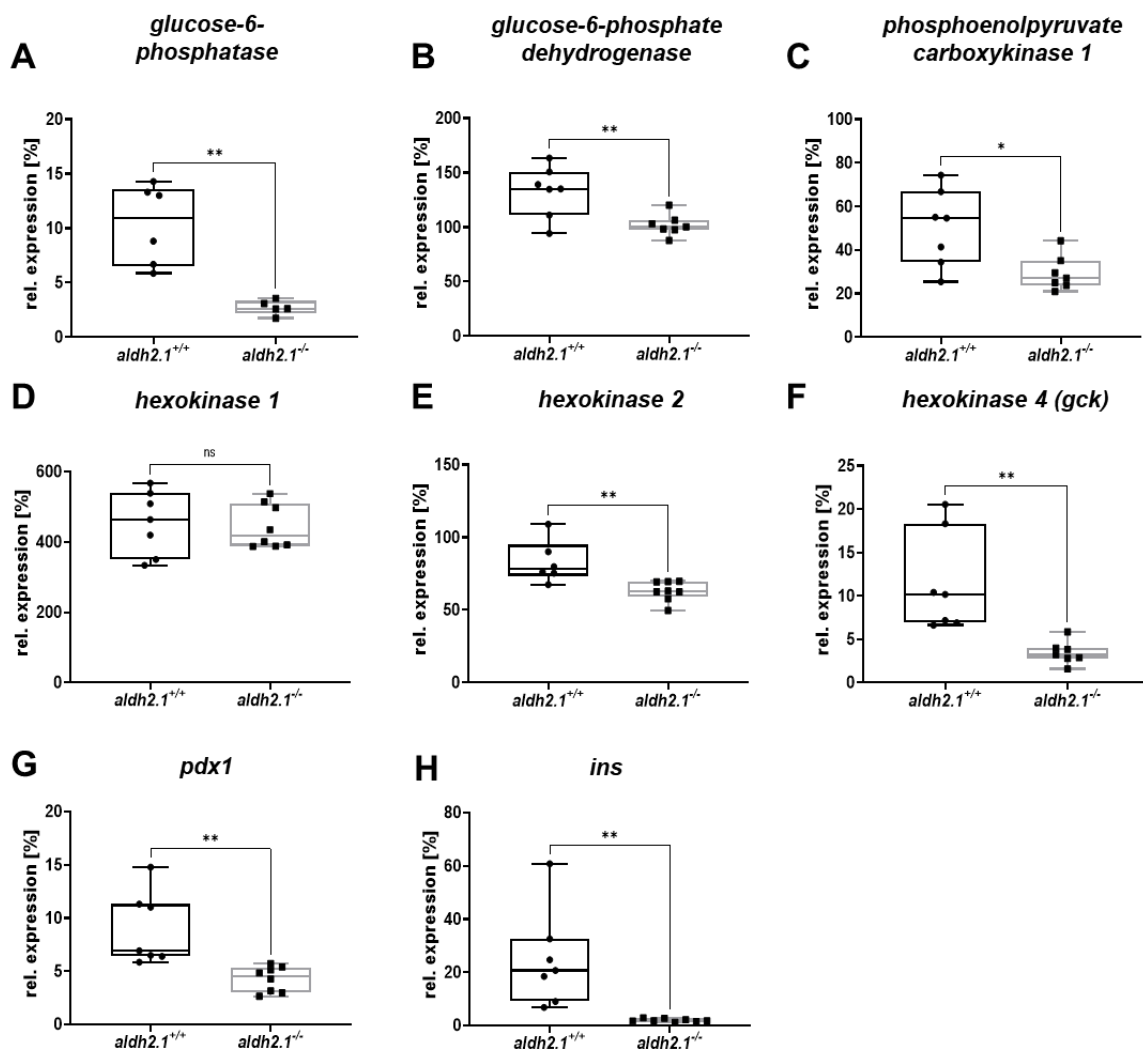


Figure 22 Inhibition of glucose-6-phosphatase / glucokinase and *ins* / *pdx1* gene expression in *aldh2.1*^{-/-} mutants. A-F Expression of key regulatory genes of glycolysis and gluconeogenesis. Strongest down regulation in *aldh2.1*^{-/-} larvae was observed for *g6pc* (A) and *gck* (F). *g6pd* (B), *pck1* (C) and *hk2* (E) were also significantly down regulated. *hk1* (D) gene expression was unchanged. Additionally, *pdx1* (G) and *ins* (H) gene expression was strongly reduced in *aldh2.1*^{-/-} larvae. Gene expression was quantified via RT-qPCR with 96 hpf zebrafish larvae and normalized to *arnt2*, n = 5-8 clutches, 50 larvae per clutch. Statistical analysis was done via Student's t-test, ns = not significant, * p < 0.05, ** p < 0.01, *** p < 0.001, **** p < 0.0001.

2.6 Pharmacological interference studies

2.6.1 Exogenous AA caused angiogenic alterations in hyaloid vasculature, impairment of glucose metabolism and alteration of MAPK signaling

Analysis of *aldh2.1*^{-/-} mutants identified microvascular complications in retinal vessels, but it remained unclear whether these alterations were directly induced by the *aldh2.1*^{-/-} mutant or indirectly by increased endogenous AA and subsequently impaired glucose metabolism and stress signaling. In order to address this question, I incubated wild type zebrafish larvae with AA and repeated prior analyses of retinal hyaloid structures and RT-qPCR for selected gene expressions. Toxicity tests for AA in zebrafish larvae were done beforehand and revealed a tolerance of up to 500 μM AA (Figure 23A, B). Analysis of hyaloid vessels in 120hpf old larvae incubated with 50μM AA (Figure 24) showed that exogenous AA can mimic the microvascular complications as seen in *aldh2.1*^{-/-} mutants, but does not amplify it. Between *aldh2.1*^{+/+} zebrafish larvae with and without AA incubation there is a 1.36-fold increase of branch points. Branch points between *aldh2.1*^{+/+} without exogenous acetaldehyde and *aldh2.1*^{-/-} with and without AA treatment were also increased by a factor of 1.3-1.5. Supplementary to retinal analysis, RT-qPCR was performed with AA-incubated wild type zebrafish larvae. Results displayed a 1.53-fold upregulation of JNK1 (Figure 25B) expression and a 1.77-fold downregulation of p38α MAPK (Figure 25C) expression. Additionally, ERK1 (Figure 25A) also shows a slight increase in expression. Intriguingly, after AA treatment *g6pc* (Figure 25D) and *gck* (Figure 25E) expression decreased by factor 2.18 and 1.84, while *pepck* (Figure 25F) was not significantly reduced.

In conclusion, the data shows that impaired glucose metabolism in *aldh2.1*^{-/-} mutants is caused by AA. Due to the loss of *aldh2.1*, AA is not detoxified and accumulates and downregulates *gck* and *g6pc*. In addition, AA was also identified as the driver of increased angiogenesis in *aldh2.1*^{-/-} retinal vasculature.

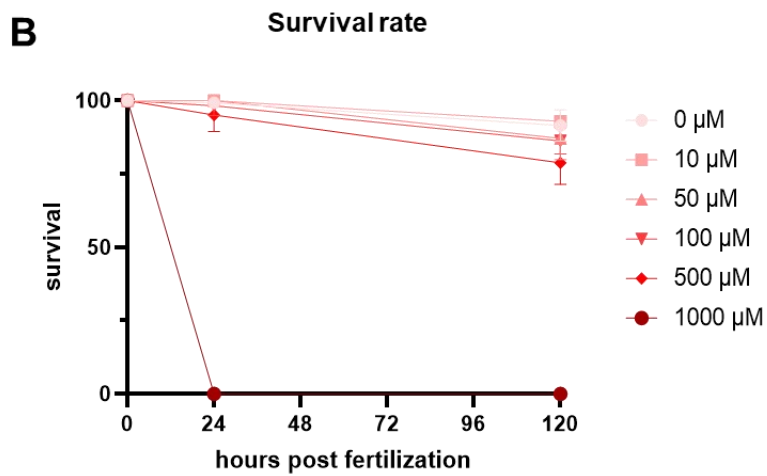
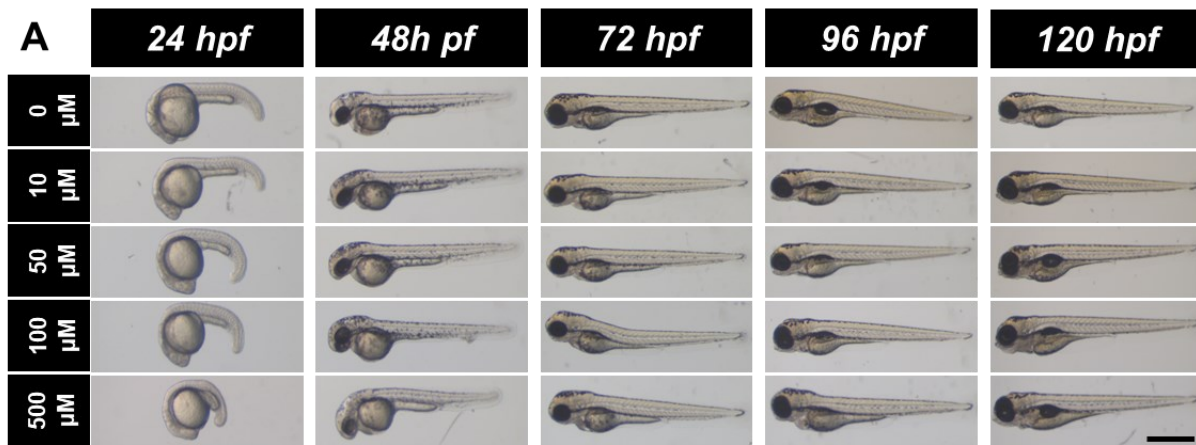


Figure 23 Zebrafish larvae displayed no morphological alterations at 120 hpf after incubation with up to 500 μM AA. A Representative microscopic images of zebrafish larvae between 24 hpf and 120 hpf displayed normal development up to 500 μM AA treatment. Black scale bar: 500 μm . **B** Quantification of survival rates showed high lethality of 1000 μM AA treated larvae.

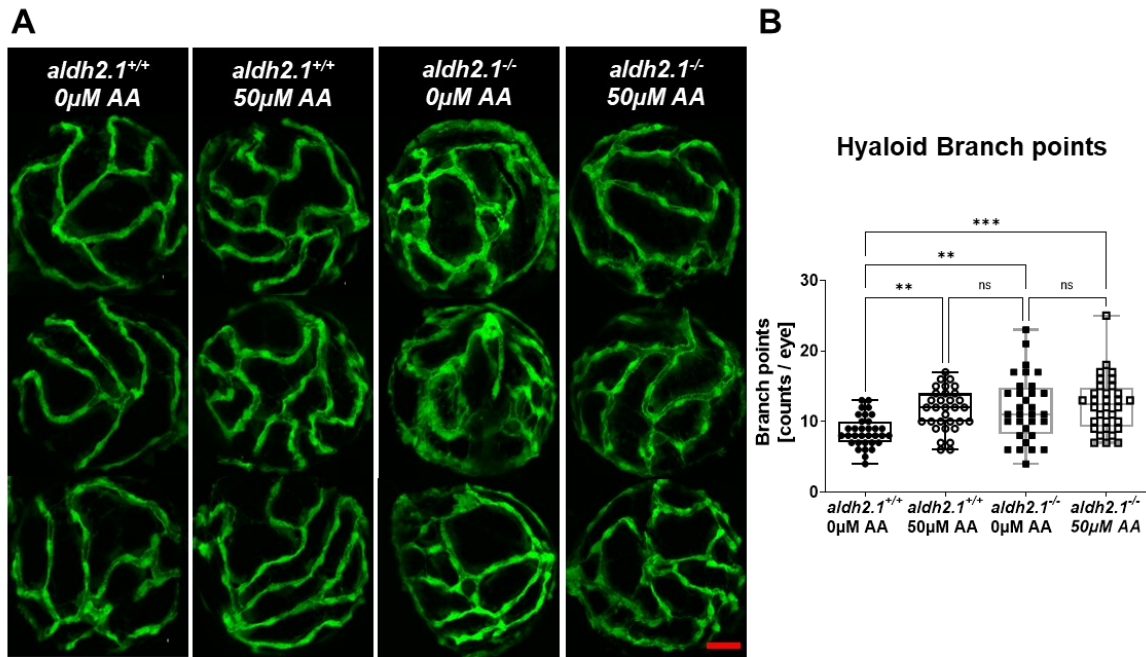


Figure 24 Exogenous AA caused angiogenic alterations in hyaloid vasculature **A** Representative confocal images of hyaloid vasculature in zebrafish larvae at 120 hpf with and without AA treatment. Red scale bar: 20 μ m. **B** Quantification of larval hyaloid vasculature showed increased numbers of branch points in *aldh2.1*^{+/+} larvae after AA (50 μ m) treatment, which was not further enhanced in *aldh2.1*^{-/-} larvae, n = 32-33 eyes per group.

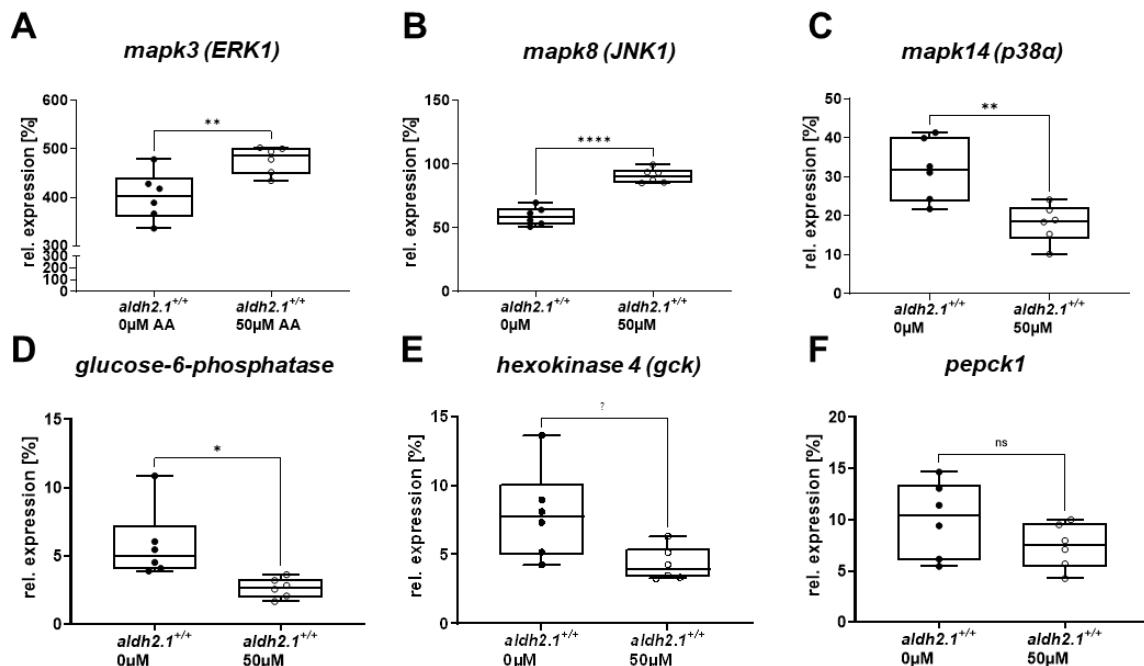


Figure 25 Exogenous AA caused angiogenic impairment of glucose metabolism and alteration of MAPK signaling. **A-C** Gene expression of MAPK family members. ERK1 gene expression (**C**) was increased in *aldh2.1*^{+/+} larvae after AA treatment. Additionally, *aldh2.1*^{+/+} larvae with 50 μ M AA treatment exhibited increased JNK1 gene expression (**D**) and decreased p38 α gene expression (**E**). **D-F** Gene expression of selected genes of glycolysis and gluconeogenesis. Reduced gene expression of *g6pc* (**F**) and *gck* (**G**) after AA treatment. *pepck* gene expression (**H**) was also reduced, although not significantly. Gene expression was quantified via RT-qPCR with 96 hpf zebrafish larvae and normalized to *arnt2*, n = 6 clutches, 50 larvae per clutch. Statistical analysis was done via Student's t-test, ns = not significant, *p < 0.05, **p < 0.01, ***p < 0.001, ****p < 0.0001.

2.6.2 Inhibition of p38 MAPK caused similar, but not identical angiogenic alterations in hyaloid vasculature in *aldh2.1*^{+/+} zebrafish larvae

To provide further evidences that the MAPKs could be a mechanistic link between increased AA levels, *aldh2.1* knockout and microvascular complications, zebrafish larvae were incubated with the selective p38 MAPK inhibitor 4-(4-Fluorophenyl)-2-(4-methylsulfinylphenyl)-5-(4-pyridyl)1H-imidazole and selective JNK inhibitor 1,3-Benzothiazol-2-yl-(2-((2-(3-pyridinyl)ethyl)amino)-4-pyrimidinyl)acetonitrile. Analysis of hyaloid vessels performed with p38 MAPK inhibitor-incubated *aldh2.1*^{+/+} and *aldh2.1*^{-/-} zebrafish larvae (Figure 26) displayed similar results as prior studies on *aldh2.1*^{-/-} mutants (Figure 10) and larvae treated with AA (Figure 24). *aldh2.1*^{+/+} zebrafish hyaloid vasculature exhibited a 1.34-fold increase in branch points after treatment with p38 MAPK inhibitor. Treatment of *aldh2.1*^{-/-} mutants could not increase branch point formation any further. This is in line with previous RT-qPCR results, as p38 MAPK mRNA expression is already significantly downregulated in *aldh2.1*^{-/-} mutants. On the other hand, analysis of hyaloid vessels performed with JNK inhibitor incubated *aldh2.1*^{+/+} and *aldh2.1*^{-/-} zebrafish larvae (Figure 27) did not achieve the presumed results. The visualization of hyaloid vessels displayed opposite effects as hypothesized before. The zebrafish hyaloid vasculature of *aldh2.1*^{+/+} and *aldh2.1*^{-/-} larvae exhibited a 2.34-fold and 1.49-fold increase in branch points after treatment with JNK inhibitor, while it was anticipated that the count of branch points in incubated larvae should be lower than untreated larvae.

In summary, the experiments suggest, that *aldh2.1*^{-/-} knockout leads to an increased retinal angiogenesis in the eyes of zebrafish via imbalance of MAPKs, including but not limited to loss of p38 MAPK function induced by AA. Additionally, while it was anticipated that the count of branch points in JNK inhibitor-incubated larvae should be lower than untreated larvae, this proof of concept seemed to be lacking, as the downregulation of JNK – instead of activation as seen in the *aldh2.1*^{-/-} zebrafish mutants – has further, unforeseen detrimental effects. Lastly, because incubation with p38 MAPK inhibitor did only result in a non-significant increase of hyaloid vessel branch points in *aldh2.1*^{-/-} knockout larvae compared to *aldh2.1*^{+/+} larvae, this series of pharmacological interventions suggested that p38 MAPK is not the sole underlying mechanism of this phenotype.

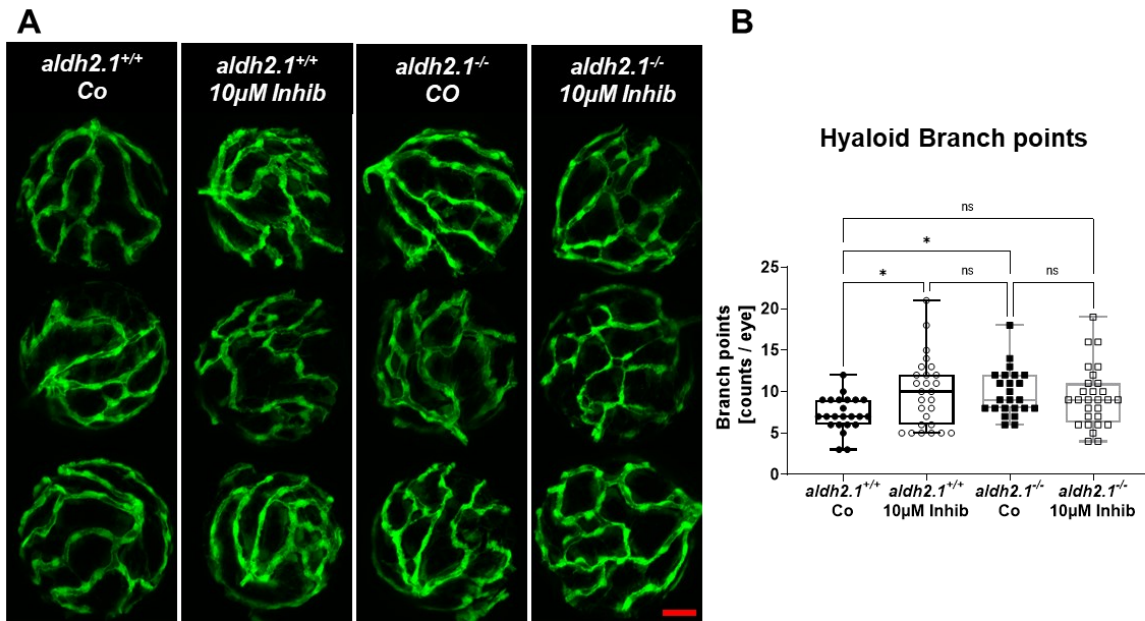


Figure 26 Inhibition of p38 MAPK caused angiogenic alterations in hyaloid vasculature in *aldhd2.1*^{+/+} larvae. **A** Representative confocal images of hyaloid vasculature in zebrafish larvae at 120 hpf with and without p38 MAPK inhibitor treatment. Red scale bar: 20 µm. **B** Quantification of larval hyaloid vasculature showed increased amount of branch points in *aldhd2.1*^{+/+} larvae with MAPK inhibitor comparable to *aldhd2.1*^{-/-} mutants, n = 23-28 eyes per group. Statistical analysis was done via Student's t-test, ns = not significant, *p < 0.05.

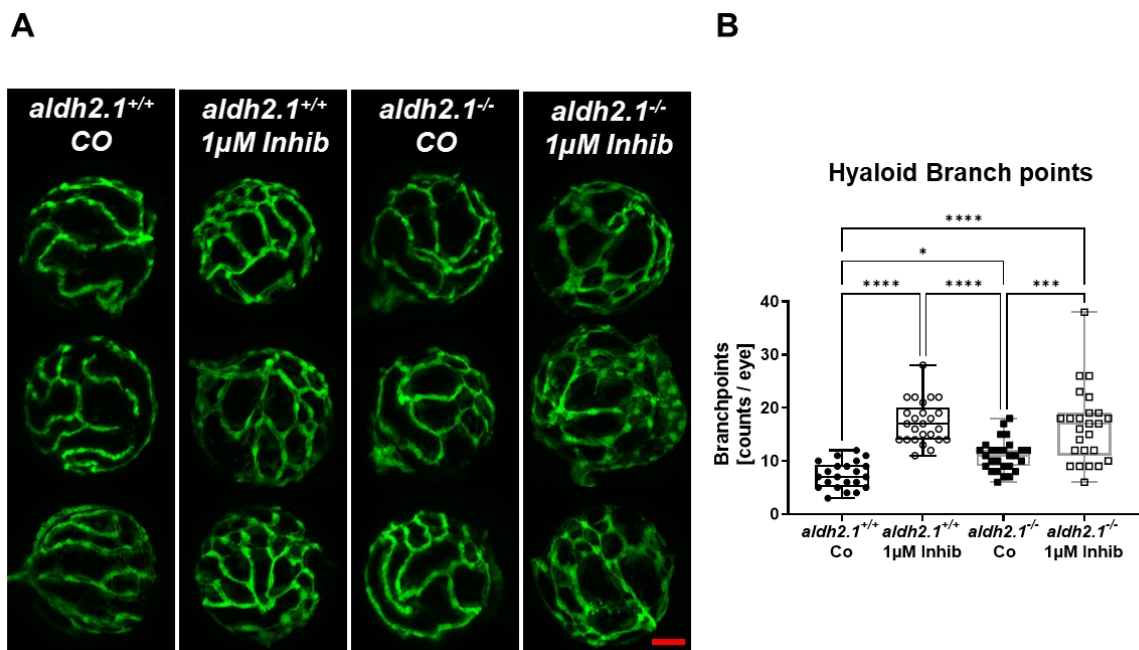


Figure 27 Inhibition of JNK caused angiogenic alterations in hyaloid vasculature in *aldhd2.1*^{+/+} larvae. **A** Representative confocal images of hyaloid vasculature in zebrafish larvae at 120 hpf with and without JNK inhibitor treatment. Red scale bar: 20 µm. **B** Quantification of larval hyaloid vasculature showed increased amount of branch points in *aldhd2.1*^{+/+} and *aldhd2.1*^{-/-} larvae with JNK inhibitor compared to the respective groups without treatment, n = 22-27 eyes per group. Statistical analysis was done via Student's t-test, ns = not significant, *p < 0.05, **p < 0.01, ***p < 0.001, ****p < 0.0001.

3. Discussion

Parts of this chapter are found in the following publication and have been originally written by myself:

Accumulation of Acetaldehyde in *aldh2.1*^{-/-} Zebrafish Causes Increased Retinal Angiogenesis and Impaired Glucose Metabolism

David Philipp Wohlfart, Bowen Lou, Chiara Simone Middel, Jakob Morgenstern, Thomas Fleming, Carsten Sticht, Ingrid Hausser, Rüdiger Hell, Hans-Peter Hammes, Julia Szendrödi, Peter Paul Nawroth, Jens Kroll

The paper published by the journal Redox Biology in 2022.

In this thesis, the aldehyde dehydrogenase isoform of *aldh2*, *aldh2.1*^{-/-}, was genetically knocked out in zebrafish to investigate its role on detoxification of reactive carbonyl species and subsequent phenotypic consequences. The main findings of this thesis are summarized in Figure 28.

The primary and secondary structure but also the function of Aldh2.1 enzyme of the zebrafish protein is comparable to the human and mouse orthologues. It not only has a similar overall amino acid sequence and preserved active sites, but also mainly detoxifies the same small reactive metabolite, acetaldehyde. Furthermore, Aldh2.1 enzyme was identified to metabolize MG; 4-HNE, MDA and ACR in zebrafish. Consequently, AA accumulated *in vivo* and the increased endogenous AA in *aldh2.1*^{-/-} zebrafish then resulted in activation of angiogenesis in the trunk and retinal blood vessels comparable to morphological hallmarks also observed in diabetic retinopathy. These microvascular damages can be explained by an imbalanced regulation of MAPKs, namely JNK and p38 kinase finally caused a reduction of vascular mural cell coverage on retinal blood vessels. Additionally, a contribution of AA to lowered postprandial blood glucose levels could be uncovered by decreasing *gck* and *g6pc* gene expression, which are key regulators of glycolysis and gluconeogenesis.

Further evidence collected in this work indicate that a longer exposure to accumulation of higher concentrations of AA may be needed to raise changes in basal morphology, kidney morphology and a broader metabolite panel, as no differences could be

observed between *aldh2.1*^{+/+} and *aldh2.1*^{-/-} mutants in the zebrafish larvae and young adult stages.

Overall, this thesis identified a novel mechanism of how RCS can specifically impair the glucose metabolism and induce angiogenesis in both larvae and adult zebrafish without concomitant hyperglycemia.

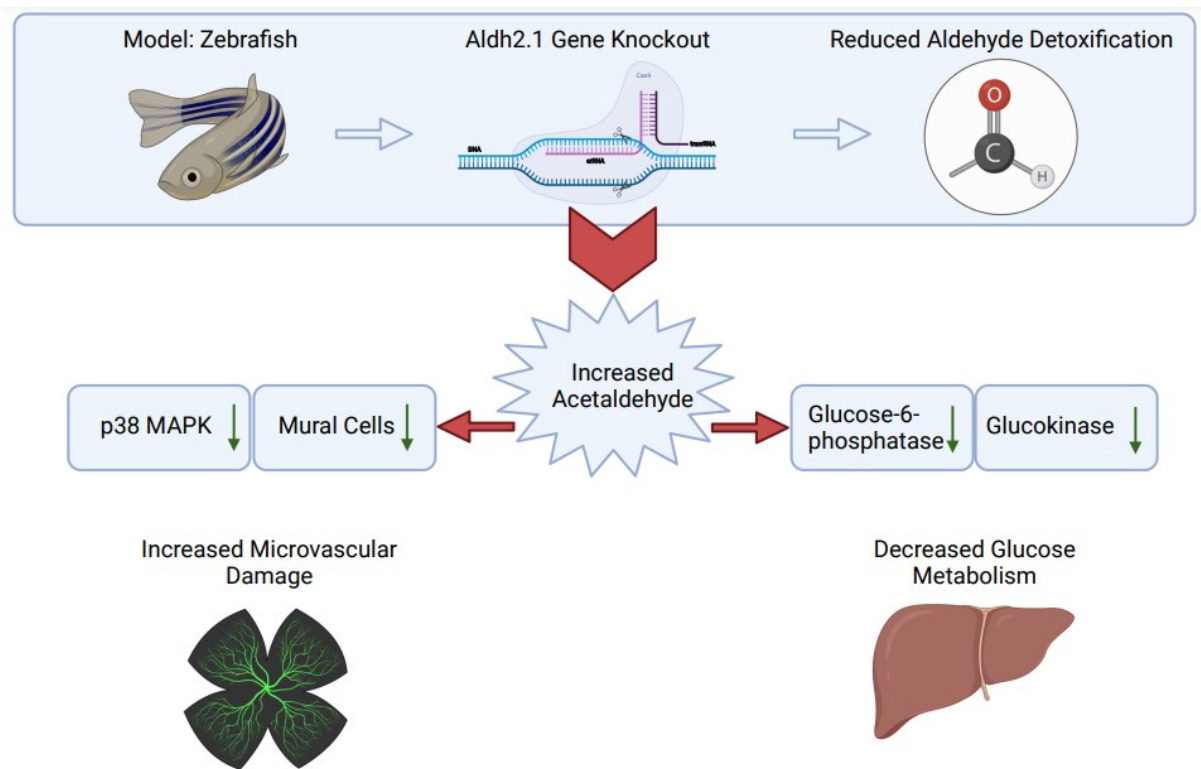


Figure 28 Graphical Abstract for the role of Aldh2.1 in zebrafish. Starting from the larval stage, functional loss of Aldh2.1 through gene knockout leads to decreased RCS detoxification and total Aldh enzyme activity. Subsequently, AA accumulates in zebrafish larvae and in liver of zebrafish adults and causes an altered regulation of specific gene expression leading to organ complications. On one side, an imbalance of the MAPKs p38 and JNK and a lowering of mural cells manifests leading to increased microvascular damage in retinal blood vessels. On the other side, key regulator of glycolysis and gluconeogenesis: gck and g6pc gene expression was inhibited causing an impaired glucose sensitivity and consequently lowered postprandial blood glucose.

3.1 *aldh2.1*^{-/-} zebrafish display increased angiogenesis and hallmarks of retinopathy without hyperglycemia

This study showed that increased endogenous AA in *aldh2.1*^{-/-} mutants led to an onset of diabetic retinopathy. Aldh2 is known to have a leading function in the protection of mitochondria, specifically loss of *aldh2* triggers an increase of ROS formation through CYP2E1, Nrf2 and TNF- α ^{27,66,67,78,79} and subsequently RCS^{56,57,151}. Additionally, altered function of Aldh2 and correspondingly AA correlates with numerous

cardiovascular and metabolic diseases including but not limited to ischemia and myocardial dysfunction^{13,34,36,60,81,100,152}. Research studies with ethanol in pathophysiologically relevant concentrations so far focused on cardiovascular disease, cancer and specific liver diseases. The essential roles of *aldh2* and its homologues for such pathological conditions is therefore unquestionable. Several of these studies focused on complications in liver and pancreas, as these two organs are also key damaged organs by alcohol abuse^{23,27,28,31,32,60}. But these studies on alcohol abuse, *aldh2*, and organ complications often focus too much on ethanol and neglected other involved species like acetaldehyde. In recent reviews, a more direct role of AA has been described, as the liver damage as a consequence of alcohol abuse has been attributed to AA instead of ethanol⁶³.

In human metabolism, acetaldehyde is the oxidized product of ethanol through alcohol dehydrogenase (Adh) and can be metabolized by Aldh2, therefore ethanol and AA should be investigated collectively. In addition, AA may be introduced into the human body by foods and tobacco smoke, providing a rationale to also research this RCS independently of any alcohol context^{63,74,75,79}.

However, one big challenge in investigating acetaldehyde, is the lack of appropriate measurement methods. A reliable measurement of acetaldehyde in blood and other biological samples has been exceedingly difficult to accomplish because of its high reactivity. Hence it was difficult to directly prove the effects of endogenous AA on whole organisms in the past, while addition of exogenous AA often resulted in difficulties with appropriate dosing. Making it difficult to distinguish between specific effects of AA at low doses and side-effects at overdoses in such commonly used animal models. The zebrafish model surprisingly offers a solution to these challenges, as they are water-based organisms. Reactive species, like AA, could therefore be added with lower concentrations into the surrounding water at early development stages, enabling the study on effects of various RCS on whole organism through diffusion into zebrafish larvae. Furthermore, it was possible to measure AA contents in zebrafish for the first time by handling them according to an adjusted protocol of Jeong *et al*¹⁵³. Consequently, the observed developed retinopathy and microvascular complications in *aldh2.1^{-/-}* zebrafish could be attributed to AA via appropriate pharmacological treatment and measurement of endogenous AA.

Supplementary, unbiased expression data in combination with pharmacological intervention studies illuminated the mechanism and showed an imbalance of JNK and p38 MAPK expression in *aldh2.1*^{-/-} zebrafish. Currently it is unknown through which mechanism these two MAPK family members are activated in *aldh2.1*^{-/-} zebrafish. There are many possibilities which include most environmental stressors, interleukin or tumor necrosis factor α and more^{154–159}. Both stress-activated protein kinases are also well known to have multiple functions in angiogenesis. p38 MAPK can act as a molecular switch for VEGF-induced angiogenesis and subsequently vascular hyperpermeability *in vitro* and *in vivo* while also regulating myocardial regeneration. The JNK family is involved in the ROS-induced endothelial angiogenesis and is suggested to regulate activation of pro-angiogenic factors like VEGF and MMP9^{138,141–143,157,160}. Moreover, vascular mural cell dropout, as exhibited in the trypsin digestion, has long been theorized to be a key player in microvascular homeostasis and recent studies have shown that loss of mural cells increases the susceptibility of the retinal vasculature to VEGF signaling and retinal angiogenesis. Mural cells are critical for a correct functioning of the retinal network and they are suggested to have a protective role for endothelial cells under stress conditions like hyperglycemia and ROS^{161–164}. Thus, the onset of retinopathy in *aldh2.1*^{-/-} larvae and adults was driven by an altered regulation of the MAPK family members and enhanced through reduction of vascular mural cell coverage. As a source of this phenomenon the reactive metabolite AA was identified independently of hyperglycemia or ethanol exposure.

3.2 AA causes an impaired glucose sensitivity and glucose mobilization via inhibition of glycolysis and gluconeogenesis gene expression

Pharmacological studies identified AA as a cause for impaired glucose sensitivity and glucose mobilization via blocking expression of key regulatory enzymes of glycolysis and gluconeogenesis, namely *gck* and *g6pc*, which ultimately led to lowered postprandial blood glucose concentrations in *aldh2.1*^{-/-} mutants. The human homologue of *aldh2.1*, *aldh2*, has already been extensively studied for its importance of ethanol detoxification. However, research on alcohol mediated stress complications mainly comprises the effect of ethanol on cardiac disease, cancer and liver disease, whereas studies directly on its metabolites, like AA and FAEE, in combination with metabolomic diseases, such as diabetes mellitus, are scarce^{13,23,37}. Intriguingly, observations made in diabetic patients already connected alcohol consumption and

hypoglycemic episodes^{26,69,82}, but the underlying mechanism on how alcohol inhibits both glycolysis and gluconeogenesis remained unexplored. This study now provided an explanation, namely that the important upstream factor causative for this phenomenon is not ethanol directly, but AA. AA blocks *g6pc* expression - a finding that has already been hypothesized several years ago and subsequently inhibits formation of glucose from glucose-6-phosphate and its release into the blood stream¹⁴⁸. Deficiency in the *g6pc* enzyme system is known to be the cause for impaired glucose homeostasis and neutrophil induced apoptosis^{145–147,165}. Moreover, AA also induced a decreased expression of *gck* – a condition that has been linked to β -cell insulin secretion in response to glucose. *gck* is known to have an impact on the glucose threshold for insulin release, subsequently leading to various complications like maturity onset diabetes of the young, type 2 (MODY2), reactive hypoglycemia and congenital hyperinsulinism^{150,166–170}. Intriguingly, insulin gene expression is severely downregulated in *aldh2.1*^{-/-} zebrafish larvae, augmenting the hypothesis that *aldh2* through AA has a high relevance for alcohol abuse mediated complications such as impaired regulation of glucose homeostasis and hypoglycemia.

3.3 Loss of Aldh2.1 does not alter glomeruli morphology

Although AA induced imbalance of MAPKs and subsequently pathophysiological alterations in zebrafish embryonal and adult retinal vasculature was established, effects on renal and glomeruli health could not be observed. PAS and EM visualizations did not reveal any alterations of parameters in glomeruli. In the preceding studies it was observed, that embryonal and adult renal alterations are accompanied by hyperglycemia. For instance, incubation of zebrafish with MG and increase of endogenous MG through *glo1* knockout was insufficient to cause alterations of kidneys¹²³. In contrast, zebrafish models with damaged renal health like *pdx1*^{-/-} and *akr1a1a*^{-/-} were observed in conjunction with hyperglycemia caused by decreased pancreatic health and development or increased insulin resistance, thereby suggesting only auxiliary impact of RCS and RCS detoxification systems to kidney damages^{16,171}.

In conclusion, even though literature suggest that *aldh2* adopts a protective role for kidney injury, research about the pathogenic impact of AA and ethanol is ongoing. The healthy kidneys and glomeruli in *aldh2.1*^{-/-} zebrafish can be seen as confirmation for

existing studies where kidney injury is not caused by RCS alone, but rather results from further complications like hyperglycemia.

3.4 Reactive metabolites as upstream factors of glucose metabolism and microvascular complications in zebrafish

RCS are spontaneously formed in the metabolism and are considered dangerous molecules because they can modify and impair the function of DNA, phospholipids and proteins^{17,46,50–52}. This modification of and binding to biomolecules often leads to production and accumulation of advanced lipoxidation and glycation end products (ALEs, AGEs) and is considered to be the cause for a wide range of pathogenic effects in the development and progression of various diseases including diabetes mellitus, neurological disorders and cancer^{54,92,172–175}. In addition to more general pathogenic effects of AGEs and ALEs the selected RCS with subsequent downstream signaling became a main focus of metabolic disease research in recent years. In several studies it could be shown, that the loss of enzymes detoxifying specific reactive species not only resulted in an accumulation of this RCS, but also subsequently altered the glucose metabolism and induced and enhanced the development of diabetic complications, establishing RCS as upstream factors and regulators to glucose homeostasis and hyperglycemia. Among the first enzymes described, loss of *glo1* in zebrafish increased MG concentrations and was accompanied by an impaired glucose tolerance^{123,132,176}. In follow-up studies in *aldh3a1* knockout zebrafish mutants, increased 4-HNE concentrations disrupted the pancreas formation, followed by inhibition of insulin expression and secretion, and finally facilitating hyperglycemia and a retinal vasodilatory phenotype¹⁵. In addition, increased ACR in *akr1a1a* zebrafish mutants led to insulin resistance and consequently to diabetic retinopathy and diabetic nephropathy¹⁶.

A major outcome of the present study is, that increased AA concentration in *aldh2.1*^{-/-} mutant zebrafish impaired glucose metabolism, causing decreased blood glucose levels, and induced an activation of angiogenesis and onset of retinopathy with morphological changes often seen in diabetic patients¹⁶¹. These observations together lead to the novel insight, that RCS can regulate glucose homeostasis and organ health during metabolic diseases. Currently, RCS need to be discussed as upstream factors of hyperglycemia, retinopathy and more. For example, the knockout of *aldh2.1* with subsequent accumulation of AA also induced microvascular alterations in the retina, but independent of any hyperglycemia. Contrariwise, lowered post-prandial blood

glucose was observed in the mutant fish. In all other preceding zebrafish studies with detoxification enzymes like *glo1*, *aldh3a1* and *akr1a1a* the diabetic complication observed by the specifically accumulated RCS was always accompanied by hyperglycemic conditions as a result of either insulin secretion and/or peripheral insulin resistance. Hence, it could never be fully excluded that hyperglycemia in such fish was the underlying cause to the microvascular damage in addition to other specific effects of the accumulated RCS. For instance, the progression of microvascular complications like diabetic retinopathy is traditionally attributed to hyperglycemia^{99,100,177}, even if that hyperglycemia may be caused through imbalanced RCS metabolism. Whereas this study reveals that microvascular phenotype observed in onset of diabetic retinopathy can be established without involvement of hyperglycemia.

Together, the data have identified a specific signature of individual RCS and their corresponding detoxifying enzyme systems, causing a specific metabolic and organ pathology ranging from altered glucose metabolism, impaired glucose tolerance, loss of pancreatic insulin expression, insulin resistance to hyperglycemia. Additionally, the independence of AA induced organ damages to hyperglycemia during decreased RCS detoxification observed in these study warrants the high importance to identify the specific mechanisms and pathways downstream of AA and other reactive metabolites.

3.5 Conclusion and future perspectives

In summary, this study has two major findings providing novel insight in the impaired glucose metabolism through the ethanol detoxification pathway and the emergence of retinopathy without hyperglycemia through acetaldehyde alone. Additionally, the data has several important implications and raises a couple of questions about RCS in diabetes research and clinical translation.

Firstly, this study on *aldh2.1* together with previous data of RCS detoxification enzymes in zebrafish show that internally produced RCS are upstream factors of impaired glucose metabolism, hyperglycemia and diabetes related organ and microvascular complications and therefore have an important, unexplored regulating function. Secondly, the interplay and crosstalk of RCS and their corresponding enzyme systems must be identified. Their mechanisms of activation and how they are altered in different disease conditions needs to be investigated to improve comprehension of their impact on organ health and in metabolic diseases. Whether the detoxification systems are supplementary factor in organ damages or if they are gatekeepers needs to be

illuminated. Lastly, it seems now more than essential to address the translation from zebrafish to human. Even though zebrafish has implemented itself as a powerful animal model for diabetes and late diabetic complications in the last decade, it needs to be investigated whether the identified signature of altered RCS in diseased zebrafish also exists in human diseases. It is currently unknown to what extent RCS induce the late diabetic complications and whether they regulate glucose homeostasis and hyperglycemia in human. Additionally, RCS could potentially be designated as biomarkers for the different subtypes of diabetes further improving the process of prediction for late diabetic complications and their therapeutic treatment.

4. Material and Methods

4.1 Material

4.1.1 Equipment

Product	Company
Table Centrifuge	Carl Roth GmbH
Microcentrifuge Mikro 200R	Hettich
Benchtop centrifuge Rotina 420R	Hettich
T100™ Thermal Cycler	BioRad
Glucometer Freedom Lite	Abbott
Heating / Shaking Block	HLC
See Saw Rocker	Stuart
Water bath AQUAline AL12	Lauda
Western Blot system	BioRad
Agarose gel chamber	Peqlab Biotechnologie GmbH
Electrophoresis power supply	Consort
Leica HI1210 water bath	Leica
Leica RM2235 microtome	Leica
Vertical Micropipette Puller P30	Sutter Instruments
BioPhotometer D30	Eppendorf
UV Transilluminator	INTAS
Leica MZ 10 F Microscope	Leica
TCS SP5 DS upright Scanner	Leica
Leica DM6000 B confocal Microscope	Leica
Leica EL 6000 UV-Lamp	Leica
Dry cabinet Memmert UNB 300	Memmert
Balance 440-47N and ABS	Kern
Electronic Balance	Kern
Quantstudio 3 qPCR – Cycler	Thermo Fischer Scientific
Chemi – Smart 5000	PeqLab
Pneumatic PicoPump PV 820	World Precision Instruments (WPI)
Jun-Air 3-4 Quiet Running Compressor	Jun-Air
pH-meter ProfiLine 197i	WTW ProfiLine
Hamilton syringe (Glastight® #1705)	Hamilton

Pipettes	Eppendorf
BX51 upright microscope	Olympus Life Science
XC10 camera	Olympus Life Science

4.1.2 Chemicals

If not indicated separately, all chemicals used during the experiments were purchased at least in analytical grade from the following companies:

AppliChem GmbH

Carl Roth GmbH

Merck AG Roche

Diagnostics GmbH

Sigma Aldrich Chemie GmbH

Thermo Fisher Scientific Inc.

Cell Signaling Technology Europe B.V.

4.1.3. Consumables

Product	Company
Blood glucose test-stripes (Lite)	FreeStyle Lite
Conical tubes (15 ml, 50 ml)	Falcon
Cover slips (22x22 mm)	Menzel Gläser
Dumont Tweezers	NeoLabs
Disposable scalpel	NeoLabs
Needle 20G – 30G x1 ½"	BD Microlance
Nitrile Gloves	BioWorld
Nitrocellulose membrane 0.22 µm	Whatman
PCR tubes (0.2 ml)	Star Labs
Quantitative PCR 96-well reaction plates	Life Technologies
Adhesive Optical Film	Biozym
Petri dishes (5 cm, 10 cm; quadratic)	Greiner
6-, 24- and 96- well plates	Greiner

Pipette tips (1000, 200, 10 μ l)	TipOne Star Labs
Pipette filter tips (1000, 100, 20 and 10 μ l)	Nerbe plus GmbH
Stainless steel beads (5 mm)	Qiagen
Syringes (1 mL)	BD Plastipak
Whatman filter paper	Sigma Aldrich
pH-Fix 0-14	Macherey-Nagel
Safe-Lock tubes (0.5, 1.5 and 2.0 ml)	Eppendorf
Serological pipettes (5, 10, 25 and 50 ml)	Falcon
Superfrost ultra plus® microscope slides	Thermo Scientific
Pasteur Pipettes	Hirschmann

4.1.4 Solutions

Solution	Components
10x ERM	20 g NaCl 0.6 g KCl 0.54 g CaCl ₂ *6H ₂ O 3.2 g MgSO ₄ *7H ₂ O 0.01 g Methylene blue Ad 1 L MilliQ water
50x TAE	242 g TrisBase 57.1 mL conc. acetic acid 100 mL 0.5 M EDTA pH 8.6 ad 1 L MilliQ water
Tricaine	400 mg Tricaine powder 97.9 mL MilliQ water ~2.1 mL 1 M Tris (pH 9) Ad to pH ~7 and 100 mL MilliQ water
5x PTU	304 g PTU ad 1L MilliQ water
Lysis buffer	133 μ L of 1.5 M Tris/HCl, pH8 40 μ L 0.5 M EDTA 60 μ L Tween 60 μ L Glycerol

10x PBS	ad 20 mL MilliQ water 400 g NaCl 10 g KCl 72,09 g Na ₂ HPO ₄ * H ₂ O 10 g KH ₂ PO ₄ ad 5 L MilliQ water
5x Laemmli	8.34 mL Tris/HCl, pH 6.8 5 g SDS 0.25 g bromophenol blue 25 mL glycerol 3.45 g DTT ad 50 mL MilliQ water
4% PFA	10 mL 10x PBS 80 mL MilliQ water 4 g PFA ad 100 mL MilliQ water
Hematoxylin	1 g Hematoxylin 0.2 g Sodium iodate (NaIO ₃) 50 g Potassium alum (KAl(SO ₄) ₂ *12 H ₂ O) 50 g Chloral hydrate (C ₂ H ₃ Cl ₃ O ₂) 1 g Citric acid (C ₆ H ₈ O ₇) ad 1 L MilliQ water
Sulfurous water	600 mL MilliQ water 30 mL 1 M HCl 36 mL 10% Sodium metasilphite (Na ₂ S ₂ O ₅)
10x electrophoresis buffer	144 g glycine 30 g Tris 10 g SDS ad 1 L MilliQ water
10x blotting buffer	30.28 g Tris 106.6 g Glycine ad 1 L MilliQ water
NP40 lysis buffer	0.87 g NaCl 5 mL 1M Tris/HCl, pH 7.4

	1.8 mL 0.5 M Na ₂ EDTA, pH 8
	1 bottle Proteinase inhibitor cocktail
	10 mL 10% Nonidet P40 solution
	10 mL Glycerol
	ad 100 ml MilliQ water
1%-Periodic Acid Solution	1 g Periodic acid ad 100 mL MilliQ water
Mayer's hemalum solution	Millipore
DPX mounting medium	Thermo Fisher Scientific
Horseradish Peroxides substrate	Supersignal™ Thermo Scientific

4.1.5 Oligonucleotides

Oligonucleotides were purchased from Sigma Aldrich.

CRISPR-construct name	Primer sequence (5' to 3')
Aldh2.1-CRISPR-for	TAGGGCTCTCCCTGGCGCCGCA
Aldh2.1-CRISPR-rev	AAACTGCGGCCAGGGAGAGC
Aldh3b1-CRISPR-for	GGAGGGCCAGAAGCAGG
Aldh3b1-CRISPR-rev	CCTGCTTCTGGCCCTCC
Aldh9a1b-CRISPR-for	GGCCTGTTCAATGTGGTTC
Aldh9a1b-CRISPR-rev	GAACCACATTGAACAGGCC

Genotyping primer name	Primer sequence (5' to 3')
Aldh2.1- gt 2.1 fw1	CCCTGCTGTGCAGTGTATTG
Aldh2.1- gt 2.3 fw2	CTGGCATGGCAATAAACACA
Aldh2.1- gt 2.4 rv2	TGCATCGAGAGAGATGCTGCCT
Aldh3b1 fwd - 2	ACAAATGCAGCAAATGCAACAA
Aldh3b1 rev -3	TGTCAGCCTGAGCATATGTTTAC
Aldh9a1b fwd 1	CAGTTGTTTTGACCCCTGTGC
Aldh9a1b rev 2	ACCGAAGGGTGAAGACAGAG

qPCR primer name	Primer sequence (5' to 3')
aldh2.1-qPCR-left	CGCACTGTATATCGCCAGTTTA
aldh2.1-qPCR-right	GGACCAAACCCTGGGATAAT

aldh3b1-qPCR-for	CATGACTCTTCCTGGTTTACCC
aldh3b1-qPCR-rev	TGATAGTTGCCCATCCCCT
aldh9a1b-qPCR-for	GGAGCAAGCCAAGAACGA
aldh9a1b-qPCR-rev	GGATCTGCAGGGCTGAAA
qPCR mapk3 fw2	GCTCCTGAGAGGGACAGTCATC
qPCR mapk3 rv2	TCGCAGGTCGTCTGGAGTTTT
qPCR mapk7 fw2	CTGGATCGGCCTTGTCGGT
qPCR mapk7 rv2	GATCAATGGTTTCCGGCTGGC
qPCR mapk8 fw1	CCGGCCTCGCTAGCACA
qPCR mapk8 rv1	ACCTCGGTGGACATGGACGA
qPCR mapk11 fw1	GCTTCTTCGGGGCCTTAAGTACA
qPCR mapk11 rv1	CATTCACGGCTACATTGCTTGGC
qPCR mapk12a fw2	ACCAAATGTTAACCCGCAAGCGAT
qPCR mapk12a rv2	CCTCTGCTGCTGTTATCCGGC
qPCR mapk14b fw1	TCCCGGCACAGATCACATTG
qPCR mapk14b rv1	TTTTCATCAAGAGCTCAGGCC
b2m_qPCR_Left	ACTGCTGAAGAACGGACAGG
b2m_qPCR_Right	GCAACGCTCTTTGTGAGGTG
arnt2_qPCR_Left	AGCCAGACAGAGGTCTTCCA
arnt2_qPCR_Right	CCGAGGTCAGCAAAGTCTTC
VEGFR2 (KDR):f1	TAAACAGCAGCGGTGTGCCA
VEGFR2 (KDR):r1	CAGTCCACGTGGCCATCCATT
FGFR2 F1	GGCCCATGAGCTCCCTGTTT
FGFR2 R1	ACGGTCGGTCACTCACTGGA
G6Pase_qPCR_Left	TCACAGCGTTGCTTTCAATC
G6Pase_qPCR_Right	AACCCAGAAACATCCACAGC
G6PDH_qPCR_Left	CGTCTTTTGTGGCAGTCAGA
G6PDH_qPCR_Right	TGATGGGTGGTGTCTTTCTCA
cPEPCK_qPCR_Left	ATCACGCATCGCTAAAGAGG
cPEPCK_qPCR_Right	CCGCTGCGAAATACTTCTTC
hk1_qPCR_Left	ATGATAGCGGCACAGCTTCT
hk1_qPCR_Right	GTTGGTGTCTCGTGCCAATC
hk2_qPCR_Left	TGAGGTCAGTCTCGTCCAGT
hk2_qPCR_Right	TCTTAATCGACAGGCCACCG

gck_qPCR_Left	AATCACCGCTGACCTGCTAT
gck_qPCR_Right	GCCACTTCACATACGCAATG
glo1-qPCR-for	AGCAGACAATGCTGCGGGTG
glo1-qPCR-rev	CTACGGGAGAACGTCCAGGC
2-INS_qPCR_Left	GGTCGTGTCCAGTGTAAGCA
2-INS_qPCR_Right	GGAAGGAAACCCAGAAGGGG
Pdx1_RT-PCR_Left	ACACGCACGCATGGAAAGGACA
Pdx1_RT-PCR_Right	GCGGGCGCGAGATGTATTTGTT
notch1a-qPCR-left	CATCACCCCTTCCAGCAGTCT
notch1a-qPCR-right	CTGAAGAGCTCCACCCATGT

4.1.6 Further materials

Product	Company
RNeasy Mini Kit	Qiagen
Great Salt Lake artemia cysts	Sanders
Fluoromount-G™	eBioscience/Invitrogen/Thermo Fishe
GoTaq® Green Master Mix	Promega
TetraMin fish flake food	Tetra
Paraplast Plus® (=Paraffin)	Sigma
Tissue-Clear®	Tissue-Tek®, Sakura Finetek
Pierce™ BCA Protein Assay Kit	Thermo Fischer Scientific
MAK263-1KT Glucose Assay Kit	Sigma Aldrich
PowerSybr Green PCR Master Mix	Thermo Fischer Scientific
Maxima First strand cDNA Kit	Thermo Fischer Scientific
4-Hydroxynonenal (4-HNE) ELISA Kit E4645	Biovision
Acrolein (ACR) ELISA Kit MBS7213206	MyBioSource Inc
Gene Ruler DNA ladder mix	Thermo Fisher Scientific
MEGashortscript™ T7	invitrogen by Thermo Fisher Scientific
mMESSAGE mMACHINE™ T7	invitrogen by Thermo Fisher Scientific
Quick-hardening mounting medium	Sigma-Aldrich
JNK Inhibitor V; CAS 345987-15-7	EMD Millipore
P38 MAPK Inhibitor, SB203580	EMD Millipore

4.1.7 Plasmids

Plasmid	Company
pT7-gRNA	Addgene
pT3TS-nCas9n	Addgene

4.1.9 Antibodies

Primary antibodies for Aldh isoforms were generated with the support of GPCF Unit Antibodies, DKFZ Heidelberg, Germany.

Primary antibodies for β -Actin was purchased from Santa Cruz Biotechnology, Inc.

Secondary antibodies were purchased from Dako, Agilent Technolgy.

4.1.10

Zebrafish transgenic lines

All experimental procedures on animals were approved by the local government authority Regierungspräsidium Karlsruhe and by the Medical Faculty Mannheim (G-98/15 and I-21/04) and carried out in accordance with the approved guidelines. Zebrafish (*Danio rerio*) adults and embryos of the transgenic lines Tg(fli1:EGFP) were utilized during this study.¹²⁴

4.2 Methods

Parts of this chapter are found in the following publication and have been originally written by myself:

Accumulation of Acetaldehyde in *aldh2.1*^{-/-} Zebrafish Causes Increased Retinal Angiogenesis and Impaired Glucose Metabolism

David Philipp Wohlfart, Bowen Lou, Chiara Simone Middel, Jakob Morgenstern, Thomas Fleming, Carsten Sticht, Ingrid Hausser, Rüdiger Hell, Hans-Peter Hammes, Julia Szendrödi, Peter Paul Nawroth, Jens Kroll

The paper published by the journal Redox Biology in 2022.

4.2.1 Study approval

All experimental procedures on animals were approved by the local government authority Regierungspräsidium Karlsruhe and by Medical Faculty Mannheim (G-98/15 and I-21/04) and carried out in accordance with the approved German laws and guidelines.

4.2.2 Zebrafish husbandry

Zebrafish lines were raised, staged and held under standard husbandry conditions in the Mannheim zebrafish core unit, Department for Vascular Biology. Embryos were held and raised in ERM at 28.5 °C for 144 hours before being transferred to adult boxes. Adult Zebrafish were kept under a 13-hour light / 11-hour dark cycle. Fish older than 72 hours-post-fertilization (hpf) and younger than 1 month-post fertilization (mpf) are referred to as larvae. From 1 – 3 mpf they are referred to as juveniles and after 90 days-post-fertilization (dpf) as adults ¹⁷⁸. Feeding of zebrafish took place twice a day, freshly hatched *Artemia salina* in the morning and fish flake food in the afternoon.

4.2.3 Generation of Zebrafish single gene knockout mutants

Mutant generation, from the design of CRISPR – oligonucleotides to the injection of CRISPR/Cas9-RNA for *aldh2.1*, *aldh3b1* and *aldh9a1b*, was performed in collaboration with Bowen Lou. Briefly: the technique used one guide RNA (gRNA), which was designed using the free software tool ZiFiT Targeter 4.2 and cloned into a T7-driven promoter expression vector (pT7-gRNA). Additionally, the pT3TS-nCas9n Vector was used in vitro for transcription to attain Cas9 mRNA. Following the protocol of the manufacturer for mRNA Synthesis, the mMESSAGE mMACHINE T3 Transcription Kit and the MEGashortscript T7 Kit were used for Cas9 mRNA and gRNA respectively. Afterwards a solution of KCl (0.1 M) containing gRNA (200 pg / L) and Cas9 mRNA was injected into one-cell stage zebrafish embryos ¹¹⁷. The resulting adult mosaic zebrafish (F0) were analyzed for germline transmission of the target gene mutation via Sanger sequencing of PCR products. Positive mutants were bred selectively. Mutations were identified by evaluation of the chromatograms and use of Yost tools Poly Peak Parser ¹⁷⁹.

4.2.4 Dissection of adult zebrafish and blood glucose measurement

Adult Zebrafish were isolated in single boxes and fasted overnight for 16-18 h prior to preparation. Then, fish were used either directly or first fed with 0.5 g flakes for one hour followed by another hour in fresh water for postprandial measurement. Afterwards fish were euthanized in ice water for two minutes and blood was extracted from caudal vessels and measured by a glucometer¹⁸⁰. Immediately after, the fish were transferred to an experimental platform covered with ice-cold PBS. For Metabolomics, RT-qPCR or Western Blot analysis, organs were isolated, transferred, weighed and snap frozen in liquid nitrogen and then stored at -80 °C. Alternatively, for visualization via either Confocal Microscopy or Histology, organs were isolated and transferred into PFA / PBS (4%) for at least 24 hours before further analysis. Lastly, for Electron Microscopy kidneys were isolated and transferred into Glutaraldehyde (3%) in Cacodylate (0.1 M) before further handling.

4.2.5 Microscopy and analysis of larvae trunks

Single gene knockout 4 dpf old zebrafish larvae (Tg(fli1:EGFP)) were anaesthetized with tricaine solution (0.003%) and separated into a 96-well plate, lying on the side. Larvae were then imaged via confocal fluorescence microscope DM6000B with Leica TCS SP5 DS scanner with 600Hz, 1024x512 pixels and 1 µm z-stacks. Quantification of alterations in trunk vessels was counted in the 6th to 22nd pair of intersegment vessels (ISV). The first 5 ISVs and the dorsal longitudinal anastomotic vessel (DLAV) were skipped. Newly developed blood vessels between ISVs were referred as 'hyper branches', while altered ISVs, i.e. malformed or missing in general were categorized as 'abnormal'.

4.2.6 Microscopy and analysis of larvae hyaloids

Larvae retinal hyaloid vasculature was imaged at 5 dpf. Larvae were anesthetized in 0.003 % tricaine and fixed in PFA / PBS (4%) for 24 h at 4 °C. Fixed larvae were washed in PBS three times for 15 minutes at RT before incubation in Trypsin / EDTA solution (0.25%) buffered at pH 7.8 with TRIS (1.5 M) for 80 minutes at 37 °C. Afterwards, larvae were washed three times for 15 minutes and stored in PBS until preparation. According to Jung's protocol¹⁷⁷, the larvae retinal hyaloid vasculature was then dissected under a stereoscope and visualized via confocal fluorescence

microscope DM6000B with Leica TCS SP5 DS scanner with 20x0.7 objective, 600Hz, 1024x1024 pixels, zoom 4 and 1.5 μ m z-stacks. Images were evaluated for vascular diameters and neovascularization using Leica Application Suite X and ImageJ. Vascular diameters were measured at 15 μ m distance from the inner optical circle (IOC) for at least 4 blood vessels. Vascularization was quantified via branch points within the circumference of the hyaloid ¹⁷⁷.

4.2.7 Microscopy and analysis of adult retinal vasculature

For the imaging of adult retinal vasculature PFA – fixed zebrafish eyes were obtained as described above, followed by a microdissection of the retina. The retina microdissection was prepared according to Wigganhauser *et al.* PFA - fixed zebrafish adult eyes were transferred to an agarose platform covered with PBS ¹²⁶. Rectus and oblique extraocular muscles were detached and the cornea was punctured to remove the lens. Thereafter, cornea and sclera were separated from the remaining intraocular tissue followed by the retinal pigment epithelium/choroid and the truncated optic nerve. The dissected retina was then washed and transferred onto a glass slide, immersed in mounting medium and covered with a cover slide. Confocal images for phenotype evaluation were acquired using the confocal fluorescence microscope DM6000 B with Leica TCS SP5 DS scanner utilizing a 20 \times 0.7 objective, 600 Hz, 1024 \times 1024 pixels and 1.5 μ m Z-steps. For evaluation Leica Application Suite X, Gimp2 and ImageJ were used. Imaged retinas were divided into three subcategory areas according to their respective vessel density and distance to the IOC: low density, middle density and high-density areas. Whereas low- and high-density areas made up 25% and middle density areas made up 50% of the whole retina. Within these areas vascularization was quantified by counting of vessel branches.

4.2.8 Retinal digest preparation

Retinal digest preparations were performed in collaboration with the laboratory of Prof. Dr. Hans-Peter Hammes by Chiara Simone Middel according to an established protocol by Dietrich *et al* ¹⁶². After preparation of the eye from the zebrafish head, it was transferred into formalin (4%) for fixation for 48 h. After fixation, the retina was dissected according to the protocol mentioned above. Following the dissection, the retina was transferred into double distilled water (ddH₂O) and incubated at 37 °C

overnight. It was then transferred into porcine trypsin (3%) in Tris-HCl (0.2 M) and incubated further for 1.5 h at 37 °C.

The retina was then transferred to a microscope slide and the retinal cells were removed from the vasculature by dropping ddH₂O from a syringe on top of the retina. The cells were removed from the slide through water aspiration, and the vasculature was left to air-dry.

The retinal digest preparations were stained using Mayer's Hemalum solution. The slides were briefly placed in ddH₂O and then moved to fresh undiluted Mayer's hemalum solution for 7 minutes. Afterwards, they were placed in room temperature tap-water for 2 minutes and then incubated subsequently with 70 %, 80 %, 96 % and finally 99.8 % ethanol for 5 minutes each. The slides were placed in two changes of xylene and kept there for 5 minutes each before being covered with cover slips and DPX mounting medium.

Images of the stained digest preparations were taken at 200x magnification using the BX51 upright microscope with an XC10 camera. Determination of the vessel diameter and the number of endothelial cells and pericytes was performed using the Cell-F software (Olympus Optical). The cells were counted in six to eight randomly selected areas in a circular area of the intermediate third of the retina, leaving out the area close to the entrance of the optic artery into the retina and the peripheral area. Endothelial cells and pericytes were distinguished by their distinct location and morphology. The cells were counted within a length of 200 µm, and the vessel diameter was measured. The cell numbers were then calculated as number of cells per mm² of capillary area.

4.2.9 Analysis of adult zebrafish kidneys

4.2.9.1 Periodic acid-Schiff stain

Kidneys were dissected from the fish body as described above and fixed in PFA (4%) for at least 24 hours, followed by washing steps in PBS for 15 minutes, then 2x with ethanol (70%) for 15 minutes, and finally in ethanol (70%) overnight at 4 °C. Afterwards, the kidneys were dehydrated through stepwise increase of the ethanol concentrations and finally in xylene. Kidneys were then transferred into melted paraffin for 15 minutes at 62 °C before being transferred into a mold with liquid paraffin. They were incubated for another 2 hours at 62 °C and then orientated in the mold. Lastly, the paraffin was solidified at room temperature. The solidified blocks were sectioned (4 µm) using a microtome and the tissue slices were transferred on to glass slides. Deparaffinization

was obtained by incubating twice with Tissue Clear twice for 10 minutes and hydrated by downward graded ethanol concentrations and finally ddH₂O. After hydration the slides were immersed in periodic acid solution (1%) for 10 minutes at RT followed by Schiff's reagent for 20 minutes. Subsequently, SO₂-water was utilized for three 2-minute washing steps. The slides were rinsed in running tap water for 5 minutes and counterstained in hematoxylin solution for 5 minutes and rinsed again in running deionized water for 5 minutes. Before visualization, the kidneys had to be dehydrated once more through upward graded ethanol concentrations, Tissue Clear and butyl acetate and mounted with a quick-hardening mounting medium. Brightfield imaging of the slides was done with the Zeiss Axio Scan.Z1. For evaluation the software tool Zen 2.3 lite was used.

4.2.9.2 Electron microscopy

Imaging of zebrafish kidneys by Electron Microscopy (EM) was prepared in collaboration with the Institute of Pathology IPH at Heidelberg University Hospital. Kidneys for EM study were fixed for at least 2 h at room temperature in glutaraldehyde (3%) solution in cacodylate buffer (0.1 M, pH 7.4), cut into pieces of $\approx 1 \text{ mm}^3$, washed in buffer, post-fixed for 1 h at 4 °C in aqueous osmium tetroxide (1%), rinsed in water, dehydrated through graded ethanol solutions, transferred into propylene oxide, and embedded in epoxy resin (Glycid Ether 100). Semithin and ultrathin sections were cut with an ultramicrotome (Reichert Ultracut E). Semithin sections of 1 μm were stained with methylene blue. 60–80 nm ultrathin sections were treated with uranyl acetate and lead citrate, and examined with an electron microscope JEM 1400 equipped with a 2K TVIPS CCD Camera TemCam F216. Kidneys were fixed in buffered formalin (10%) for Periodic acid-Schiff staining, removed, routinely embedded in paraffin, and cut into 4 μm -thick sections. For quantification of GBM on EM sections, up to 15 images were analyzed per genotype.

4.2.10 Generation of lysates from zebrafish larvae

Embryo and larvae samples were anaesthetized with 0.003 % tricaine in different developmental time points between 24 hpf and 120 hpf and collected in a clutch of 50. The yolk sac was removed by rigorous pipetting and centrifuging for 5 minutes at 14000 rpm. After removing the supernatant, the sample was snap-frozen in liquid nitrogen. Prior to each assay, zebrafish larvae were homogenized in assay buffer repeatedly pipetting with a 1 mL syringe with a 25 G needle.

4.2.11 Western Blot analysis

For western blot analysis, larvae / adult organs were incubated for 10 min with sodium-vanadate (2 mM) in 1×PBS on ice to inhibit phosphatases. Afterwards, they were lysed in NP40 lysis buffer (NaCl (150 mmol L⁻¹), Tris-HCl (50 mmol L⁻¹), pH 7.4, 1 % NP40, EDTA (10 mmol L⁻¹), 10 % glycerol, protease inhibitors) using a 1 mL syringe and a 25 G needle. Followed by incubation on ice for 30 minutes on a shaker. The supernatant containing the protein lysate was diluted 5:1 with 5x Laemmli sample buffer and heated to 95 °C for 5 min, separated via SDS-PAGE, and then transferred to a nitrocellulose membrane for antibody incubation. Visualization by enhanced chemiluminescence (ECL) was acquired after incubation with Horseradish Peroxides substrate (HRP) using the Chemi – Smart 5000 detection machine and software (PeqLab).

4.2.12 Pharmacological treatment of zebrafish embryos / larvae

Fertilized zebrafish embryos were transferred into 5 cm petri dishes. Each petri dish held 30 embryos in 10 mL ERM. At 24 hpf the chorion was removed using tweezers. Treatment with either acetaldehyde (final concentrations of 10 µM to 5 mM, Sigma-Aldrich) or p38 MAPK inhibitor (final concentration of 10 µM, EMD Millipore, SB 203580) or JNK MAPK inhibitor (final concentration of 1 µM, EMD Millipore, CAS 345987-15-7) started at 4 hpf and was refreshed daily at 24, 48, 72, 96 hpf.

4.2.13 Enzyme Activity assays

Total Enzyme activity for Aldh, Akr and Glo1 was performed in collaboration with Dr. Jakob Morgenstern from the Department of Internal Medicine I and Clinical Chemistry, Heidelberg University Hospital, and was measured using 96 hpf old zebrafish larvae at 25 °C.

Total Aldh enzyme activity was determined in Tris-HCl (0.5 mM, pH 9.5) containing DL-2-amino-1propanol (10 mM), NAD (0.5 mM) and one of the following: MG (2 mM) or 4-HNE (4 mM) or AA (5 mM) or MDA or ACR as substrates by measuring the rate of NADH formation at 340 nm ⁴⁶.

Glo1 enzyme activity was determined spectro-photometrically by monitoring the change in absorbance at 235 nm caused by the formation of S-D-lactoylglutathione ¹⁸¹.

Total Akr activity was determined in the assay mixture containing potassium phosphate (100 mM), DL-glyceraldehyde (10 mM) / ACR (5 mM), and NADPH (0.1 mM) by measuring the rate of reduction of NADPH at 340 nm.

The total enzyme activity of Aldh, Akr and Glo1 is described in units, where 1 unit is the amount of enzyme that catalyzes the formation of 1 μmol of NAD(P)H/min / 1 μmol of NAD(P)/min or 1 μmol S-D-lactoylglutathione/min respectively.

4.2.14 Measurements of glucose and reactive metabolites

4.2.14.1 Methylglyoxal assay

MG, 3-DG, and glyoxal were measured in collaboration with Dr. Thomas Fleming from the Department of Internal Medicine I and Clinical Chemistry, Heidelberg University Hospital, using a LC-MS/MS setup with 96 hpf old zebrafish larvae lysates according to Thornalley *et al* protocol^{182,183}. Briefly, the zebrafish larvae sample was treated with precipitation solution (Trichloroacetic acid 20% w/v in 0.9% NaCl) and incubated with an internal standard. Afterwards it was derivatized with 1,2-Diaminobenzene. Lastly the quantification was done using the XEVO TQ-S tandem quadrupole mass spectrometer.

4.2.14.2 Acetaldehyde assay

AA was measured in collaboration with Dr. Jakob Morgenstern from the Department of Internal Medicine I and Clinical Chemistry, Heidelberg University Hospital, utilizing a LC-MS/MS setup with lysates from 96 hpf old zebrafish larvae according to an adjusted protocol of Jeon *et al*¹⁵³. As internal standard acetaldehyde-d4 was used.

4.2.14.3 Whole Body Glucose

Glucose content was determined according to the manufacturer's instruction of MAK263-1KT Glucose Assay Kit (Sigma Aldrich) with lysates from 96 hpf old zebrafish larvae.

4.2.14.4 4-HNE assay

4-HNE was determined according to the manufacturer's instruction of 4-Hydroxynonenal ELISA Kit (Biovision, cat. # E4645) with lysates from 96 hpf old larvae.

4.2.14.5 Acrolein assay

Protein-bound acrolein was determined according to manufacturer's instruction of Acrolein ELISA Kit (MyBioSource Inc cat. # MBS7213206) with 96 hpf old larvae lysates.

4.2.15 Isolation of genomic DNA

Whole-body zebrafish larvae or cut fins of adults were prepared in a 0.2 mL reaction tube and 20 μ L lysis buffer. The first step was an incubation at 98 °C for 10 minutes and a subsequent addition of 10 μ L protein kinase-K (10 mg/mL). The reaction mix was then incubated at 55 °C for at least 4 hours before gently mixing it and incubating once more at 55 °C for 1 hour. To inactivate any protein kinase K the mix was then heated up to 98 °C for 10 minutes before being used in further experiments or alternatively being stored at -20 °C.

4.2.16 Isolation of total RNA and reverse transcription

Total RNA was isolated from homogenized zebrafish larvae or adult organs using RNeasy Mini Kit according to the manufacturer's instruction (Qiagen). RNA was reverse transcribed into cDNA by Maxima First Strand cDNA Synthesis Kit (Thermo Fischer Scientific) following the manufacturer's instructions. Isolated RNA could either be used directly or was stored at -80 °C.

4.2.17 (Reverse-transcription quantitative) Polymerase Chain Reaction (RT-qPCR)

4.2.17.1 Primer Design

Primer design was done using the NCBI primer blast tool (<https://www.ncbi.nlm.nih.gov/tools/primer-blast/>).

4.2.17.2 Polymerase Chain Reaction

PCR was performed using 12.5 μ L GoTaq® Green Master Mix (Promega), 2 μ L of forward and reverse primer each, as well as 6.5 μ L sterile MilliQ H₂O and lastly 2 μ L template DNA. The following cycles were used. A first denaturation at 95 °C for 3-minutes was followed by 35 cycles of denaturation at 95 °C for 30 s, annealing at the primer specific annealing temperature for 45 s and an elongation step at 72 °C. The elongation time was specifically selected depending on the DNA construct used and

varied between 30 and 60 seconds. A longer elongation step for another 10 minutes at 72 °C after the 35 cycles finalized the amplification. Afterwards the samples were either used directly or stored at -20 °C.

4.2.17.3 Reverse-transcription quantitative Polymerase Chain Reaction

RT-qPCR was done with PowerSYBR™ Green PCR Master Mix in 96 - well reaction plates utilizing the Quant Studio 3 Real-Time-PCR-System (Thermo Fischer Scientific). The reaction mix contained 1 µL mix of forward and reverse primer, 5 µL Power SYBR Green PCR Master Mix and 4 µL cDNA mix prepared in RNase-free H₂O, in a total volume of 10 µL.

4.2.18 Genotyping

Genotyping for *aldh2.1*^{-/-}, *aldh3b1*^{-/-} and *aldh9a1b*^{-/-} knockout zebrafish mutants was done by purification of PCR products with the QIAquick PCR Purification Kit according to the manufacturers protocol. Afterwards DNA concentration was determined photometrically and the samples were diluted, mixed with primer, and sent to Eurofins genomics for a Sanger sequencing. The results were analyzed with Yost tools Poly Peak Parser.¹⁷⁹

4.2.19 RNA-Sequence Analysis

Total RNA was isolated from homogenized zebrafish larvae (120 hpf) or organs using RNeasy Mini Kit according to the manufacturer's instruction as described in 4.2.15. Library construction and sequencing were performed by BGISEQ-500 (Beijing Genomic Institution, www.bgi.com, BGI). Gene expression analysis was performed by the Core-Lab for Microarray Analysis, Centre for Medical Research (ZMF) by Dr. Carsten Sticht. The main procedure utilized R and bioconductor with the NGS analysis package systempipeR. For quality control of raw sequencing reads FastQC (Babraham Bioinformatics) was used. Afterwards the low-quality reads were removed with the trim_galore software (version 0.6.4). Lastly, the resulting reads could be aligned to the zebrafish genome version danRer11 from UCSC and counted using kallisto version 0.46.1. For further analysis the count data was then transformed to log₂-counts per million (logCPM) using the voom-function in the limma package. The differential expression analysis was performed using the limma package in R. A false positive rate

of $\alpha = 0.05$ with FDR correction was taken as the level of significance. The data is available on <https://www.ncbi.nlm.nih.gov/geo/query/acc.cgi?acc=GSE189416>.

4.2.20 Metabolomic Analysis

Metabolomic Analysis assays were performed in collaboration with Gernot Poschet and Elena Heidenreich at the Metabolomics Core Technology Platform at the Centre of Organismal Studies Heidelberg. Adenosine compounds, thiols, free amino acids, fatty acids and primary metabolites were measured in lysates taken from 96 hpf old zebrafish larvae utilizing either ultra-performance liquid chromatography with fluorescence detection (UPLC-FLR) or semi-targeted GC-MS.

4.2.21 Protein Sequence Alignment

The amino acid sequences of Aldh2.1, Aldh3b1 and Aldh9a1b protein from zebrafish, human and mouse were accessed by Uniprot database. For comparison the selected sequences were aligned using Clustal Omega Multiple Sequence Alignment.

4.2.22 Statistical Analysis

Experimental results are expressed as median using box plots 5 – 95 % confidence intervals with whiskers. Statistical significance between different groups was analyzed using Student's t-test. GraphPad Prism 8.3.0 was used for analyses and p values of 0.05 were considered as significant and marked as: * $p < 0.05$. Further niveaus are partially mentioned: ** $p < 0.01$, *** $p < 0.001$, **** $p < 0.0001$.

Abbreviations

Abbreviation	Full form
%	Percent
°C	Degree Celsius
μL	Microliter
μm	Micrometer
μM	Micromolar
AA	Acetaldehyde
ADH	Alcohol dehydrogenase
ACR	Acrolein
AGE	Advanced glycation end product
AKR	Aldo keto reductase
AKT	Protein kinase B
ALDH	Aldehyde dehydrogenase
bp	Base pairs
BSA	Bovine serum albumin
Cas9	CRISPR associated protein 9
cDNA	Complementary deoxyribonucleic acid
CKD	Chronic kidney disease
Co	Control
CoA	Co-enzymeA
CRISPR	Clustered regularly-interspaced short pa
DM	Diabetes Mellitus
DME	Diabetic macular edema
DLAV	Dorsal longitudinal anastomotic vessel
DKFZ	German Cancer Research Center
DN	Diabetic nephropathy
DNA	Deoxyribonucleic acid
dpf	Days after post fertilization
DR	Diabetic retinopathy
EGFP	Enhanced green fluorescent protein
ESRD	End-stage renal disease
ER	Endoplasmic reticulum

eNOS	Endothelial nitric oxide synthase
FAEE	Fatty acid ethyl-ester
fli1	Friend leukemia integration1
GBM	Glomerular basement membrane
GC-MS	Gas chromatography-mass spectrometry
GDM	Gestational diabetes
Glo1	Glyoxalase1
Glut	Glucose transporter
Gly	Glycine
gRNA	Guide RNA
GSEA	Gene set enrichment analysis
GST	Glutathione S-transferase
H2O	Water
HbA1C	Glycated hemoglobin
HK	Hexokinase
hpf	Hours after post fertilization
HPLC	High performance liquid chromatography
Hz	Hertz
kb	Kilo bases
KCl	Potassium chloride
IDDM	Insulin-dependent diabetes mellitus
IFG	Impaired fasting glycaemia
IGT	Impaired glucose tolerance
Ins	Insulin
Insb	Insulin b
Insra	Insulin receptor isoform a
Insr	Insulin receptor isoform b
IOC	Inner optic circle
ISV	Intersegment vessel
LB	Lysogeny broth
LC-MS/MS	Liquid chromatography-tandem mass spectrometry
LD50	Median lethal dose
Leu	Leucine
Lys	Lysine

M	Molar
MARD	Mild age-related diabetes
MAPK	Mitogen-activated Protein Kinase
MDA	Malondialdehyde
MG	Methylglyoxal
mM	Millimolar
MO	Morpholino
MOD	Mild obesity-related diabetes
MODY	Maturity onset diabetes of the young
mTORC1	Mammalian target of rapamycin complex 1
mRNA	Messenger RNA
n	Number of samples
NaCl	Sodium chloride
NADH	Nicotinamide adenine dinucleotide
NADPH	Nicotinamide adenine dinucleotide phosphate
NCBI	National Center for Biotechnology Information
NF	Normal feeding
NPDR	Non-proliferative diabetic retinopathy
nmol	Nanomole
NOX	NADPH oxidase
OF	Overfeeding
Orn	Ornithine
p	p-value
PAM	Protospacer adjacent motif
PAS	Periodic acid Schiff
PBS	Phosphate buffered saline
PCA	Principal component analysis
PCR	Polymerase chain reaction
PDR	Proliferative diabetic retinopathy
Pdx1	Pancreatic and duodenal homeobox 1
PFA	Paraformaldehyde
PFK	Phosphofructokinase
Phe	Phenylalanine
PKC	Protein kinase C

pmol	Picomol
Pro	Proline
PTU	Phenylthiourea
p70-S6K	Ribosomal protein S6 kinase
PUFAs	Polyunsaturated fatty acids
RCS	Reactive carbonyl species
ROS	Reactive-oxygen species
RPE	Retinal pigmented epithelium
rpm	Rounds per minute
RT-PCR	Reverse transcription polymerase chain reaction
RT-qPCR	Real time-quantitative polymerase chain reaction
SAID	Severe autoimmune diabetes
SA	Segmental artery
SD	Standard deviation
SDS	Sodium dodecyl sulfate
SIDD	Severe insulin-deficient diabetes
SIRD	severe insulin-resistant diabetes
SNOs	S-nitrosothiols
SV	Segmental vein
T1DM	Type 1 diabetes
T2DM	Type 2 diabetes
TCA	Tricarboxylic acid
Tg	Transgenic
Thr	Threonine
Tris	Tris-aminomethan
Tyr	Tyrosine
UCP2 / UPLC-FSR	Ultra-performance liquid chromatography with fluorescence Detection
UV	Ultraviolet
Val	Valine
VEGF	Vascular endothelial growth factor
4-HNE	4-Hydroxynonenal
3-HPMA	N-acetyl-S-(3-hydroxypropyl)-L-cysteine
3DG	3-deoxyglucosone

References

1. Sophos, N. A. & Vasiliou, V. Aldehyde dehydrogenase gene superfamily: the 2002 update. *Chemico-biological interactions* **143-144**, 5–22; 10.1016/s0009-2797(02)00163-1 (2003).
2. Jackson, B. Update on the aldehyde dehydrogenase gene (ALDH) superfamily. *Human genomics* **5**, 1–21; 10.1186/1479-7364-5-4-283 (2011).
3. Vasiliou, V., Thompson, D. C., Smith, C., Fujita, M. & Chen, Y. Aldehyde dehydrogenases: from eye crystallins to metabolic disease and cancer stem cells. *Chemico-biological interactions* **202**, 2–10; 10.1016/j.cbi.2012.10.026 (2013).
4. Münzel, T. & Daiber, A. The potential of aldehyde dehydrogenase 2 as a therapeutic target in cardiovascular disease. *Expert opinion on therapeutic targets* **22**, 217–231; 10.1080/14728222.2018.1439922 (2018).
5. Blatter, E. E., Abriola, D. P. & Pietruszko, R. Aldehyde dehydrogenase. Covalent intermediate in aldehyde dehydrogenation and ester hydrolysis. *The Biochemical journal* **282 (Pt 2)**, 353–360; 10.1042/bj2820353 (1992).
6. Lassen, N. *et al.* Antioxidant function of corneal ALDH3A1 in cultured stromal fibroblasts. *Free radical biology & medicine* **41**, 1459–1469; 10.1016/j.freeradbiomed.2006.08.009 (2006).
7. Marchitti, S. A., Chen, Y., Thompson, D. C. & Vasiliou, V. Ultraviolet Radiation: Cellular Antioxidant Response and the Role of Ocular Aldehyde Dehydrogenase Enzymes. *Eye & contact lens* **37**, 206–213; 10.1097/ICL.0b013e3182212642 (2011).
8. Chen, Y., Koppaka, V., Thompson, D. C. & Vasiliou, V. ALDH1A1: From Lens and Corneal Crystallin to Stem Cell Marker. *Experimental eye research* **102C**, 105–106; 10.1016/j.exer.2011.04.008 (2011).
9. Vasiliou, V., Pappa, A. & Estey, T. Role of human aldehyde dehydrogenases in endobiotic and xenobiotic metabolism. *Drug metabolism reviews* **36**, 279–299; 10.1081/dmr-120034001 (2004).
10. Tsai, S.-H. *et al.* Aldehyde dehydrogenase 2 protects against abdominal aortic aneurysm formation by reducing reactive oxygen species, vascular inflammation, and apoptosis of vascular smooth muscle cells. *FASEB journal : official publication of the Federation of American Societies for Experimental Biology* **34**, 9498–9511; 10.1096/fj.201902550RRR (2020).
11. Xu, T. *et al.* Aldehyde dehydrogenase 2 protects against acute kidney injury by regulating autophagy via the Beclin-1 pathway. *JCI insight* **6**; 10.1172/jci.insight.138183 (2021).
12. Ahmed Laskar, A. & Younus, H. Aldehyde toxicity and metabolism: the role of aldehyde dehydrogenases in detoxification, drug resistance and carcinogenesis. *Drug metabolism reviews* **51**, 42–64; 10.1080/03602532.2018.1555587 (2019).
13. Chen, C.-H., Ferreira, J. C. B. & Mochly-Rosen, D. ALDH2 and Cardiovascular Disease. *Advances in experimental medicine and biology* **1193**, 53–67; 10.1007/978-981-13-6260-6_3 (2019).
14. Marchitti, S. A., Bocker, C., Stagos, D. & Vasiliou, V. Non-P450 aldehyde oxidizing enzymes: the aldehyde dehydrogenase superfamily. *Expert opinion on drug metabolism & toxicology* **4**, 697–720; 10.1517/17425255.4.6.697 (2008).
15. Lou, B. *et al.* Elevated 4-hydroxynonenal induces hyperglycaemia via Aldh3a1 loss in zebrafish and associates with diabetes progression in humans. *Redox biology* **37**, 101723; 10.1016/j.redox.2020.101723 (2020).
16. Qi, H. *et al.* Reduced Acrolein Detoxification in akr1a1a Zebrafish Mutants Causes Impaired Insulin Receptor Signaling and Microvascular Alterations. *Advanced science (Weinheim, Baden-Wurtemberg, Germany)* **8**, e2101281; 10.1002/adv.202101281 (2021).
17. Liu, G., Ji, W., Huang, J., Liu, L. & Wang, Y. 4-HNE expression in diabetic rat kidneys and the protective effects of probucol. *Journal of endocrinological investigation* **39**, 865–873; 10.1007/s40618-015-0428-y (2016).
18. Goedde, H. W. & Agarwal, D. P. Pharmacogenetics of aldehyde dehydrogenase (ALDH). *Pharmacology & therapeutics* **45**, 345–371; 10.1016/0163-7258(90)90071-9 (1990).

19. Klyosov, A. A., Rashkovetsky, L. G., Tahir, M. K. & Keung, W. M. Possible role of liver cytosolic and mitochondrial aldehyde dehydrogenases in acetaldehyde metabolism. *Biochemistry* **35**, 4445–4456; 10.1021/bi9521093 (1996).
20. Muto, M. *et al.* Association of aldehyde dehydrogenase 2 gene polymorphism with multiple oesophageal dysplasia in head and neck cancer patients. *Gut* **47**, 256–261; 10.1136/gut.47.2.256 (2000).
21. Yokoyama, A. *et al.* Alcohol and aldehyde dehydrogenase gene polymorphisms influence susceptibility to esophageal cancer in Japanese alcoholics. *Alcoholism, clinical and experimental research* **23**, 1705–1710 (1999).
22. Matsuda, T., Yabushita, H., Kanaly, R. A., Shibutani, S. & Yokoyama, A. Increased DNA damage in ALDH2-deficient alcoholics. *Chemical research in toxicology* **19**, 1374–1378; 10.1021/tx060113h (2006).
23. Boffetta, P. & Hashibe, M. Alcohol and cancer. *The Lancet. Oncology* **7**, 149–156; 10.1016/S1470-2045(06)70577-0 (2006).
24. Chen, J. *et al.* Association Between Aldehyde dehydrogenase-2 Polymorphisms and Risk of Alzheimer's Disease and Parkinson's Disease: A Meta-Analysis Based on 5,315 Individuals. *Frontiers in neurology* **10**, 290; 10.3389/fneur.2019.00290 (2019).
25. Joshi, A. U. *et al.* Aldehyde dehydrogenase 2 activity and aldehydic load contribute to neuroinflammation and Alzheimer's disease related pathology. *Acta neuropathologica communications* **7**, 190; 10.1186/s40478-019-0839-7 (2019).
26. Fernández-Checa, J. C., Kaplowitz, N., Colell, A. & García-Ruiz, C. Oxidative Stress and Alcoholic Liver Disease. *Alcohol Health and Research World* **21**, 321–324 (1997).
27. Huang, Q.-H. *et al.* Polydatin Protects Rat Liver against Ethanol-Induced Injury: Involvement of CYP2E1/ROS/Nrf2 and TLR4/NF- κ B p65 Pathway. *Evidence-based complementary and alternative medicine : eCAM* **2017**, 7953850; 10.1155/2017/7953850 (2017).
28. Petersen, O. H. Different Effects of Alcohol on the Liver and the Pancreas. *Function (Oxford, England)* **2**, zqab008; 10.1093/function/zqab008 (2021).
29. Thomes, P. G. *et al.* Natural Recovery by the Liver and Other Organs after Chronic Alcohol Use. *Alcohol research : current reviews* **41**, 5; 10.35946/arcr.v41.1.05 (2021).
30. Zhao, P., Kalhorn, T. F. & Slattery, J. T. Selective mitochondrial glutathione depletion by ethanol enhances acetaminophen toxicity in rat liver. *Hepatology (Baltimore, Md.)* **36**, 326–335; 10.1053/jhep.2002.34943 (2002).
31. Zhao, P. & Slattery, J. T. Effects of ethanol dose and ethanol withdrawal on rat liver mitochondrial glutathione: implication of potentiated acetaminophen toxicity in alcoholics. *Drug metabolism and disposition: the biological fate of chemicals* **30**, 1413–1417; 10.1124/dmd.30.12.1413 (2002).
32. Rocco, A., Compare, D., Angrisani, D., Sanduzzi Zamparelli, M. & Nardone, G. Alcoholic disease: Liver and beyond. *World Journal of Gastroenterology : WJG* **20**, 14652–14659; 10.3748/wjg.v20.i40.14652 (2014).
33. Cederbaum, A. I. Cytochrome P450 2E1-dependent oxidant stress and upregulation of anti-oxidant defense in liver cells. *Journal of gastroenterology and hepatology* **21 Suppl 3**, S22-5; 10.1111/j.1440-1746.2006.04595.x (2006).
34. Zhang, Y. & Ren, J. ALDH2 in alcoholic heart diseases: molecular mechanism and clinical implications. *Pharmacology & therapeutics* **132**, 86–95; 10.1016/j.pharmthera.2011.05.008 (2011).
35. Ma, H., Guo, R., Yu, L., Zhang, Y. & Ren, J. Aldehyde dehydrogenase 2 (ALDH2) rescues myocardial ischaemia/reperfusion injury: role of autophagy paradox and toxic aldehyde. *European Heart Journal* **32**, 1025–1038; 10.1093/eurheartj/ehq253 (2010).
36. Budas, G. R., Disatnik, M.-H., Chen, C.-H. & Mochly-Rosen, D. Activation of aldehyde dehydrogenase 2 (ALDH2) confers cardioprotection in protein kinase C epsilon (PKC ϵ) knockout mice. *Journal of molecular and cellular cardiology* **48**, 757–764; 10.1016/j.yjmcc.2009.10.030 (2009).
37. Chen, C.-H., Sun, L. & Mochly-Rosen, D. Mitochondrial aldehyde dehydrogenase and cardiac diseases. *Cardiovascular Research* **88**, 51–57; 10.1093/cvr/cvq192 (2010).

38. Chang, J. S., Hsiao, J.-R. & Chen, C.-H. ALDH2 polymorphism and alcohol-related cancers in Asians: a public health perspective. *Journal of biomedical science* **24**, 19; 10.1186/s12929-017-0327-y (2017).
39. Li, H. *et al.* Refined geographic distribution of the oriental ALDH2*504Lys (nee 487Lys) variant. *Annals of human genetics* **73**, 335–345; 10.1111/j.1469-1809.2009.00517.x (2009).
40. Jarl, J. & Gerdtham, U.-G. Time pattern of reduction in risk of oesophageal cancer following alcohol cessation--a meta-analysis. *Addiction (Abingdon, England)* **107**, 1234–1243; 10.1111/j.1360-0443.2011.03772.x (2012).
41. Bagnardi, V. *et al.* Alcohol consumption and site-specific cancer risk: a comprehensive dose-response meta-analysis. *British journal of cancer* **112**, 580–593; 10.1038/bjc.2014.579 (2015).
42. Murata, C. *et al.* Inactive aldehyde dehydrogenase 2 worsens glycemic control in patients with type 2 diabetes mellitus who drink low to moderate amounts of alcohol. *Alcoholism, clinical and experimental research* **24**, 5S-11S (2000).
43. Dakeishi, M., Murata, K., Sasaki, M., Tamura, A. & Iwata, T. Association of alcohol dehydrogenase 2 and aldehyde dehydrogenase 2 genotypes with fasting plasma glucose levels in Japanese male and female workers. *Alcohol and alcoholism (Oxford, Oxfordshire)* **43**, 143–147; 10.1093/alcalc/agm173 (2008).
44. Yin, G. *et al.* ALDH2 polymorphism is associated with fasting blood glucose through alcohol consumption in Japanese men. *Nagoya journal of medical science* **78**, 183–193 (2016).
45. Xu, F. *et al.* ALDH2 genetic polymorphism and the risk of type II diabetes mellitus in CAD patients. *Hypertension research : official journal of the Japanese Society of Hypertension* **33**, 49–55; 10.1038/hr.2009.178 (2010).
46. Vander Jagt, D. L. & Hunsaker, L. A. Methylglyoxal metabolism and diabetic complications: roles of aldose reductase, glyoxalase-I, betaine aldehyde dehydrogenase and 2-oxoaldehyde dehydrogenase. *Chemico-biological interactions* **143-144**, 341–351; 10.1016/s0009-2797(02)00212-0 (2003).
47. Semchyshyn, H. M. Reactive carbonyl species in vivo: generation and dual biological effects. *TheScientificWorldJournal* **2014**, 417842; 10.1155/2014/417842 (2014).
48. Davies, S. S. & Zhang, L. S. Reactive Carbonyl Species Scavengers—Novel Therapeutic Approaches for Chronic Diseases. *Current pharmacology reports* **3**, 51–67; 10.1007/s40495-017-0081-6 (2017).
49. Schalkwijk, C. G. & Stehouwer, C. D. A. Methylglyoxal, a Highly Reactive Dicarbonyl Compound, in Diabetes, Its Vascular Complications, and Other Age-Related Diseases. *Physiological reviews* **100**, 407–461; 10.1152/physrev.00001.2019 (2020).
50. Hanssen, N. M. J., Stehouwer, C. D. A. & Schalkwijk, C. G. Methylglyoxal stress, the glyoxalase system, and diabetic chronic kidney disease. *Current opinion in nephrology and hypertension* **28**, 26–33; 10.1097/MNH.0000000000000465 (2019).
51. Alfarhan, M., Jafari, E. & Narayanan, S. P. Acrolein: A Potential Mediator of Oxidative Damage in Diabetic Retinopathy. *Biomolecules* **10**; 10.3390/biom10111579 (2020).
52. Vehkala, L. *et al.* Plasma IgA antibody levels to malondialdehyde acetaldehyde-adducts are associated with inflammatory mediators, obesity and type 2 diabetes. *Annals of medicine* **45**, 501–510; 10.3109/07853890.2013.841322 (2013).
53. Mano, J. Reactive carbonyl species: their production from lipid peroxides, action in environmental stress, and the detoxification mechanism. *Plant physiology and biochemistry : PPB* **59**, 90–97; 10.1016/j.plaphy.2012.03.010 (2012).
54. Vistoli, G. *et al.* Advanced glycooxidation and lipoxidation end products (AGEs and ALEs): an overview of their mechanisms of formation. *Free radical research* **47 Suppl 1**, 3–27; 10.3109/10715762.2013.815348 (2013).
55. Thornalley, P. J. Protein and nucleotide damage by glyoxal and methylglyoxal in physiological systems--role in ageing and disease. *Drug metabolism and drug interactions* **23**, 125–150; 10.1515/dmdi.2008.23.1-2.125 (2008).

56. Mahreen, R., Mohsin, M., Nasreen, Z., Siraj, M. & Ishaq, M. Significantly increased levels of serum malonaldehyde in type 2 diabetics with myocardial infarction. *International journal of diabetes in developing countries* **30**, 49–51; 10.4103/0973-3930.60006 (2010).
57. Esterbauer, H., Schaur, R. J. & Zollner, H. Chemistry and biochemistry of 4-hydroxynonenal, malonaldehyde and related aldehydes. *Free radical biology & medicine* **11**, 81–128; 10.1016/0891-5849(91)90192-6 (1991).
58. Ayala, A., Muñoz, M. F. & Argüelles, S. Lipid peroxidation: production, metabolism, and signaling mechanisms of malondialdehyde and 4-hydroxy-2-nonenal. *Oxidative medicine and cellular longevity* **2014**, 360438; 10.1155/2014/360438 (2014).
59. Tian, C.-J. & Zhen, Z. Reactive Carbonyl Species: Diabetic Complication in the Heart and Lungs. *Trends in endocrinology and metabolism: TEM* **30**, 546–556; 10.1016/j.tem.2019.05.005 (2019).
60. Chen, Y.-C., Peng, G.-S., Wang, M.-F., Tsao, T.-P. & Yin, S.-J. Polymorphism of ethanol-metabolism genes and alcoholism: correlation of allelic variations with the pharmacokinetic and pharmacodynamic consequences. *Chemico-biological interactions* **178**, 2–7; 10.1016/j.cbi.2008.10.029 (2009).
61. Colell, A. *et al.* Transport of reduced glutathione in hepatic mitochondria and mitoplasts from ethanol-treated rats: effect of membrane physical properties and S-adenosyl-L-methionine. *Hepatology (Baltimore, Md.)* **26**, 699–708; 10.1002/hep.510260323 (1997).
62. Guo, R., Scott, G. I. & Ren, J. Involvement of AMPK in Alcohol Dehydrogenase Accentuated Myocardial Dysfunction Following Acute Ethanol Challenge in Mice. *PLoS ONE* **5**; 10.1371/journal.pone.0011268 (2010).
63. Le Daré, B., Lagente, V. & Gicquel, T. Ethanol and its metabolites: update on toxicity, benefits, and focus on immunomodulatory effects. *Drug metabolism reviews* **51**, 545–561; 10.1080/03602532.2019.1679169 (2019).
64. Michoudet, C. & Baverel, G. Metabolism of acetaldehyde in human and baboon renal cortex. Ethanol synthesis by isolated baboon kidney-cortex tubules. *FEBS letters* **216**, 113–117; 10.1016/0014-5793(87)80767-6 (1987).
65. Bishehsari, F. *et al.* Alcohol and Gut-Derived Inflammation. *Alcohol research : current reviews* **38**, 163–171 (2017).
66. Cederbaum, A. I. CYP2E1--biochemical and toxicological aspects and role in alcohol-induced liver injury. *The Mount Sinai journal of medicine, New York* **73**, 657–672 (2006).
67. Jing, L. *et al.* Chronic alcohol intake-induced oxidative stress and apoptosis: role of CYP2E1 and calpain-1 in alcoholic cardiomyopathy. *Molecular and cellular biochemistry* **359**, 283–292; 10.1007/s11010-011-1022-z (2012).
68. Maurel, D. B., Boisseau, N., Benhamou, C. L. & Jaffre, C. Alcohol and bone: review of dose effects and mechanisms. *Osteoporosis international : a journal established as result of cooperation between the European Foundation for Osteoporosis and the National Osteoporosis Foundation of the USA* **23**, 1–16; 10.1007/s00198-011-1787-7 (2012).
69. Tetzschner, R., Nørgaard, K. & Ranjan, A. Effects of alcohol on plasma glucose and prevention of alcohol-induced hypoglycemia in type 1 diabetes-A systematic review with GRADE. *Diabetes/metabolism research and reviews* **34**; 10.1002/dmrr.2965 (2018).
70. Varga, Z. V., Matyas, C., Paloczi, J. & Pacher, P. Alcohol Misuse and Kidney Injury: Epidemiological Evidence and Potential Mechanisms. *Alcohol research : current reviews* **38**, 283–288 (2017).
71. Guo, R. & Ren, J. Alcohol and Acetaldehyde in Public Health: From Marvel to Menace. *International Journal of Environmental Research and Public Health* **7**, 1285–1301; 10.3390/ijerph7041285 (2010).
72. Ueno, F. *et al.* Influence of alcohol and acetaldehyde on cognitive function: findings from an alcohol clamp study in healthy young adults. *Addiction (Abingdon, England)* **117**, 934–945; 10.1111/add.15733 (2022).
73. Jakkampudi, A. *et al.* Fatty acid ethyl ester (FAEE) associated acute pancreatitis: An ex-vivo study using human pancreatic acini. *Pancreatology : official journal of the International Association of Pancreatology (IAP) ... [et al.]* **20**, 1620–1630; 10.1016/j.pan.2020.10.027 (2020).

74. LENTI, C. Formazione di acetaldeide da treonina nel fegato. *Bollettino della Societa italiana di biologia sperimentale* **28**, 1382–1383 (1952).
75. LENTI, C. & GRILLO, M. A. Attivazione con piridoxalfosfato, glutatione, adenosin-5-fosfato e adenosina del processo di formazione di acetaldeide dalla d, 1-treonina nel fegato. *Bollettino della Societa italiana di biologia sperimentale* **28**, 1970–1973 (1952).
76. Endo, J. *et al.* Metabolic remodeling induced by mitochondrial aldehyde stress stimulates tolerance to oxidative stress in the heart. *Circulation research* **105**, 1118–1127; 10.1161/CIRCRESAHA.109.206607 (2009).
77. Steinmetz, C. G., Xie, P., Weiner, H. & Hurley, T. D. Structure of mitochondrial aldehyde dehydrogenase: the genetic component of ethanol aversion. *Structure (London, England : 1993)* **5**, 701–711; 10.1016/s0969-2126(97)00224-4 (1997).
78. Nakamura, Y. *et al.* Acetaldehyde accumulation suppresses Kupffer cell release of TNF-Alpha and modifies acute hepatic inflammation in rats. *Journal of gastroenterology* **39**, 140–147; 10.1007/s00535-003-1278-5 (2004).
79. Zhang, X., Li, S.-Y., Brown, R. A. & Ren, J. Ethanol and acetaldehyde in alcoholic cardiomyopathy: from bad to ugly en route to oxidative stress. *Alcohol (Fayetteville, N.Y.)* **32**, 175–186; 10.1016/j.alcohol.2004.01.005 (2004).
80. Li, S.-Y. *et al.* Overexpression of aldehyde dehydrogenase-2 (ALDH2) transgene prevents acetaldehyde-induced cell injury in human umbilical vein endothelial cells: role of ERK and p38 mitogen-activated protein kinase. *The Journal of biological chemistry* **279**, 11244–11252; 10.1074/jbc.M308011200 (2004).
81. Li, S.-Y. *et al.* Attenuation of acetaldehyde-induced cell injury by overexpression of aldehyde dehydrogenase-2 (ALDH2) transgene in human cardiac myocytes: role of MAP kinase signaling. *Journal of molecular and cellular cardiology* **40**, 283–294; 10.1016/j.yjmcc.2005.11.006 (2006).
82. van de Wiel, A. Diabetes mellitus and alcohol. *Diabetes/metabolism research and reviews* **20**, 263–267; 10.1002/dmrr.492 (2004).
83. Diagnosis and Classification of Diabetes Mellitus. *Diabetes Care* **32**, S62-7; 10.2337/dc09-S062 (2009).
84. Harreiter, J. & Roden, M. Diabetes mellitus – Definition, Klassifikation, Diagnose, Screening und Prävention (Update 2019). *Wiener klinische Wochenschrift* **131**, 6–15; 10.1007/s00508-019-1450-4 (2019).
85. Petersmann, A. *et al.* Definition, Classification and Diagnosis of Diabetes Mellitus. *Experimental and clinical endocrinology & diabetes : official journal, German Society of Endocrinology [and] German Diabetes Association* **127**, S1-S7; 10.1055/a-1018-9078 (2019).
86. Czech, M. P. Insulin action and resistance in obesity and type 2 diabetes. *Nature medicine* **23**, 804–814; 10.1038/nm.4350 (2017).
87. Duckworth, W. *et al.* Glucose control and vascular complications in veterans with type 2 diabetes. *The New England journal of medicine* **360**, 129–139; 10.1056/NEJMoa0808431 (2009).
88. Kirkman, M. S., Mahmud, H. & Korytkowski, M. T. Intensive Blood Glucose Control and Vascular Outcomes in Patients with Type 2 Diabetes Mellitus. *Endocrinology and metabolism clinics of North America* **47**, 81–96; 10.1016/j.ecl.2017.10.002 (2018).
89. Zoungas, S. *et al.* Effects of intensive glucose control on microvascular outcomes in patients with type 2 diabetes: a meta-analysis of individual participant data from randomised controlled trials. *The lancet. Diabetes & endocrinology* **5**, 431–437; 10.1016/S2213-8587(17)30104-3 (2017).
90. Ismail-Beigi, F. *et al.* Effect of intensive treatment of hyperglycaemia on microvascular outcomes in type 2 diabetes: an analysis of the ACCORD randomised trial. *Lancet (London, England)* **376**, 419–430; 10.1016/S0140-6736(10)60576-4 (2010).
91. Ahlqvist, E., van Zuydam, N. R., Groop, L. C. & McCarthy, M. I. The genetics of diabetic complications. *Nature reviews. Nephrology* **11**, 277–287; 10.1038/nrneph.2015.37 (2015).
92. Augustine, J. *et al.* The Role of Lipoxidation in the Pathogenesis of Diabetic Retinopathy. *Frontiers in endocrinology* **11**, 621938; 10.3389/fendo.2020.621938 (2020).

93. Brownlee, M. Biochemistry and molecular cell biology of diabetic complications. *Nature* **414**, 813–820; 10.1038/414813a (2001).
94. Giacco, F. & Brownlee, M. Oxidative stress and diabetic complications. *Circulation research* **107**, 1058–1070; 10.1161/CIRCRESAHA.110.223545 (2010).
95. Domingueti, C. P. *et al.* Diabetes mellitus: The linkage between oxidative stress, inflammation, hypercoagulability and vascular complications. *Journal of diabetes and its complications* **30**, 738–745; 10.1016/j.jdiacom.2015.12.018 (2016).
96. Ahlqvist, E. *et al.* Novel subgroups of adult-onset diabetes and their association with outcomes: a data-driven cluster analysis of six variables. *The lancet. Diabetes & endocrinology* **6**, 361–369; 10.1016/S2213-8587(18)30051-2 (2018).
97. Cheung, N., Mitchell, P. & Wong, T. Y. Diabetic retinopathy. *Lancet (London, England)* **376**, 124–136; 10.1016/S0140-6736(09)62124-3 (2010).
98. Fong, D. S., Aiello, L. P., Ferris, F. L. & Klein, R. Diabetic retinopathy. *Diabetes Care* **27**, 2540–2553; 10.2337/diacare.27.10.2540 (2004).
99. Kern, T. S., Antonetti, D. A. & Smith, L. E. H. Pathophysiology of Diabetic Retinopathy: Contribution and Limitations of Laboratory Research. *Ophthalmic research* **62**, 196–202; 10.1159/000500026 (2019).
100. Lechner, J., O'Leary, O. E. & Stitt, A. W. The pathology associated with diabetic retinopathy. *Vision research* **139**, 7–14; 10.1016/j.visres.2017.04.003 (2017).
101. Sabarudin, A. *et al.* Recent advances in nephropathy biomarker detections using paper-based analytical devices. *Analytical sciences : the international journal of the Japan Society for Analytical Chemistry* **38**, 39–54; 10.2116/analsci.21SAR10 (2022).
102. Samsu, N. Diabetic Nephropathy: Challenges in Pathogenesis, Diagnosis, and Treatment. *BioMed research international* **2021**, 1497449; 10.1155/2021/1497449 (2021).
103. Arora, M. K. & Singh, U. K. Molecular mechanisms in the pathogenesis of diabetic nephropathy: an update. *Vascular pharmacology* **58**, 259–271; 10.1016/j.vph.2013.01.001 (2013).
104. Donate-Correa, J. *et al.* Inflammatory Targets in Diabetic Nephropathy. *Journal of Clinical Medicine* **9**; 10.3390/jcm9020458 (2020).
105. Kopel, J., Pena-Hernandez, C. & Nugent, K. Evolving spectrum of diabetic nephropathy. *World journal of diabetes* **10**, 269–279; 10.4239/wjd.v10.i5.269 (2019).
106. Valencia, W. M. & Florez, H. How to prevent the microvascular complications of type 2 diabetes beyond glucose control. *BMJ (Clinical research ed.)* **356**, i6505; 10.1136/bmj.i6505 (2017).
107. Vinik, A. I. Diabetic neuropathy: pathogenesis and therapy. *The American journal of medicine* **107**, 17S-26S; 10.1016/s0002-9343(99)00009-1 (1999).
108. Vinik, A. I. Diagnosis and management of diabetic neuropathy. *Clinics in geriatric medicine* **15**, 293–320 (1999).
109. Vinik, A. I. & Erbas, T. Diabetic autonomic neuropathy. *Handbook of clinical neurology* **117**, 279–294; 10.1016/B978-0-444-53491-0.00022-5 (2013).
110. Vinik, A. I., Erbas, T. & Casellini, C. M. Diabetic cardiac autonomic neuropathy, inflammation and cardiovascular disease. *Journal of diabetes investigation* **4**, 4–18; 10.1111/jdi.12042 (2013).
111. Feldman, E. L. *et al.* Diabetic neuropathy. *Nature reviews. Disease primers* **5**, 41; 10.1038/s41572-019-0092-1 (2019).
112. Heckler, K. & Kroll, J. Zebrafish as a Model for the Study of Microvascular Complications of Diabetes and Their Mechanisms. *International journal of molecular sciences* **18**; 10.3390/ijms18092002 (2017).
113. Howe, K. *et al.* The zebrafish reference genome sequence and its relationship to the human genome. *Nature* **496**, 498–503; 10.1038/nature12111 (2013).
114. Menke, A. L., Spitsbergen, J. M., Wolterbeek, A. P. M. & Woutersen, R. A. Normal anatomy and histology of the adult zebrafish. *Toxicologic pathology* **39**, 759–775; 10.1177/0192623311409597 (2011).

115. Lawrence, C. Advances in zebrafish husbandry and management. *Methods in cell biology* **104**, 429–451; 10.1016/B978-0-12-374814-0.00023-9 (2011).
116. Moulton, J. D. Using Morpholinos to Control Gene Expression. *Current protocols in nucleic acid chemistry* **68**, 4.30.1-4.30.29; 10.1002/cpnc.21 (2017).
117. Jao, L.-E., Wentz, S. R. & Chen, W. Efficient multiplex biallelic zebrafish genome editing using a CRISPR nuclease system. *Proceedings of the National Academy of Sciences of the United States of America* **110**, 13904–13909; 10.1073/pnas.1308335110 (2013).
118. Maddison, L. A., Joest, K. E., Kammeyer, R. M. & Chen, W. Skeletal muscle insulin resistance in zebrafish induces alterations in β -cell number and glucose tolerance in an age- and diet-dependent manner. *American journal of physiology. Endocrinology and metabolism* **308**, E662-9; 10.1152/ajpendo.00441.2014 (2015).
119. Marín-Juez, R., Jong-Raadsen, S., Yang, S. & Spaink, H. P. Hyperinsulinemia induces insulin resistance and immune suppression via Ptpn6/Shp1 in zebrafish. *The Journal of endocrinology* **222**, 229–241; 10.1530/JOE-14-0178 (2014).
120. Toyoshima, Y. *et al.* The role of insulin receptor signaling in zebrafish embryogenesis. *Endocrinology* **149**, 5996–6005; 10.1210/en.2008-0329 (2008).
121. Salehpour, A., Rezaei, M., Khoradmehr, A., Tahamtani, Y. & Tamadon, A. Which Hyperglycemic Model of Zebrafish (*Danio rerio*) Suits My Type 2 Diabetes Mellitus Research? A Scoring System for Available Methods. *Frontiers in cell and developmental biology* **9**, 652061; 10.3389/fcell.2021.652061 (2021).
122. Wiggenhauser, L. M. *et al.* Activation of Retinal Angiogenesis in Hyperglycemic *pdx1*^{-/-} Zebrafish Mutants. *Diabetes* **69**, 1020–1031; 10.2337/db19-0873 (2020).
123. Lodd, E. *et al.* The combination of loss of glyoxalase1 and obesity results in hyperglycemia. *JCI insight* **4**; 10.1172/jci.insight.126154 (2019).
124. Lawson, N. D. & Weinstein, B. M. In vivo imaging of embryonic vascular development using transgenic zebrafish. *Developmental biology* **248**, 307–318; 10.1006/dbio.2002.0711 (2002).
125. Middel, C. S., Hammes, H.-P. & Kroll, J. Advancing Diabetic Retinopathy Research: Analysis of the Neurovascular Unit in Zebrafish. *Cells* **10**; 10.3390/cells10061313 (2021).
126. Wiggenhauser, L. M., Kohl, K., Dietrich, N., Hammes, H.-P. & Kroll, J. Studying Diabetes Through the Eyes of a Fish: Microdissection, Visualization, and Analysis of the Adult *tg(fli:EGFP)* Zebrafish Retinal Vasculature. *Journal of Visualized Experiments : JoVE*; 10.3791/56674 (2017).
127. Wiggenhauser, L. M. & Kroll, J. Vascular Damage in Obesity and Diabetes: Highlighting Links Between Endothelial Dysfunction and Metabolic Disease in Zebrafish and Man. *Current vascular pharmacology* **17**, 476–490; 10.2174/1570161116666181031101413 (2019).
128. Olsen, A. S., Sarras, M. P. & Intine, R. V. Limb regeneration is impaired in an adult zebrafish model of diabetes mellitus. *Wound repair and regeneration : official publication of the Wound Healing Society [and] the European Tissue Repair Society* **18**, 532–542; 10.1111/j.1524-475X.2010.00613.x (2010).
129. Gleeson, M., Connaughton, V. & Arneson, L. S. Induction of hyperglycaemia in zebrafish (*Danio rerio*) leads to morphological changes in the retina. *Acta diabetologica* **44**, 157–163; 10.1007/s00592-007-0257-3 (2007).
130. Bellier, J. *et al.* Methylglyoxal, a potent inducer of AGEs, connects between diabetes and cancer. *Diabetes research and clinical practice* **148**, 200–211; 10.1016/j.diabres.2019.01.002 (2019).
131. Rabbani, N. & Thornalley, P. J. Glyoxalase 1 Modulation in Obesity and Diabetes. *Antioxidants & redox signaling* **30**, 354–374; 10.1089/ars.2017.7424 (2019).
132. Schumacher, D. *et al.* Compensatory mechanisms for methylglyoxal detoxification in experimental & clinical diabetes. *Molecular metabolism* **18**, 143–152; 10.1016/j.molmet.2018.09.005 (2018).
133. Vasiliou, V., Pappa, A. & Petersen, D. R. Role of aldehyde dehydrogenases in endogenous and xenobiotic metabolism. *Chemico-biological interactions* **129**, 1–19; 10.1016/s0009-2797(00)00211-8 (2000).

134. Singh, S. *et al.* Aldehyde Dehydrogenases in Cellular Responses to Oxidative/electrophilic Stress. *Free radical biology & medicine* **56**, 89–101; 10.1016/j.freeradbiomed.2012.11.010 (2012).
135. Koppaka, V. *et al.* Aldehyde dehydrogenase inhibitors: a comprehensive review of the pharmacology, mechanism of action, substrate specificity, and clinical application. *Pharmacological reviews* **64**, 520–539; 10.1124/pr.111.005538 (2012).
136. Beisswenger, P. J., Howell, S. K., Touchette, A. D., Lal, S. & Szwegold, B. S. Metformin reduces systemic methylglyoxal levels in type 2 diabetes. *Diabetes* **48**, 198–202; 10.2337/diabetes.48.1.198 (1999).
137. Rezzola, S., Paganini, G., Semeraro, F., Presta, M. & Tobia, C. Zebrafish (*Danio rerio*) embryo as a platform for the identification of novel angiogenesis inhibitors of retinal vascular diseases. *Biochimica et biophysica acta* **1862**, 1291–1296; 10.1016/j.bbadis.2016.04.009 (2016).
138. Jopling, C., Suñe, G., Morera, C. & Izpisua Belmonte, J. C. p38 α MAPK regulates myocardial regeneration in zebrafish. *Cell cycle (Georgetown, Tex.)* **11**, 1195–1201; 10.4161/cc.11.6.19637 (2012).
139. Ricard, N., Zhang, J., Zhuang, Z. W. & Simons, M. Isoform-Specific Roles of ERK1 and ERK2 in Arteriogenesis. *Cells* **9**; 10.3390/cells9010038 (2019).
140. Ricard, N. *et al.* Endothelial ERK1/2 signaling maintains integrity of the quiescent endothelium. *The Journal of experimental medicine* **216**, 1874–1890; 10.1084/jem.20182151 (2019).
141. Issbrücker, K. *et al.* p38 MAP kinase--a molecular switch between VEGF-induced angiogenesis and vascular hyperpermeability. *FASEB journal : official publication of the Federation of American Societies for Experimental Biology* **17**, 262–264; 10.1096/fj.02-0329fje (2003).
142. Chang, L. & Karin, M. Mammalian MAP kinase signalling cascades. *Nature* **410**, 37–40; 10.1038/35065000 (2001).
143. Wang, Z., Yang, J., Qi, J., Jin, Y. & Tong, L. Activation of NADPH/ROS pathway contributes to angiogenesis through JNK signaling in brain endothelial cells. *Microvascular research* **131**, 104012; 10.1016/j.mvr.2020.104012 (2020).
144. Batlle, R. *et al.* Regulation of tumor angiogenesis and mesenchymal-endothelial transition by p38 α through TGF- β and JNK signaling. *Nature communications* **10**, 3071; 10.1038/s41467-019-10946-y (2019).
145. Nordlie, R. C. Metabolic regulation by multifunctional glucose-6-phosphatase. *Current topics in cellular regulation* **8**, 33–117; 10.1016/b978-0-12-152808-9.50009-2 (1974).
146. Nordlie, R. C. Multifunctional glucose-6-phosphatase: cellular biology. *Life sciences* **24**, 2397–2404; 10.1016/0024-3205(79)90447-8 (1979).
147. Nordlie, R. C. & Foster, J. D. A retrospective review of the roles of multifunctional glucose-6-phosphatase in blood glucose homeostasis: Genesis of the tuning/retuning hypothesis. *Life sciences* **87**, 339–349; 10.1016/j.lfs.2010.06.021 (2010).
148. Brecher, A. S. & Lehti, M. D. A hypothesis linking hypoglycemia, hyperuricemia, lactic acidemia, and reduced gluconeogenesis in alcoholics to inactivation of glucose-6-phosphatase activity by acetaldehyde. *Alcohol (Fayetteville, N.Y.)* **13**, 553–557; 10.1016/s0741-8329(96)00067-5 (1996).
149. Méndez-Lucas, A., Hyroššová, P., Novellasdemunt, L., Viñals, F. & Perales, J. C. Mitochondrial phosphoenolpyruvate carboxykinase (PEPCK-M) is a pro-survival, endoplasmic reticulum (ER) stress response gene involved in tumor cell adaptation to nutrient availability. *The Journal of biological chemistry* **289**, 22090–22102; 10.1074/jbc.M114.566927 (2014).
150. Lenzen, S. A Fresh View of Glycolysis and Glucokinase Regulation: History and Current Status*. *The Journal of biological chemistry* **289**, 12189–12194; 10.1074/jbc.R114.557314 (2014).
151. Mano, J. & Biswas, M. S. Analysis of Reactive Carbonyl Species Generated Under Oxidative Stress. *Methods in molecular biology (Clifton, N.J.)* **1743**, 117–124; 10.1007/978-1-4939-7668-3_11 (2018).
152. Uchida, K. Role of reactive aldehyde in cardiovascular diseases. *Free radical biology & medicine* **28**, 1685–1696; 10.1016/s0891-5849(00)00226-4 (2000).

153. Jeong, H.-S. *et al.* Validation and Determination of the Contents of Acetaldehyde and Formaldehyde in Foods. *Toxicological research* **31**, 273–278; 10.5487/TR.2015.31.3.273 (2015).
154. Bellahcene, M. *et al.* Activation of p38 mitogen-activated protein kinase contributes to the early cardiodepressant action of tumor necrosis factor. *Journal of the American College of Cardiology* **48**, 545–555; 10.1016/j.jacc.2006.02.072 (2006).
155. Bengal, E., Aviram, S. & Hayek, T. p38 MAPK in Glucose Metabolism of Skeletal Muscle: Beneficial or Harmful? *International journal of molecular sciences* **21**; 10.3390/ijms21186480 (2020).
156. Chuang, S. M., Liou, G. Y. & Yang, J. L. Activation of JNK, p38 and ERK mitogen-activated protein kinases by chromium(VI) is mediated through oxidative stress but does not affect cytotoxicity. *Carcinogenesis* **21**, 1491–1500 (2000).
157. Davis, R. J. Signal transduction by the JNK group of MAP kinases. *Cell* **103**, 239–252; 10.1016/s0092-8674(00)00116-1 (2000).
158. Hoene, M. *et al.* Activation of the mitogen-activated protein kinase (MAPK) signalling pathway in the liver of mice is related to plasma glucose levels after acute exercise. *Diabetologia* **53**, 1131–1141; 10.1007/s00125-010-1666-3 (2010).
159. Whitmarsh, A. J., Yang, S. H., Su, M. S., Sharrocks, A. D. & Davis, R. J. Role of p38 and JNK mitogen-activated protein kinases in the activation of ternary complex factors. *Molecular and cellular biology* **17**, 2360–2371; 10.1128/MCB.17.5.2360 (1997).
160. Nebreda, A. R. & Porras, A. p38 MAP kinases: beyond the stress response. *Trends in biochemical sciences* **25**, 257–260; 10.1016/s0968-0004(00)01595-4 (2000).
161. Hammes, H.-P. Pericytes and the pathogenesis of diabetic retinopathy. *Hormone and metabolic research = Hormon- und Stoffwechselforschung = Hormones et metabolisme* **37 Suppl 1**, 39–43; 10.1055/s-2005-861361 (2005).
162. Dietrich, N. & Hammes, H.-P. Retinal digest preparation: a method to study diabetic retinopathy. *Methods in molecular biology (Clifton, N.J.)* **933**, 291–302; 10.1007/978-1-62703-068-7_19 (2012).
163. Caceres, L. *et al.* Frizzled 4 regulates ventral blood vessel remodeling in the zebrafish retina. *Developmental dynamics : an official publication of the American Association of Anatomists* **248**, 1243–1256; 10.1002/dvdy.117 (2019).
164. Park, D. Y. *et al.* Plastic roles of pericytes in the blood-retinal barrier. *Nature communications* **8**, 15296; 10.1038/ncomms15296 (2017).
165. Shieh, J.-J., Pan, C.-J., Mansfield, B. C. & Chou, J. Y. In islet-specific glucose-6-phosphatase-related protein, the beta cell antigenic sequence that is targeted in diabetes is not responsible for the loss of phosphohydrolase activity. *Diabetologia* **48**, 1851–1859; 10.1007/s00125-005-1848-6 (2005).
166. Heredia, V. V., Carlson, T. J., Garcia, E. & Sun, S. Biochemical basis of glucokinase activation and the regulation by glucokinase regulatory protein in naturally occurring mutations. *The Journal of biological chemistry* **281**, 40201–40207; 10.1074/jbc.M607987200 (2006).
167. Matschinsky, F. M. Banting Lecture 1995. A lesson in metabolic regulation inspired by the glucokinase glucose sensor paradigm. *Diabetes* **45**, 223–241; 10.2337/diab.45.2.223 (1996).
168. Osbak, K. K. *et al.* Update on mutations in glucokinase (GCK), which cause maturity-onset diabetes of the young, permanent neonatal diabetes, and hyperinsulinemic hypoglycemia. *Human mutation* **30**, 1512–1526; 10.1002/humu.21110 (2009).
169. Šimčíková, D., Kocková, L., Vackářová, K., Těšínský, M. & Heneberg, P. Evidence-based tailoring of bioinformatics approaches to optimize methods that predict the effects of nonsynonymous amino acid substitutions in glucokinase. *Scientific reports* **7**, 9499; 10.1038/s41598-017-09810-0 (2017).
170. Toulis, K. A., Nirantharakumar, K., Pourzitaki, C., Barnett, A. H. & Tahrani, A. A. Glucokinase Activators for Type 2 Diabetes: Challenges and Future Developments. *Drugs* **80**, 467–475; 10.1007/s40265-020-01278-z (2020).
171. Wiggerhauser, L. M. *et al.* pdx1 Knockout Leads to a Diabetic Nephropathy- Like Phenotype in Zebrafish and Identifies Phosphatidylethanolamine as Metabolite Promoting Early Diabetic Kidney Damage. *Diabetes* **71**, 1073–1080; 10.2337/db21-0645 (2022).

172. Altomare, A. *et al.* Lipid peroxidation derived reactive carbonyl species in free and conjugated forms as an index of lipid peroxidation: limits and perspectives. *Redox biology* **42**; 10.1016/j.redox.2021.101899 (2021).
173. Gianazza, E. *et al.* Lipid Peroxidation in Atherosclerotic Cardiovascular Diseases. *Antioxidants & redox signaling* **34**, 49–98; 10.1089/ars.2019.7955 (2021).
174. Gianazza, E., Brioschi, M., Fernandez, A. M. & Banfi, C. Lipoxidation in cardiovascular diseases. *Redox biology* **23**, 101119; 10.1016/j.redox.2019.101119 (2019).
175. Gugliucci, A. Glycation as the glucose link to diabetic complications. *The Journal of the American Osteopathic Association* **100**, 621–634 (2000).
176. Moraru, A. *et al.* Elevated Levels of the Reactive Metabolite Methylglyoxal Recapitulate Progression of Type 2 Diabetes. *Cell metabolism* **27**, 926-934.e8; 10.1016/j.cmet.2018.02.003 (2018).
177. Jung, S.-H., Kim, Y. S., Lee, Y.-R. & Kim, J. S. High glucose-induced changes in hyaloid-retinal vessels during early ocular development of zebrafish: a short-term animal model of diabetic retinopathy. *British journal of pharmacology* **173**, 15–26; 10.1111/bph.13279 (2016).
178. Kimmel, C. B., Ballard, W. W., Kimmel, S. R., Ullmann, B. & Schilling, T. F. Stages of embryonic development of the zebrafish. *Developmental dynamics : an official publication of the American Association of Anatomists* **203**, 253–310; 10.1002/aja.1002030302 (1995).
179. Hill, J. T. *et al.* Poly peak parser: Method and software for identification of unknown indels using sanger sequencing of polymerase chain reaction products. *Developmental dynamics : an official publication of the American Association of Anatomists* **243**, 1632–1636; 10.1002/dvdy.24183 (2014).
180. Zang, L., Shimada, Y., Nishimura, Y., Tanaka, T. & Nishimura, N. Repeated Blood Collection for Blood Tests in Adult Zebrafish. *Journal of Visualized Experiments : JoVE*; 10.3791/53272 (2015).
181. McLellan, A. C. & Thornalley, P. J. Glyoxalase activity in human red blood cells fractionated by age. *Mechanisms of ageing and development* **48**, 63–71; 10.1016/0047-6374(89)90026-2 (1989).
182. Thornalley, P. J. & Rabbani, N. Assay of methylglyoxal and glyoxal and control of peroxidase interference. *Biochemical Society transactions* **42**, 504–510; 10.1042/BST20140009 (2014).
183. Rabbani, N. & Thornalley, P. J. Measurement of methylglyoxal by stable isotopic dilution analysis LC-MS/MS with corroborative prediction in physiological samples. *Nature protocols* **9**, 1969–1979; 10.1038/nprot.2014.129 (2014).